

URINE-BASED CANCER DETECTION  
VIA EXPRESSION-TARGETED GENE DELIVERY

AN ABSTRACT

SUBMITTED ON THE NINETEENTH DAY OF MAY 2015

TO THE DEPARTMENT OF CHEMICAL AND BIOMOLECULAR ENGINEERING

IN PARTIAL FULFILLMENT OF THE REQUIREMENTS

OF THE SCHOOL OF SCIENCE AND ENGINEERING

OF TULANE UNIVERSITY

FOR THE DEGREE

OF

DOCTOR OF PHILOSOPHY

BY

Yunlan Fang

YUNLAN FANG

APPROVED:

W. Godbey

W. GODBEY, PH.D.  
DIRECTOR

D. Blake

DIANE A. BLAKE, PH.D.

A. Skaja

ANNE SKAJA ROBINSON, PH.D.

N. Pesika

NOSHIR S. PESIKA, PH.D.

## **Abstract**

The overall objective of this project was to design and develop a urine-based assay as a means of early cancer detection. Through expression-targeted gene delivery, cancer cells were to be induced into expressing reporter proteins that would be secreted and detected via lateral flow assay. The work began *in vitro*, but progressed into the bladder in an orthotopic model of transitional cell carcinoma. As opposed to existing blood- or urine-based cancer diagnosis methods that work via detection of a limited number of cancer biomarkers, the method developed in this thesis is not limited to secreted cancer-specific molecules. Instead, genes were engineered that placed cancer-specific DNA elements (promoters and enhancers) upstream of exons that encode secreted proteins. Following non-virally mediated gene delivery, the transgenes, expressed preferentially in cancer cells, yielded the expression of the secretable reporters, which were detected in cell supernatants *in vitro* or in the urine *in vivo*.

A good orthotopic bladder model was required to test therapeutic/diagnostic agents. In traditional methods to establish an orthotopic murine bladder model, mechanical damage (electrocautery) or chemical denudation are widely used to disrupt the glycosaminoglycan layer lining on the urothelium for the purpose of increasing the tumor-take rate. We compared gene delivery efficiencies, via the *Gaussia luciferase* (*G.luc*) reporter, in murine models with versus without urothelial burn injury via

electrocautery. It was found that urine samples collected at 24 hours after the third treatment from tumor-bearing mice having initially received the burn injuries contained significantly lower luciferase levels than those from the counterpart “no burn” mice ( $p < 0.05$ ). This finding also held true in tumor-free mice having received burns versus no burns. Considering the fact that the tumor-take rate of the no-burn model was 80%, as opposed to 87.5% tumor-take in the burn model, the burn-free tumor-instillation regimen was chosen for the murine model of transitional cell carcinoma, upon which the expression-targeted diagnostic was tested.

The cyclooxygenase-2 promoter ( $P_{cox2}$ ) and osteopontin promoter ( $P_{opn}$ ) were selected to drive the expression of *G.luc* both *in vitro* and *in vivo*. Each promoter yielded cancer-specificity in that, following transfections, the reporter was expressed well in the murine bladder carcinoma cell line MB49 as opposed to little-to-no expression in normal murine fibroblasts (MF). In control experiments *in vivo*,  $P_{cox2}$ -*G.luc*- and  $P_{opn}$ -*G.luc*-treated mice without tumors did not secrete significantly higher levels of G.luc than did tumor-free mice undergoing treatments with the pUC19 null vector. However, tumor-bearing mice that were treated with  $P_{cox2}$ -*G.luc* did secrete significantly higher levels of G.luc than did tumor-bearing mice treated with the null vector. Trials utilizing  $P_{opn}$ -*G.luc* treatments did not yield a significant increase in G.luc expression versus negative controls. A positive correlation was established between maximal G.luc levels observed and bladder weight ( $R^2=0.94$ ). Although  $P_{cmv}$ -,  $P_{cox2}$ -, and  $P_{opn}$ -driven transgene expressions followed different kinetics in cultured MB49 cells, *G.luc* expression driven by the three promoters displayed similar expression profiles in the bladder model. Local

maxima were observed in urine samples collected at 24- and 48- hours post-transfection (and at 72-hours when experiments were carried out that far). This periodicity in luciferase detection spikes may have been the result of a masking of G.luc signal by some factor(s) that were present in the urine in a circadian fashion.

Further development of the detection system involved branching out from G.luc in the search for additional secretable reporters that could be detected in the urine. Genes encoding *beta-2-microglobulin* ( $\beta 2m$ ), the *beta*-subunit of *human chorionic gonadotropin* ( $\beta hCG$ ), the *prostate specific antigen* (*psa*), and *secreted alkaline phosphatase* (*seap*), were selected based upon their sizes, expression levels in healthy individuals, and detectability by currently-available ELISA-based methods. A library of promoters and reporters would open the door to multiple cancer-detection assays being performed simultaneously with a single test. It was found that the transcription of the delivered transgenes  $\beta hCG$  and *psa*, and the secretion of the corresponding protein products, were more active in bladder carcinoma cells than in the colon carcinoma cells tested *in vitro*. *In vivo*, the PSA and SEAP reporters were elevated in tumor-bearing mice having undergone treatments with  $P_{cox2}$ -driven transgenes encoding these proteins. Results indicated that  $\beta 2m$  was not a good reporter for the detection system. While  $\beta hCG$  was not examined *in vivo* because of reports that it could cause an up-regulation in cancer cell proliferation, a non-bioactive fragment of  $\beta hCG$  could potentially be very useful, based on the exciting data obtained *in vitro* using the  $\beta hCG$  reporter with detection taking place in home-pregnancy kits. On the targeting side, both  $P_{cox2}$  and  $P_{opn}$  were able to yield relatively high levels of downstream gene expression in bladder carcinoma cells. *In vivo*

results demonstrated the utility of the detection system for bladder tumors, and existing urine-based lateral assays showed proof-of-concept for a potential home-based cancer detection system.

URINE-BASED CANCER DETECTION  
VIA EXPRESSION-TARGETED GENE DELIVERY

A DISSERTATION

SUBMITTED ON THE NINETEENTH DAY OF MAY 2015

TO THE DEPARTMENT OF CHEMICAL AND BIOMOLECULAR ENGINEERING

IN PARTIAL FULFILLMENT OF THE REQUIREMENTS

OF THE SCHOOL OF SCIENCE AND ENGINEERING

OF TULANE UNIVERSITY

FOR THE DEGREE

OF

DOCTOR OF PHILOSOPHY

BY

Yunlan Fang

YUNLAN FANG

APPROVED :

W T Godbey

W T. GODBEY, PH.D.  
DIRECTOR

DA Blake

DIANE A. BLAKE, PH.D.

A Skaja

ANNE SKAJA ROBINSON, PH.D.

Noshir S. Pesika

NOSHIR S. PESIKA, PH.D.

© Copyright by Yunlan Fang, 2015

All Rights Reserved

## **Acknowledgements**

I would like to express my deepest gratitude to my advisor Dr. W Godbey, who provides me the great opportunity to work in his laboratory at Tulane University. His creativity and enthusiasm to cancer research is contagious, leading me into the world of bioengineering. His patient guidance helps me develop scientific thinking skills and the ability to conduct research more independently.

My sincere thanks to the dissertation committee: Dr. Diane Blake, Dr. Anne Robinson, and Dr. Noshir Pesika, for their insightful and constructive advices about my research, as well as for their continued support and encouragement.

I would also express my gratitude to Dr. Scott Grayson and students in his laboratory for offering me an opportunity to collaborate with them and expanding my knowledge on polymer chemistry.

I would like to thank Dr. Daniel Shantz, Dr. Bruce Gibb, Dr. Vijay John, and Dr. Yiping Chen for the access to their facilities.

I would also like to thank my fellow lab mates in Dr. Godbey's laboratory: Dr. Xiujuan Zhang, Dr. Georgina Dobek, Daniel Balazs, Dr. Xuguang Chen, Jacqueline Scapa, Benjamin Wolfson, Frederick Twigg and Natalee Buisson, for providing me assistance and making a fun research atmosphere.

I would like to expand my gratitude to Dr. Georgina Dobek, Amy and technicians in the Department of Comparative Medicine, for helping me take care of animals.

I am also grateful to all faculty and staff members, and my friends in the CBE department. Their assistance and accompany are indispensable for me to work and live well here.

Finally, I would like to thank my husband Xuguang, my parents, my parents-in-law and my grandparents for their unswerving belief on me, encouraging me to chase my dreams with their endless love.

# Table of Contents

<b>Acknowledgements .....</b>	<b>ii</b>
<b>List of Tables .....</b>	<b>vii</b>
<b>List of Figures.....</b>	<b>viii</b>
<b>Chapter 1. Background .....</b>	<b>1</b>
1.1. Cancer Screening and Detection .....	1
1.2. Expression-targeted gene delivery in cancer.....	6
1.3. Reporter system.....	11
1.4. Lateral flow chromatographic immunoassays .....	17
1.5. Goals of Dissertation.....	19
<b>Chapter 2. Effect of Electrocautery on a Murine Orthotopic Bladder Tumor Model as it Relates to Gene Delivery .....</b>	<b>21</b>
2.1. Introduction.....	21
2.2. Materials and Methods .....	25
2.2.1. <i>Murine orthotopic tumor model</i> .....	25
2.2.2. <i>In vivo transfections</i> .....	26
2.2.3. <i>Histology</i> .....	27
2.2.4. <i>Statistics</i> .....	27
2.3. Results.....	27
2.3.1. <i>In vivo transfections</i> .....	27
2.3.2. <i>Bladder weight</i> .....	31
2.3.3. <i>H&amp;E staining</i> .....	32
2.4. Discussion.....	34
2.5. Conclusion .....	35
<b>Chapter 3. Non-invasive Detection of Bladder Cancer via Expression-targeted Gene Delivery .....</b>	<b>37</b>
3.1. Introduction.....	37
3.2. Materials and Methods .....	41
3.2.1. <i>Plasmid Construction</i> .....	41
3.2.2. <i>In vitro transfections</i> .....	41
3.2.3. <i>Murine orthotopic tumor model</i> .....	42
3.2.4. <i>In vivo transfections</i> .....	43
3.2.5. <i>In vitro serum deprivation and shock</i> .....	44
3.2.6. <i>Identification of signal inhibitors in urine</i> .....	44
3.2.7. <i>Statistics</i> .....	45
3.3. Results.....	45
3.3.1. <i>In vitro transfections</i> .....	45
3.3.2. <i>In vivo transfections</i> .....	48

3.3.3.	<i>Establishing the best time to collect urine for analysis</i>	52
3.3.4.	<i>In vitro time course secreted gaussia luciferase assay</i>	58
3.3.5.	<i>In vitro serum deprivation and shock</i>	58
3.3.6.	<i>Presence of a Masking Factor?</i>	61
3.3.7.	<i>Correlation between G.LUC levels and tumor burden</i>	64
3.4.	Discussion	67
3.5.	Conclusion	72

## **Chapter 4. Cancer Detection Using Expression-targeted Gene Delivery to Drive Expression of Urine-borne Reporters ..... 73**

4.1.	Introduction	73
4.2.	Materials and Methods	79
4.2.1.	<i>Cells</i>	79
4.2.2.	<i>Plasmid construction</i>	80
4.2.3.	<i>In vitro transfections</i>	82
4.2.4.	<i>Real-time quantitative PCR</i>	83
4.2.5.	<i>Reporter assay for cell culture</i>	85
4.2.6.	<i>Murine orthotopic tumor model</i>	86
4.2.7.	<i>In vivo transfections</i>	86
4.2.8.	<i>Urine-based reporter assays</i>	87
4.2.9.	<i>Statistics</i>	87
4.3.	Results	87
4.3.1.	<i>First detection of reporters</i>	87
4.3.2.	<i>Transcription of reporter genes when expression-targeting was employed</i>	90
4.3.3.	<i>Lateral flow immunoassay results for cell culture</i>	96
4.3.4.	<i>Reporter expression, in vitro, as determined by immunoassays</i>	100
4.3.5.	<i>Reporter expression, in vivo, as determined by immunoassays</i>	104
4.4.	Discussion	107
4.5.	Conclusion	112

## **Conclusions ..... 113**

## **Appendix A An Evaluation of Gene Delivery using Cyclic Poly(ethylene imine) and Exact Linear Analogs ..... 115**

A1.	Introduction	115
A2.	Methods and Materials	119
A2.1.	<i>DNA protection and complex stability assay</i>	119
A2.2.	<i>Cells and Media</i>	120
A2.3.	<i>Transfection experiments</i>	120
A2.4.	<i>Luciferase Assay</i>	120
A2.5.	<i>Viability assay</i>	121
A2.6.	<i>Dynamic Light Scattering Measurements</i>	121
A2.7.	<i>Zeta Potential Measurements</i>	122
A3.	Results	122
A3.1.	<i>DNA protection and complex stability assay</i>	122
A3.2.	<i>Gene delivery</i>	123
A3.3.	<i>Cell viability</i>	126
A3.4.	<i>Further characterization</i>	127
A4.	Discussion	129
A5.	Conclusion	131

## **Appendix B Plasmid Maps ..... 133**

**List of References..... 148**

## List of Tables

**Table 1.1.** US Food and Drug Administration-approved cancer biomarkers.

**Table 1.2.** Examples of cancer-specific promoters in cancer gene therapy.

**Table 1.3.** Luciferase reporters Features.

**Table 2.1.** Common pretreatment methods to disrupt the integrity of bladder urothelium.

**Table 3.1.** Specific gravity of urine samples collected at 6am and 6pm from tumor-bearing mice and normal mice.

## List of Figures

**Figure 1.1.** Schematic view of lateral flow assay.

**Figure 2.1.** Bladder cancer staging.

**Figure 2.2.** Reporter luminescence following transfection with the indicated plasmids on healthy mice.

**Figure 2.3.** Reporter luminescence following transfection with the indicated plasmids on tumor-bearing mice.

**Figure 2.4.** Bladder weights of burned or unburned tumor-bearing mice.

**Figure 2.5.** H&E staining on bladder tumor tissues

**Figure 3.1.** Secreted G. luciferase levels, measured as intensity (counts per second), of the supernatants of transfected of MF cells or MB49 cells.

**Figure 3.2.** Luminescence intensities of supernatants of MB49 cells treated with  $P_{cmv}$ -*G.luc*,  $P_{cox2}$ -*G.luc*, or  $P_{opn}$ -*G.luc*.

**Figure 3.3.** Reporter luminescence following transfection with the indicated plasmids.

**Figure 3.4.** Luciferase levels detected in urine samples from tumor-bearing mice.

**Figure 3.5.** Profiles of G.LUC intensities in the urine of tumor-bearing mice transfected with  $P_{cmv}$ -*G.luc*,  $P_{cox2}$ -*G.luc*, or  $P_{opn}$ -*G.luc* in the evening.

**Figure 3.6.** Representative profiles of G. luciferase intensities in the urine of mice

transfected with  $P_{cmv-luc}$  in the morning.

**Figure 3.7.** Luciferase intensity normalized to maximal intensity tested during 66h after transfection on MB49 cells that were transfected.

**Figure 3.8.** Luciferase intensities detected in luciferase-positive cell supernatants that had been diluted with urine collected from mice at either 6:00 am or 6:00 pm.

**Figure 3.9.** The relationship between maximal luciferase intensity detected in urine samples and at that times the tumor burden of tumor-bearing mice.

**Figure 4.1.** Secretion levels of three reporter proteins were compared in different cell lines that were transfected with the strong  $P_{cmv}$ .

**Figure 4.2.** Fold change in the transcription of three reporter genes, in three cell lines.

**Figure 4.3.** PCR results reflecting changes in  $\beta 2m$  transcription levels.

**Figure 4.4.** PCR results reflecting changes in  $\beta hCG$  transcription levels.

**Figure 4.5.** Fold change of  $psa$  transcription levels.

**Figure 4.6.** Lateral flow assays indicating the presence or absence of  $\beta hCG$  in cell supernatants.

**Figure 4.7.** Lateral flow assays indicating the presence or absence of PSA in cell supernatants.

**Figure 4.8.** Reporter concentrations in the supernatants of normal murine fibroblasts (MF), murine colon cancer cells (CT26.C125) and murine bladder tumor cells (MB49).

**Figure 4.9.** PSA concentrations following transfection with the indicated plasmids *in vivo*.

**Figure 4.10.** SEAP concentrations following transfection with the indicated plasmids *in*

*vivo*.

**Figure A1.** DNA protection and complex stability assay.

**Figure A2.** Transfection efficiencies and cell viability with HFF-1 cells for linear and cyclic PEI at different N:P ratios.

**Figure A3.** Results of transfections with Gaussia luciferase reporter plasmids.

**Figure A4.** Sizes and zeta potentials of transfection complexes

**Figure B1.** <sup>P</sup>*cmv-Gaussia luc* map.

**Figure B2.** <sup>P</sup>*cox2-Gaussia luc* map.

**Figure B3.** <sup>P</sup>*opn-Gaussia luc* map.

**Figure B4.** <sup>P</sup>*cmv-βhCG* map.

**Figure B5.** <sup>P</sup>*cox2-βhCG* map.

**Figure B6.** <sup>P</sup>*opn-βhCG* map.

**Figure B7.** <sup>P</sup>*cmv-β2m* map.

**Figure B8.** <sup>P</sup>*cox2-β2m* map.

**Figure B9.** <sup>P</sup>*opn-β2m* map.

**Figure B10.** <sup>P</sup>*cmv-psa* map.

**Figure B11.** <sup>P</sup>*cox2-psa* map.

**Figure B12.** <sup>P</sup>*opn-psa* map.

**Figure B13.** <sup>P</sup>*cmv-seap* map.

**Figure B14.** <sup>P</sup>*cox2-seap* map.

**Figure B15.** <sup>P</sup>*opn-seap* map.

# **Chapter 1. Background**

## **1.1. Cancer Screening and Detection**

According to the newest statistics from the American Cancer Society, about 589,430 Americans are expected to die of cancer (about 1,620 people per day) and 1,658,370 new cancer cases are expected to be diagnosed in 2015 (American Cancer Society). Cancer has become the second most common cause of death in the US. Screening is an effective approach to help detect cancer early and provide treatment opportunities before cancer progression becomes uncontrollable. For instance, since the introduction of screening, the relative 5-year survival rate of bladder cancer patients has reduced from 98% at Stage 0 to 15% at Stage IV based on people diagnosed with bladder cancer from 1988 to 2001(American Cancer Society). Hence, early detection is crucial to lowering mortality rates among cancer patients.

The history of cancer screening dates back to 1923, when George Papanicolaou developed the Pap test to diagnose cervical cancer (Mammas and Spandidos, 2012). As researchers gain a deeper understanding of cancer mechanisms, new diagnostic tools for cancer are being developed. Currently, there are a variety of methods that have been applied to cancer diagnosis. Each one is described in more detail below.

1) Biopsy. Tissue or cell samples may be taken from the suspected neoplasm to be evaluated by a pathologist. Excisional biopsies require surgery to remove the entire tumor or a debulking procedure may be performed to remove a part of it from the body, therefore local or even general anesthesia is usually required. Another biopsy technique considered less invasive than a surgical biopsy, is a fine needle biopsy or a punch biopsy. Local anesthesia is still required if a large-sized needle (core needle) is used but no incision is made (American Cancer Society). Given that a very thin needle is used, tiny pieces of tissue with a small amount of fluid are removed, therefore tissue processing can occasionally be faster than surgical biopsies. The drawback of the fine needle technique is that sometimes insufficient samples are extracted, preventing a definite diagnosis. Needle biopsies are also usually performed under the guidance of imaging tools to guarantee the samples are collected from the correct location (American Cancer Society).

2) Imaging. These techniques rely on a wide array of imaging facilities to produce pictures showing the inside of body based on the interaction of electromagnetic radiation (e.g. computed tomography (CT), positron emission tomography (PET), and magnetic resonance imaging (MRI)) with body tissues and fluids or the reflection (ultrasound) (Fass, 2008). CT uses computer-processed X-rays to create 2-dimensional slices of a scanned area and then generates a 3-dimensional image via digital geometry processing. Sometimes the temporal and spatial resolution of CT is combined with the metabolic sensitivity of PET to form images, which not only display tumor size but also show tumor metabolism and other parameters (Fass, 2008). CT is especially recommended for colorectal cancer and lung cancer screening according to American Cancer Society

screening guidelines. Mammography is another imaging technique, which uses low-energy X-rays to create pictures of breasts. This technique is a widely used breast cancer screening exam. However, high frequency electromagnetic radiation including X-rays and ultraviolet light are ionizing, which poses a potential safety hazard to people (Pierce et al., 1996). MRI uses non-ionizing radiation and serves as an alternative option for breast cancer detection. However, the high cost, limited access, and high false positive probability keep MRI from being considered as a routine screening exam. Instead MRI is used as a supplemental technique for mammography or ultrasound to assist with decision-making before mastectomy surgeries (Fass, 2008). Ultrasound technique creates images based on echoes. An ultrasound emits high-frequency sound waves, which bounce off organs and tissues creating an image. Ultrasound is better than X-rays at evaluating cancers in soft tissue and is used to tell the difference between fluid-filled cysts and solid tumors based on the different echo patterns. However, ultrasound fails to offer images as detailed as those from CT or MRI scans and cannot indicate if tumors are benign or malignant (American Cancer Society).

3) Endoscopy. This diagnostic test involves insertion of an endoscope into the body. This aids physicians by allowing them to look inside of the body via fiber optics (installed on one end of the endoscope). There are several different types of endoscopy (American Cancer Society). For example, a colonoscope is inserted into the body through the anus to check the colon and large intestine. This is considered a routine screening exam for colorectal cancer. Though colonoscopy is a sensitive diagnostic technique, it can fail to detect some small polyps (Atkin et al., 2002). Before the test, a thorough

cleansing of the colon is necessary and sedative drugs are usually administered into patients. Sometimes colonoscopy can lead to serious complications, including bleeding or rarely, perforation of the lining of colon. In recent years, capsule colonoscopy has been developed as a less invasive diagnostic procedure than conventional colonoscopy ostensibly to reduce the risk of complications (Riccioni et al., 2012).

4) Laboratory tests. Body fluids including blood, urine and tissues may be collected for a series of laboratory tests. For example, a complete blood count is used to diagnose and monitor leukemia by measuring indicators of disease, such as altered numbers of different cell types, the amount of hemoglobin, and the size of red blood cells (National Cancer Institute). Cytogenetic analysis is used to evaluate any changes in the number and structure of chromosomes in white blood cells (National Cancer Institute). A gene mutation test is used to identify if mutations occur in genes that are associated with cancer development (National Cancer Institute). Another popular laboratory test that is noteworthy, is the tumor biomarker test. A tumor biomarker is a biological molecule present in body fluids or tissues that indicates the presence of a tumor in body. It can be a protein, nucleic acid, antibody and or a peptide. Table 1.1 lists all cancer biomarkers that have been approved by the Food and Drug Administration (FDA). (Ludwig and Weinstein, 2005, Fuzery et al., 2013, Li and Chan, 2014)

**Table 1.1.** US Food and Drug Administration-approved cancer biomarkers.

Biomarkers	Type	Cancer Type	Source
$\alpha$ -Fetoprotein	Glycoprotein	Nonseminomatous testicular	Serum
HCG- $\beta$	Glycoprotein	Testicular	Serum
CA19-9	Carbohydrate	Pancreatic	Serum
CA125	Glycoprotein	Ovarian	Serum
HE4	Protein	Ovarian	Serum
OVA1	Proteins	Ovarian	Serum
Pap smear	Cervical smear	Cervical	Cervix
CEA	Protein	Colon	Serum
EGFR	Protein	Colon	Colon
Fibrin/fibrinogen Degradation product	Protein	Colon	Serum
KIT	Protein (IHC)	GI tumor	GIST
Thyroglobulin	Protein	Thyroid	Serum
PSA (total)	Protein	Prostate	Serum
PSA (complex)	Protein	Prostate	Serum
PSA (free PSA%)	Protein	Prostate	Serum
Pro2PSA	Protein	Prostate	Serum
CA15-3	Glycoprotein	Breast	Serum
CA27-29	Glycoprotein	Breast	Serum
Cytokeratins	Protein (IHC)	Breast	Breast tumor
OR and PR	Protein (IHC)	Breast	Breast tumor
HER2/NEU	Protein (IHC)	Breast	Breast tumor
HER2/NEU	Protein	Breast	Serum
HER2/NEU	DNA (FISH)	Breast	Breast tumor
Chromosomes 3,7,9, and 17	DNA (FISH)	Bladder	Urine
NMP22	Protein	Bladder	Urine
Fibrin/FDP	Protein	Bladder	Urine
BTA	Protein	Bladder	Urine
HMW CEA and mucin (immunofluorescence)	Protein	Bladder	Urine

BTA, bladder tumor-associated antigen; CA, cancer antigen; CEA, carcinoembryonic antigen; FDP, fibrin degradation protein; FIS, fluorescent in-situ hybridization; GIST, gastrointestinal stromal tumor; HCG, human chorionic gonadotropin; HE4, human epididymis protein 4; IHC, immunohistochemistry; NMP22, nuclear matrix protein 22; OVA1, multiple proteins including CA-125 II, transthyretin, apolipoprotein A1,  $\beta$ 2-microglobulin and transferrin; PSA, prostate-specific antigen.

As for bladder cancer, the main type of cancer this work would focus on, white light cystoscopy (WLC) is still the diagnostic standard (Cauberg Evelyne et al., 2011). A cystoscope with a lens or a camera on one end is inserted into the bladder through the urethra, allowing physicians to look at inside of the bladder. But WLC is not ideal for detecting small papillary bladder tumors, satellite lesions and carcinoma in situ (CIS)

(Jocham et al., 2008). Fluorescence cystoscopy is helpful to improve visualizing bladder tumors. Fluorescent dyes such as 5-aminolevulinic acid or its hexyl ester hexaminolevulinate are delivered into the bladder via a transurethral catheter and specifically absorbed by cancer cells. When a blue light is applied through the cystoscope, cancer cells will emit a red color due to the accumulation of the porphyrins in them (Cheung et al., 2013a). Narrow-band imaging improves the contrast between bladder cancer cells and normal bladder cells by filtering white light into two narrow bandwidths of light ( $\lambda=415\text{nm}$  (blue) and  $\lambda=540\text{nm}$  (green)), which are taken up by hemoglobin (Cauberg Evelyne et al., 2011, Kuznetsov et al., 2006). Because bladder tumor has vascular networks, regions of blood vessels will show darkness, increasing the visibility of tumors (Cauberg Evelyne et al., 2011). Cytology is widely used as a non-invasive urine test. Urinary markers for bladder cancer detection have been summarized in Table 1.1. For example, UroVysion<sup>®</sup> produced by Abbott Molecular Inc diagnosed bladder cancer by detecting aneuploidy in chromosomes 3,7, and 17, and loss of the 9p21 locus of the P16 tumor suppressor gene (Cheung et al., 2013a, Junker et al., 2003). In addition, the USA Food and Drugs Administration have approved a point-of-care NMP 22 test, which is produced by Stellar Pharmaceuticals, for bladder cancer detection and surveillance (Cheung et al., 2013a).

## **1.2. Expression-targeted gene delivery in cancer**

Delivery of a reporter gene into cancer cells is a very promising strategy to image cancer (Wu et al., 2003a). If these genes are delivered into the cells or tissues of interest under the control of a universal promoter, which normal cells or tissues also respond to, it is expected to cause a false-positive signal, during diagnosis. Expression-targeted gene

expression technique is aimed to manipulate cancer cells or malignant tissues to express the delivered gene but to prevent or at least minimize the delivered gene's expression in normal cells or tissues. The success of such strategy is achieved by taking advantage of cancer-specific promoters. A typical cancer-specific promoter is a region of DNA that is limited to initiating transcription of downstream a gene in cancer cells. In general, a cancer-specific promoter contains many cis-regulatory elements, which are bound by overexpressed transcription factors present in cancer cells. However, due to a lack of or an insufficiency in these transcription factors in normal cells, normal cells fail to respond to the cancer-specific promoter effectively, leading to a low or undetectable expression of the downstream gene. Table 1.2. summarizes a series of cancer-specific promoters that may be used for transcriptional targeting in cancers.

**Table 1.2.** Examples of cancer-specific promoters in cancer gene therapy.

Promoter	Cancer Type	Reference
$\alpha$ -fetoprotein (AFP)	Hepatocellular carcinoma	(Peng et al., 2013)
Carcinoembryonic antigen (CEA)	CEA-expressing tumors	(Fichera et al., 1998)
Cholecystokinin type A receptor	Pancreatic cancer	(Xie et al., 2007)
erbB2	ERBB2-expressing tumors	(Chang et al., 1999)
mucin-1 (muc1)	MUC1(DF3)-expressing tumors	(Huyn et al., 2009)
L-plastin (LP-P)	Epithelial-derived tumors	(Chung and Deisseroth, 2004)
$\alpha$ -lactalbumin (ALA)	Breast	(Li et al., 2005)
midkine (MK)	Pancreatic	(Yoshida et al., 2002)
cyclooxygenase-2 (cox-2)	Gastrointestinal	(Yamamoto et al., 2001a)
PSA/PMSA, kallikrein-2	Prostate	(Zhang et al., 2002)
Probasin (ARR2PB)	Prostate	(Zhang et al., 2000)
Tyrosinase promoter	Melanoma	(Siders et al., 1998)
Human telomerase reverse transcriptase	Not cancer type specific	(Gu et al., 2000b)
Prolactin (PRL)	Pituitary tumors	(Camper et al., 1985)
Osteocalcin 2	Osteosarcoma	(Ko et al., 1996)

Dysregulation of some gene expression takes place in almost all cancer types. Therefore, cancer-specific promoters upstream of these genes likely lack tissue specificity. Telomerase is a eukaryotic ribonucleoprotein enzyme that maintains stability of telomeres, the ends of eukaryotic chromosomes. Telomerase expression is repressed in most somatic cells and tissues, resulting in shortened telomeres when cell division occurs. However, telomerase is highly expressed in more than 85% of human cancers (Kim et al., 1994). Human telomerase reverse transcriptase (hTERT) is a crucial catalytic subunit of telomerase, playing a determinant role in telomerase activity (Gu et al., 2000a). The gene *hTERT* is overexpressed in cancer cells but repressed in most somatic cells, and expression of the <sup>P</sup>*hTERT*-directed suicide gene (*Bax*) could induce apoptosis targeted to in cancer cells and tumor tissues (Gu et al., 2000a). Survivin is an inhibitor of apoptosis protein and is overexpressed in most cancers, playing a role in enhancing cancer cell proliferation and resistance to chemotherapy. Although it is also expressed in some normal cells (e.g., primitive hematopoietic cells, T lymphocytes, and vascular endothelial cells) to regulate their growth, its expression level is much lower than that of transformed cells (Fukuda and Pelus, 2006). The <sup>P</sup>*survivin*-driven *luciferase* shows more than 200 times more cancer-specific activity than the cytomegalovirus promoter (<sup>P</sup>*cmv*) upstream of *luciferase* delivered via liposome intravenously into mice bearing lung tumor (Chen et al., 2004).

Though some of these cancer-specific promoters could be used selectively in a specific cancer type, some others lack such selectivity and work in many different types of cancer. One of the solutions to improve selectivity is to introduce some tissue-specific

elements into a non tissue-specific promoter. A lung cancer-targeted promoter system was developed by co-delivering  $P^{hTERT}$ -driven thyroid transcription factor 1 (*TTF-1*) and five tandem copies of human surfactant protein A1 promoter ( $P^{hSPA1}$ )-driven luciferase to lung cancer cells (Fukazawa et al., 2004).  $P^{hTERT}$  does not possess tissue specificity but it could drive the expression of *TTF-1*. Together with other lung-specific accessory factors, *TTF-1* could bind to the  $P^{hSPA1}$  and drive the expression of downstream gene in lung cancer cells (Fukazawa et al., 2004). Another approach is to collaborate with other regulation mechanisms to elevate specificity. A tissue specific Epithelial Cell Adhesion Molecule (EpCAM) promoter (EGP-2) drove suicide gene expression under the regulation of let-7b miRNA selectively in EpCAM-overexpressing and let-7 down regulated retinoblastoma cell lines (Danda et al., 2013). Recently, Chuah et al. used a bioinformatics approach to identify evolutionary conserved *cis-acting regulatory modules (CRMs)* that were liver-specific and some of these *CRMs* could contribute to 10- to 100-fold increase in gene expression (Chuah et al., 2014). This computational approach may be applied to search for clusters of transcription factor binding site motifs corresponding to tissue-specific cancer.

The transcriptional activity of cancer-specific promoters is another important characteristic in determining their potential in clinical therapy. Limited activity could not elicit sufficient therapeutic effects or produce reporter expression over detection sensitivity. One of the direct strategies to amplify the transcriptional activity of cancer-specific promoters is to construct multiple copies of a homologous promoter or combine heterogeneous promoters together, achieving an additive or possibly synergistic effect.

The transcriptional activity of the multiple core-*tac*-promoters cluster was increased significantly via repeating the number of the core-*tac*-promoters (Li et al., 2012). However, not all multimerization of positive elements in promoters can result in transcriptional activity elevation. Multiple copies of *β-lactoglobulin* promoter unfortunately reduced the downstream chloramphenicol acetyl transferase reporter gene expression (James et al., 2000). Multimerization of proximal *sericin1* promoter also repressed gene expression at the transcription level (Ye et al., 2015). Another strategy is to employ the approach of two-step transcriptional activation (TSTA) to improve promoter strength. In the first step, the tissue-specific promoter such as prostate specific antigen promoter (<sup>P</sup>*PSA*) directed *GAL4-VP16* fusion gene expression. The expressed GAL4-VP16 fusion protein served as transcriptional factor to interact with GAL4 response elements in a minimal promoter, which drove the expression of an imaging reporter gene (e.g., *luciferase*, *mutant HSV1 thymidine kinase enzyme*) (Iyer et al., 2001). This approach could improve imaging signal by around 5-fold compared to the traditional one step method by detecting luciferase expression after transiently transfected LNCaP cells were infused into mice (Iyer et al., 2001). The GAL4/VP16 system was also used to augment the transcriptional activity of the carcinoembryonic antigen promoter (<sup>P</sup>*CEA*) by 20 to 100 fold in CEA-positive cells compared with only 6 to 8 fold in CEA-negative cells (Koch et al., 2001). Another two-step system uses one plasmid containing <sup>P</sup>*hTERT* upstream of a constitutively activated form of *heat shock transcription factor 1* (*cHSF1*) and is followed by the heat shock protein 70B promoter (<sup>P</sup>*HSE*)-driving the cytosine deaminase (CD) gene could increase the CD expression without losing cancer specificity *in vitro* and *in vivo* (Wang et al., 2003).

### **1.3. Reporter system**

Reporter genes have been widely investigated and used to study a series of biological processes, such as evaluating transfection efficiency or studying protein subcellular localization. In order to assess the transcriptional activity of promoter elements, the promoter DNA is inserted upstream of a reporter gene. The reporter gene encodes a protein with a unique feature allowing it to be easily identified among a mixture of endogenous proteins. For example, if the reporter protein is a specific enzyme then it can catalyze a specific biochemical reaction. The constructed chimeric gene will be delivered into cultured cells or animals via gene delivery methods. The expressed reporter protein will be quantified in extracted cell/tissue, culture supernatant or body fluids. Although the quantity of reporter protein is not directly associated with transcriptional activity of promoter elements according to the central dogma, the more active promoter elements are, the more reporter protein would be generated in general (Alam and Cook, 1990).

A successful reporter system should meet the following requirements (Kain and Ganguly, 2001): (1) The reporter protein is low-to-undetectable in the host or is very easily distinguished from endogenous proteins. (2) There is a reliable, sensitive, inexpensive assay available for the reporter protein to be detected rapidly. (3) A broad linear range is offered by the assay for the reporter protein to test the changes in promoter activity. (4) The physiology of the cells, tissues and the organism is not expected to change due to the expression of the reporter gene. Various reporter proteins that are widely used in monitoring biological processes will be introduced below.

1) Chloramphenicol acetyltransferase (CAT). CAT was the first reporter protein used for studying transcription regulation (Jiang et al., 2008). It is a prokaryotic enzyme that can catalyze the transfer of acetyl group from acetyl-coenzyme A (acetyl-CoA) to chloramphenicol. Because there are no endogenous proteins such as CAT with the same enzymatic activity in mammalian cells, it is readily distinguished from other endogenous proteins. The stability of CAT is very high with a half-life of 50 hours in mammalian cells (Thompson et al., 1991). The CAT proteins are first extracted from cells and mixed thoroughly with chloramphenicol and radioactive elements, followed by adding the substrate acetyl CoA to the mixture. After the reaction is finished, the CAT activity is represented by the amount of acetylated chloramphenicol, which is normally measured by either scanning the density of the dark spots on an X-ray film or by measuring the radioactivity in each spot on the thin-layer chromatographic sheets. There are other detection methods to analyze CAT without using radioactive elements. The CAT ELISA uses anti-CAT antibody to measure the CAT protein amount directly rather than the CAT activity. Another option is to use a CAT assay based on a fluorescent derivative of chloramphenicol; the assay possesses higher sensitivity and a broader detection range than radioactive substrate (Kain and Ganguly, 2001).

2) Secreted Alkaline Phosphatase (SEAP). The SEAP protein is a truncated form of human placental alkaline phosphatase (PLAP) through the deletion of C-terminal 24 amino acids – the glycoposphatidylinositol (GPI) domain (Berger et al., 1988). Unlike PLAP, SEAP is secreted from transfected cells into the cell supernatant, making detection of SEAP much easier without lysing cells. The half-life of SEAP is around 500 hours, in

culture medium while it is about 2 hours in serum in mice (Hiramatsu et al., 2006). Unlike endogenous alkaline phosphatase, SEAP is very heat-stable and able to resist to the phosphatase inhibitor L-homoarginine. Therefore, endogenous alkaline phosphatase could be easily removed by heating samples at 65 °C and by incubation with this inhibitor, without affecting the quantification of SEAP. *p*-Nitrophenyl phosphate is a kind of substrate used for SEAP colorimetric assay. This assay is a rapid, simple to use and cost-effective test but has limitations in sensitivity and detection range. A bioluminescent assay has a higher sensitivity (compared to the colorimetric assay for luciferase) via hydrolysis of D-luciferin-*O*-phosphate. SEAP could catalyze the dephosphorylation reaction to produce free luciferin, which acts as the substrate for firefly luciferase. The most sensitive substrate in current use for the SEAP assay is CSPD [3-(4-methoxyspiro[1,2-dioxetane-3,2'(5'-chloro)-tricyclo(3.3.1.1<sup>3,7</sup>)decane]-4-yl)phenyl phosphate], which is dephosphorylated by alkaline phosphatase (AP). Dioxetane anion from the dephosphorylation step is unstable and will decompose and emit light with its activity peak at 477nm. The light signal is quantified by a luminometer or a scintillation counter.

3) Fluorescent Protein. The green fluorescent protein (GFP) was first isolated from the jellyfish *Aequorea victoria*. The luminescent protein aequorin in the organism emits blue light after interaction with Ca<sup>2+</sup> ions (Tsien, 1998). Part of this luminescent energy is transferred to GFP, making it glow green. Under the excitation of UV or blue light (major peak  $\lambda=395$  nm, minor peak  $\lambda=475$ nm), bright green light is emitted by GFP with an emission peak at  $\lambda=509$ nm, which has similar fluorescence excitation and emission

spectra to those of fluorescein (Kain et al., 1995). Fluorescent proteins are advantageous over bioluminescent reporters in that their chromophore is intrinsic to the primary structure of the proteins, without the requirement of adding a substrate or cofactor (Kain et al., 1995). Another merit of fluorescent proteins is they allow real-time monitoring of transcriptional changes in cells and organisms. When potentials of the GFP on scientific research were realized, more efforts were made to create mutants of GFP to meet different needs. For example, a single point mutation (S65T) changed GFP to possess enhanced fluorescence and photostability and shift the excitation and emission spectra (Excitation  $\lambda=488$  nm, emission  $\lambda=509$ nm) to better suit FITC filter sets (Heim et al., 1995). Other color mutants were also created to make it possible to detect more than one fluorescent protein simultaneously. Additionally, some mutants were produced to overcome GFP shortcomings. Wild type GFP is very stable and their half-life can exceed 24h *in vivo* (Andersen et al., 1998). It is not desirable since the high protein expression remains even after the activity of the promoter directing the *gfp* has weakened (Leveau and Lindow, 2001). New variants were constructed to make it more susceptible to proteases and the half-life was highly reduced (Andersen et al., 1998).

4) Luciferases. Both fluorescence and chemiluminescence processes produce photons through energy transitions from unstable excited states to ground states, allowing light signal to be observed. The absorption of light is required as an external energy to excite chromophores of fluorescence proteins while chemiluminescence proteins obtain the energy from exothermic chemical reactions (Fan and Wood, 2007). Though chemiluminescent assays generate lower light intensities than fluorescent assays,

backgrounds of chemiluminescent assays are also much lower in that no external photons are introduced into the samples. This leads to higher sensitivity chemiluminescent assays (Fan and Wood, 2007). Table 1.3. summarizes several luciferase reporters that are commonly used in biological research. For the assays using D-luciferin as a substrate, the substrate is combined with ATP and forms a luciferyl-AMP intermediate, bound to a specific luciferase. The first intermediate becomes another bound intermediate, oxyluciferin, in the presence of O<sub>2</sub>. Oxyluciferin moves from a high-energy state to the ground state by emitting yellow-green light (Thorne et al., 2010). For the assays using coelenterazine as a substrate, the specific luciferase catalyzes the oxidation of coelenterazine to generate coelenteramide and emit blue light (Thorne et al., 2010). The Cypridina Luciferase (CLuc) can catalyze the oxidation of Cypridina luciferin to Cypridina oxyluciferin and emit blue light (Thorne et al., 2010). Firefly luciferase (FLuc) and Renilla luciferase (RLuc) are two widely used luminescent reporters in cell-based assays. They have a shorter half-life than fluorescent proteins like GFP, which makes them better at monitoring transcriptional induction (Thorne et al., 2010). The secreted luciferases such as Gaussia luciferase (GLuc) and Cypridina luciferase (CLuc) have longer half-lives than those non-secreted luciferases, but secreted luciferases are more convenient because they allow real time assays without requiring lysing cells (Thorne et al., 2010).

**Table 1.3. Luciferase reporters features (Thorne et al., 2010)**

Luciferase	Firefly (FLuc)	Modified Firefly (Ultra-Glo)	Click beetle (CBLuc)	Sea pansy (RLuc)	Copepod crustacean (GLuc)	Ostracod crustacean (CLuc)
Species	<i>Photinus pyralis</i>	<i>Photuris pennsylvanica</i>	<i>Pyrophorus plagiorthalamus</i>	<i>Renilla reniformas</i>	<i>Gaussia princeps</i>	<i>Cypridina noctiluca</i>
Emission wavelength	550-570nm	550-570nm	Green: 537nm Red: 613nm	480nm	460nm	465nm
Substrates	D-luciferin/ATP			Coelenterazine		Vargulin
Secreted	No				Yes	
Half-life	3hrs	N/A	7hrs	4.5hrs	6 days	53hrs

5)  $\beta$ -Galactosidase. The enzyme  $\beta$ -galactosidase ( $\beta$ -Gal) is encoded by the *lacZ* gene from *E.coli* and can catalyze the hydrolysis of  $\beta$ -galactosides into monosaccharides. There are different substrates of  $\beta$ -Gal used for different assay formats. The colorimetric assay is a simple and cost-effective method to quantify  $\beta$ -Gal activity. The reaction substrate used for this assay is O-nitrophenyl-beta-D-galactopyranoside (ONPG). After mixing cell extracts with this substrate, the optical densities can be measured via spectrophotometer (Smale, 2010). In the fluorimetric assay,  $\beta$ -4-methylumbelliferyl  $\beta$ -D-galactopyranoside (MUG) is a commonly used substrate. MUG penetrates cells, is hydrolyzed by  $\beta$ -Gal, resulting in the fluorescent compound 4-methylumbelliferone (4MU), which can be detected using a fluorimeter (Young et al., 1993). A more sensitive chemiluminescent assay was developed using a chemiluminescent substrate (3-(4-methoxyspiro[1,2-dioxetane-3,2'-tricyclo-[3.3.1.1<sup>3,7</sup>]decan]-4-yl)phenyl- $\beta$ -D-galactopyranoside) and is capable of detecting as little as 2 fg of  $\beta$ -Gal (Jain and Magrath, 1991).

#### **1.4. Lateral flow chromatographic immunoassays**

Lateral flow chromatographic immunoassays are portable devices used to detect the presence or absence of a target analyte in body fluid sample. As we gain more understanding of the biomarkers associated with some disease/phenomena, these tests gain use as medical diagnostics. In 1988, this technology found its first real commercial application in a home pregnancy test launched by Unipath (Thornton et al., 2012). Currently, tests are available for detecting various biomolecules to identify different conditions, including drugs of abuse, diabetes, cancer, and sexually transmitted diseases.

Figure 1.1 shows a schematic view of a traditional lateral flow assay. It is composed of several layers of materials overlapping each other. The sample is loaded onto the sample pad through the sample port at the proximal end of the strip. The sample pad pretreats the sample to guarantee it is compatible with the rest of the test (Wong and Tse, 2009). Then the treated sample flows to the conjugate pad. A particulate conjugate (generally a colloidal gold, colored, fluorescent or paramagnetic latex particle) has been immobilized in the conjugate pad in advance (Wild, 2013). The particulate becomes conjugated to a biological molecule (antigen or antibody). As the sample moves from the sample pad to the conjugate pad, the immobilized conjugate interacts with the sample and become a complex if the specific analyte is present in the sample. The reaction matrix is where the protein binding happens during the test and control regions. The reaction matrix is a porous membrane and commonly made of nitrocellulose, which is inexpensive, capable of high protein-binding, and easy to handle (Yetisen et al., 2013). The other specific biological components of the assay have been immobilized on the test line and

the control line on the reaction matrix, either antibody or antigen, capturing the conjugate and even conjugate-analyte while the fluid creates two lines. There are also membranes made of other materials such as nylon and polyvinylidene fluoride (Yetisen et al., 2013). The distal end of the assay is the absorbent pad is where excess fluid passing the control line is entrapped.

In the traditional human chorionic gonadotropin (hCG) dipstick, (mouse) monoclonal anti-hCG antibody, which is conjugated to colloidal gold is deposited on the conjugate pad. The test line is coated with an anti-hCG capture antibody while the control line is coated with (goat)-anti-(mouse) antibody. If the level of hCG in the sample is greater than the sensitivity of the assay, hCG in the sample will bind to gold-antibody conjugate in the conjugate pad and migrate to the reaction matrix where the hCG-conjugate complex will bind to capture antibody on the test line and develop a red band. Whether or not hCG is in the sample, the gold-antibody conjugate in the conjugate pad migrates to the control line region and binds to the (goat)-anti-(mouse) antibody coated on it, displaying a red band on the control line.

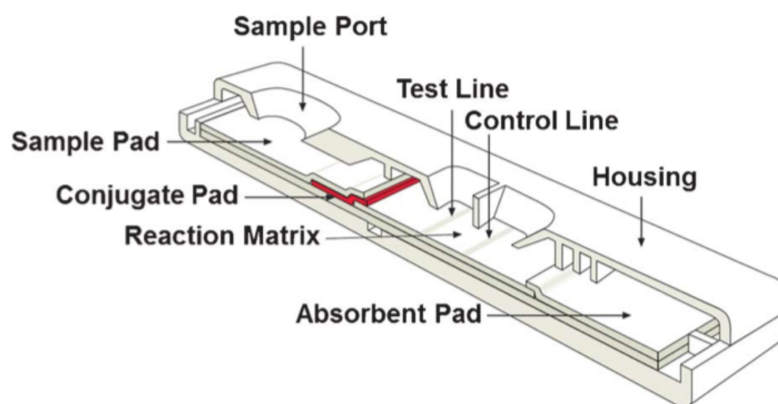


**Figure 1.1** Schematic view of lateral flow assay (Yetisen et al., 2013).

## 1.5. Goals of Dissertation

The objective of this study was to design and develop a non-invasive assay to diagnose cancer cells using the expression-targeted gene delivery technique. This strategy would manipulate cancer cells into expressing an exogenous reporter gene encoding a secreted protein, which could be detected in cell supernatant and in urine samples from organisms.

Chapter 2 describes the methods used to create a bladder orthotopic tumor model and investigates the effect of one of the pretreatment approaches (electrocautery) on gene delivery *in vivo*. The universally strong promoter ( $P_{cmv}$ )-directed gene delivery efficiency was determined via secreted luciferase expression in both tumor-bearing mice and normal mice, from both tumor models receiving electrocautery and without pretreatment with electrocautery.

Chapter 3 presents our expression-targeted gene delivery strategy and results based on two cancer-specific promoters ( $P_{cox2}$  and  $P_{opn}$ ) –directed *luciferase* gene delivery *in vitro* and *in vivo*. Kinetics profiles of promoters were studied in bladder carcinoma cells and a murine orthotopic bladder cancer model. We also investigated the correlation between tumor burden and luciferase intensities driven by different promoters.

Chapter 4 takes the treatment advantages of expression-targeted gene delivery strategy one step further using several human secreted proteins as reporters – beta-2-microglobulin( $\beta 2M$ ), human chorionic gonadotropin beta subunit ( $\beta hCG$ ), secreted

alkaline phosphatase (SEAP) and prostate specific antigen (PSA). Transcription of these delivered genes and secretion levels of their coding proteins were investigated in normal cells and transformed cells. SEAP and PSA were also utilized in cancer detection in the bladder cancer model.

Appendix A is based on a collaborative project with Dr. Grayson's group regarding the application of cyclic poly(ethylene imine) in gene delivery. Dr. Godbey designed cyclic poly(ethylene imine). Dr. Cortez and Molly Payne were responsible for synthesis of the polymers. My responsibility was to characterize the synthesized polymers and test their potential application in gene delivery.

Appendix B lists all plasmid maps that have been constructed in this work.

## **Chapter 2. Effect of Electrocautery on a Murine Orthotopic Bladder Tumor Model as it Relates to Gene Delivery**

### **2.1. Introduction**

In order to develop therapeutics or detection systems, appropriate model systems for bladder cancers must be considered. The new incidence of urinary bladder cancer in United States in 2015 is estimated at 74,000 and the mortality is approximately 16,000 (American Cancer Society). Bladder cancer incidence in men is about 4-fold above in women and it is more common in white men than black men (American Cancer Society). Typically bladder cancer is categorized as non-muscle-invasive bladder cancer (NMIBC) and muscle-invasive bladder cancer (MIBC). NMIBC accounts for about 75% of primary diagnoses with the features of high recurrent rate but low mortality rate. MIBC though takes up approximately 25% of primary diagnosis but is so fatal that about half of patients would die from it (Kamat et al., 2013). Figure 2.1 showed the T categories for bladder cancer. NMIBC includes low-grade Ta tumors, high-grade T1 tumors, and carcinoma *in situ* (CIS), all of which are confined within the muscle layer. CIS is a noninvasive flat tumor and the precursor could potentially develop into MIBC (T2 to T4) (Mertens et al., 2014).

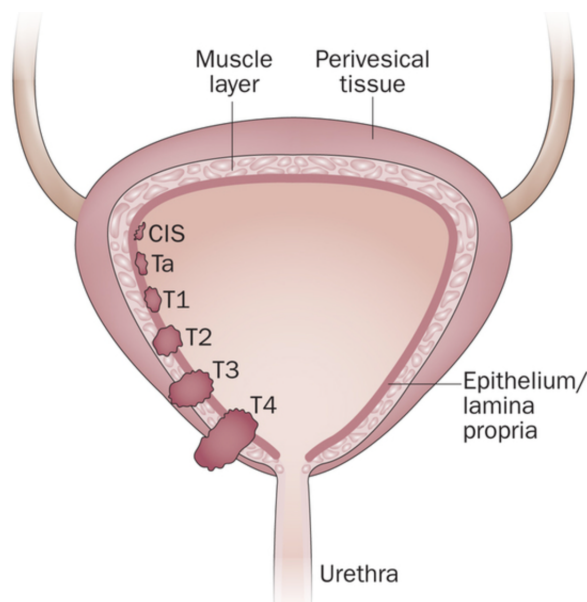


**Figure 2.1** Bladder cancer staging (Mertens et al., 2014).

In order to test diagnostic or therapeutic agents for bladder cancer, it is necessary to establish some bladder models. A good animal bladder tumor model should meet the following criteria: 1) tumors grow intravesically; 2) tumors originate from urothelial cell carcinoma and are not muscle-invasive; 3) the animal host is immunocompetent; 4) the model is easy to operate and reproduce (Chan et al., 2009a). According to the location where cells or graft material is delivered, animal models could be divided into orthotopic models and ectopic models. In the former tumor models, cancer cells or tumor sections are injected to the location where the original tumor grows. But in the ectopic tumor models, malignant cells or tumor sections are delivered to another location that is different from that of the original tumor. Subcutaneous injections are commonly seen in ectopic tumor models (Burnier and Burnier, 2013). However, orthotopic models are

preferable than ectopic models especially for studying tumor progression and anti-tumor therapy (Souba and Wilmore, 2001). Because the host microenvironment exerts critical influence in tumor development and metastasis, which could explain that specific tumors have their preference in metastasizing to specific sites. Different organs have their own unique microenvironment, providing different expression of cytokines and growth factors to affect tumor growth (Souba and Wilmore, 2001). Additionally, the site where cells are infused also has impact on tumor resistance to chemotherapeutic agents (Souba and Wilmore, 2001).

According to the tumor inducing methods, the orthotopic murine bladder tumor models could be categorized into three types: 1) induced by a chemical carcinogen such as N-methyl-N-nitrosurea (MNU), N-[4-5-nitro-2-furyl-2-thiazolyl]-formamide (FANFT) and N-butyl-N-(4-hydroxybutyl)nitrosamine; 2) human bladder cancer cells (e.g., KU7, T24 and UM-UC3 cells) are infused in nude mice in the xenograft model; 3) murine bladder cancer cells (e.g., MB49 and MBT-2 cells) are implanted in immunocompetent mice (Chan et al., 2009a). The carcinogen induction method is time-consuming (8-14 months) and not feasible for research (Chan et al., 2009a). The xenograft models neglect the immune response of the host to therapeutic agents (Chan et al., 2009a).

In this study, we used MB49 cells to establish the orthotopic bladder tumor model. This cell line was developed from C57BL/6 mice bearing 7,12-dimethylenanthracene-induced bladder cancer (Summerhayes and Franks, 1979). The bladder mucosa and the glycosaminoglycan (GAG) layer lining on the urothelium serve as a physiological barrier

against external insults (Chan et al., 2009b). In order to increase the success rate of tumor implantation, there are some methods proposed to disrupt the GAG layer for infused cells better attaching to the bladder surface, mainly including mechanical damage (electrocautery) and chemical denudation (e.g., polylysine (PLL) and silver nitrate) (Table 2.1). Electrocautery is one of the most popular methods used to disrupt the GAG layer, but few studies were performed on the effect of electrocautery on gene delivery in the orthotopic bladder tumor model. Here, *Gaussia luciferase* (*G.Luc*) as a reporter gene was used to compare the gene delivery efficiency between the bladder tumor model with electrocautery and that without electrocautery.

**Table 2.1** Common pretreatment methods to disrupt the integrity of bladder urothelium for establishing murine orthotopic bladder model.

Pretreatment	Cell populations	Dwell time	Tumor take rate	Reference
Electrocautery	I: $10^4$ II: $2 \times 10^4$ III: $5 \times 10^4$ MB49	3h	100%	(Gunther et al., 1999)
	$2 \times 10^4$ MB49	2h	100%	(Bohle et al., 2002)
	$5 \times 10^4$ MB49	2h	90%	(Jurczok et al., 2008)
	$10^5$ MB49	3h	90%	(Brocks et al., 2005)
	$10^5$ MB49	2h	77%	(Wu et al., 2003b)
0.1ml 0.01% poly-L-lysine	$10^5$ MB49-PSA	2h	100%	(Tham et al., 2011)
0.1mg/ml poly-L-lysine	$10^5$ MB49-PSA	2h	100%	(Seow et al., 2010)
8ul 1M silver nitrate	$5 \times 10^5$ MB49	2h	96.7%	(Chade et al., 2008)
5ul 0.2M silver nitrate	$5 \times 10^5$ MB49	1h	100%	(Luo et al., 2004)

## 2.2. Materials and Methods

### 2.2.1. Murine orthotopic tumor model

All experiments were performed with the approval of the Tulane University Institutional Animal Care and Use Committee. Female, 4- to 6-week-old C57Bl/6J mice (Jackson Laboratories, Bar Harbor, ME) were randomly assigned to treatment or control groups. To test the influence of electrocautery in exogenous gene expression, mice were divided into four groups: **A**: control – “unburned healthy mice” (electrocautery was not performed and no MB49 cells were instilled) **B**: the bladders of mice received electrocautery (two pulses or 2.5 W, ~0.5 seconds total) but no MB49 cells – “burned healthy mice” **C**:  $1 \times 10^5$  MB49 cells (100 ul of cells at a concentration of  $10^6$  cells/ml) were delivered into the bladders of mice not receiving electrocautery – “unburned tumor-bearing mice” **D**:  $1 \times 10^5$  MB49 cells (100 ul of cells at a concentration of  $10^6$  cells/ml)

were delivered into the bladders of mice having received electrocautery (two pulses or 2.5 W, ~0.5 seconds total) – “burned tumor-bearing mice”.

The procedure for the instillation of cells was carried out on all four groups using either MB49 cells or normal saline, as defined for each group. A total of 100  $\mu$ l was delivered via transurethral catheterization and allowed to incubate for 90 minutes. Details of the procedure can be seen in (Dobek and Godbey, 2011).

### 2.2.2. *In vivo transfections*

Mice were anesthetized via isoflurane and urine in each bladder was drained via transurethral catheterization. The 25kDa polycation poly(ethylenimine) (PEI) (Sigma-Aldrich, St. Louis, MO, USA) was diluted, titrated to pH = 7.0, and complexed with 3.6 $\mu$ g of plasmid DNA –pUC19 (New England Biolabs, Ipswich, MA, USA) or <sup>P</sup>*cmv-G.luc* (Thermo Scientific, Rockford, IL, USA), at a N:P ratio of 7.5:1 in a total volume of 100  $\mu$ l. The complexes were delivered into each bladder via transurethral catheterization. Transfection was performed for 2 hours, followed by catheter removal and animal revival.

Transfections were repeated every three days beginning on day 5 after tumor instillation, with a total of 3 transfections per mouse. At 24 hours and 48 hours after each transfection, each mouse was put in an individual cage. Urine samples were collected as the mice urinated naturally until either the required quantity of urine had been collected (20-100  $\mu$ l, depending upon the assay) or 3 hours had passed, whichever occurred first. Urine samples were then centrifuged at 1,000 x G for 10 minutes to remove larger debris,

such as red blood cells due to hematuria. G.LUC expression was measured using 20 ul urine samples, using *Gaussia* Luciferase assay kits (New England BioLabs).

14 days after tumor implantation, mice were sacrificed and bladders with tumor were collected and weighted.

### 2.2.3. *Histology*

Bladders with tumor from burned model and unburned model were collected and immersed in 4% paraformaldehyde at 4°C. The frozen tissues of non-burned tumors and the paraffin-embedded tissues of burned tumors were stained with H&E and examined at a light microscope.

### 2.2.4. *Statistics*

Luciferase activity data were log transformed to put them in the form of a normal distribution. Student's t-test was used to compare differences between group pairs.  $P < 0.05$  was used to define differences as significant.

## 2.3. Results

### 2.3.1. *In vivo transfections*

Figure 2.2 showed the effect of electrocautery on transfection in healthy mice. In unburned healthy mice, significantly elevated G.LUC levels were observed in  $P_{cmv-g.luc}$ -treated trials versus pUC19-treated trials at 24 hours and 48 hour after the first transfection, and at 24 hours after the second and third transfections. If electrocautery

was performed on normal urinary bladders prior to transfection, the <sup>P</sup>*cmv-g.luc*-treated group did not secrete significantly higher level of G.LUC than pUC19 treated group at any time points when urine samples were collected. Additionally, <sup>P</sup>*cmv-luc*-treated unburned healthy mice produced significantly higher levels of G.LUC than their burned counterparts at 24 hours after the first transfection.

It seemed that electrocautery can negatively affect transfection, which also held true in bladder orthotopic tumor model (*fig.2.3*). Whether or not electrocautery was performed prior to tumor implantation, urine samples collected at 24 hours after the third treatment from <sup>P</sup>*cmv-g.luc* treated tumor-bearing mice showed significantly elevated luciferase levels compared to pUC19-treated groups. However, at that time point, <sup>P</sup>*cmv-g.luc*-treated unburned tumor-bearing mice showed significantly higher levels of G.LUC in urine than their burned counterparts. The mean level of G.LUC that was secreted by the former group was about 4-fold of that secreted by the burned group.

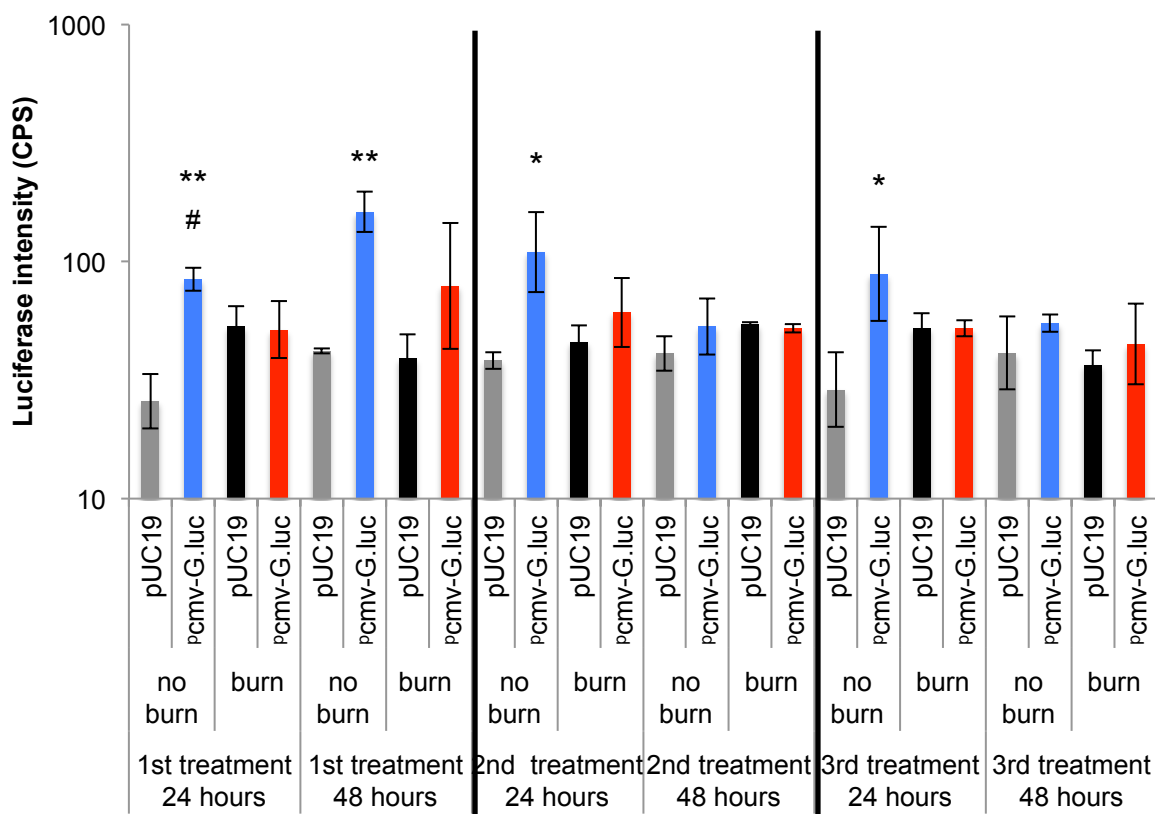


**Figure 2.2.** Reporter luminescence following transfection with the indicated plasmids on healthy mice, either receiving electrocautery or not, undergoing transfections every three days for a total of three treatments. 24- and 48-hours after each treatment, each mouse was assigned in an individual cage and stayed there about 2 hours. 2-hour urine was collected using a pipet. Data are presented on a log scale. “\*” and “\*\*” indicate significant differences between the indicated treatment group and negative control [t-test, n=3 (each group has three mice),  $p < 0.05$  (\*) or  $p < 0.01$  (\*\*)]. “#” indicate significant differences between *P<sub>cmv-luc</sub>* treated healthy mice receiving electrocautery and those without receiving electrocautery [t-test, n=3 (each group has three mice),  $p < 0.05$  (#)].

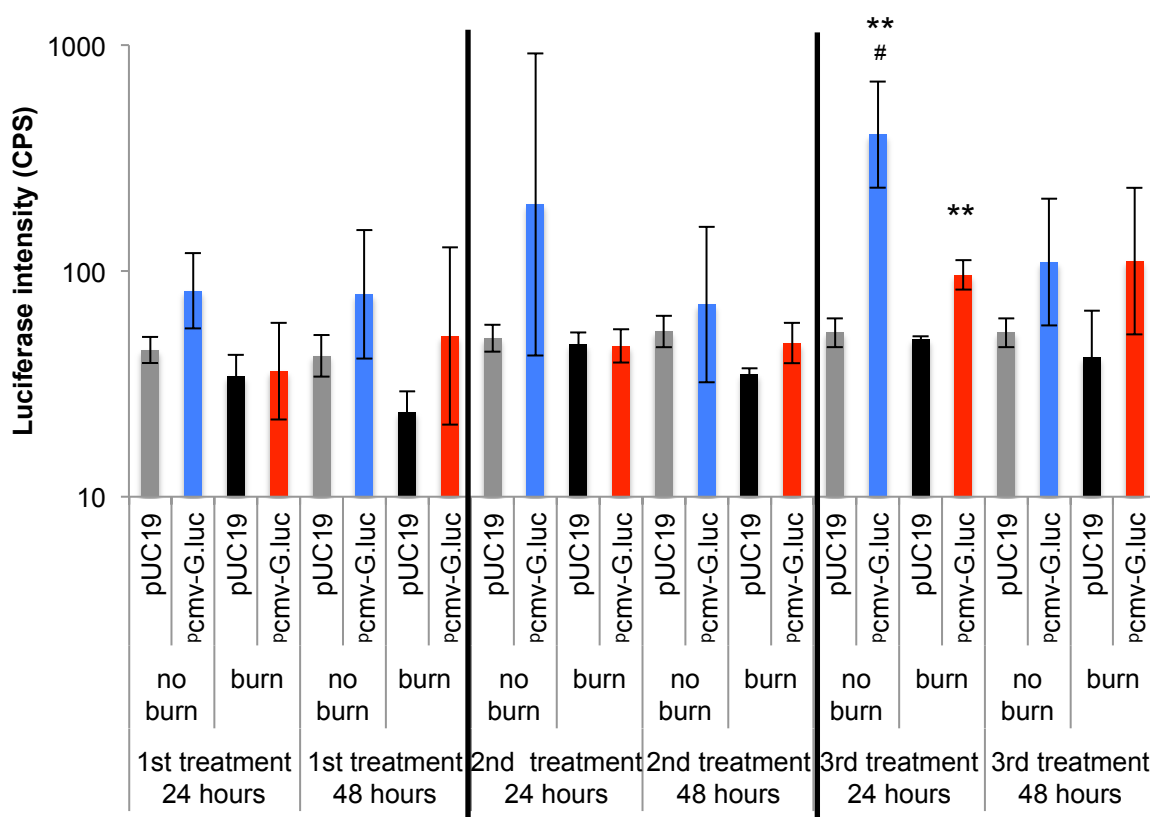


**Figure 2.3.** Reporter luminescence following transfection with the indicated plasmids on tumor-bearing mice, either receiving electrocautery or not, undergoing transfections every three days for a total of three treatments. 24- and 48-hours after each treatment, each mouse was assigned in an individual cage and stayed there up to 3 hours. Urine was collected during that period using a pipet. Data are presented on a log scale. “\*\*\*” indicates significant differences between the indicated treatment group and negative control [t-test, n=3 (each group had three mice),  $p < 0.01$  (\*\*)]. “#” indicates significant differences between  $P_{cmv-luc}$  treated tumor-bearing mice receiving electrocautery and those without receiving electrocautery [t-test, n=3 (each group had three mice),  $p < 0.05$  (#)].

### 2.3.2. Bladder weight

Figure 2.4 compared bladder weights of tumor-bearing mice between the burned group and the unburned group. Regardless of delivered plasmids (pUC19 or  $P_{cmv}$ -G.luc, unburned tumor-bearing mice did not show a significant difference in bladder weight versus burned tumor-bearing mice. However, in both pUC19 and  $P_{cmv}$ -G.luc treated tumor-bearing mice, unburned groups had tumors with a smaller variance compared to burned groups. Besides,  $P_{cmv}$ -G.luc-treated mice did not bear significantly different-sized tumors versus pUC19-treated mice whether or not electrocautery was administered.

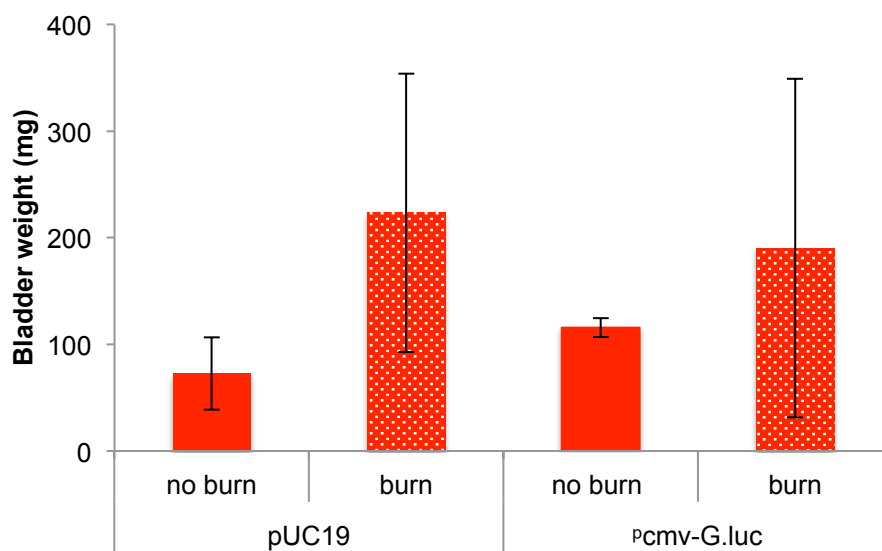


**Figure 2.4** Bladder weights of burned or unburned tumor-bearing mice. They were either transfected with negative control plasmid pUC19 or  $P_{cmv}$ -G.luc. [t-test, n=3 (each group had three mice)].

### 2.3.3. *H&E staining*

H&E staining was performed on sections from tumor-bearing bladders which received electrocautery or not prior to MB49 cells infusion. In the tumor tissue of a unburned bladder (*fig.2.5a*), the round to polygonal neoplastic cells were arranged palisading around blood vessels. Most neoplastic cells have distinctive cell border, small to moderate amount of eosinophilic, fibrillar cytoplasm, and high nuclei/cytoplasm ratio. The nuclei were round to oval and had fine chromatin with 1-2 nucleoli. The mitotic figures were 1-3/High power fields (HPF). There were mild to moderate anisocytosis and anisokaryosis. There were scattered foci of necrosis and hemorrhage. In the tumor tissue of a burned bladder (*fig.2.5b*), the neoplastic cells were more polygonal to spindle arranged in bundles. They had indistinctive cell border, moderate to large amount of eosinophilic, fibrillar cytoplasm, and variable nuclei/cytoplasm ratio. The nuclei are round to elongated and have coarsely stippled chromatin with 1 to more nucleoli. Occasionally there were multinucleate giant cells. The mitotic figures were 5-7/HPF. Severe anisocytosis and anisokaryosis were observed in these neoplastic cells. There were also scattered foci of necrosis and hemorrhage. In the burned group, there was a bladder in which neoplastic cells invaded into the muscle layer (*fig. 2.5c*). Additionally, edema was observed in one of burned tumor bladders (*fig.2.5d*). The neoplastic cells in burned bladders were more aggressive than those in unburned bladders based on higher mitosis, anisocytosis, anisokaryosis, multinucleate giant cells, and muscular invasion.

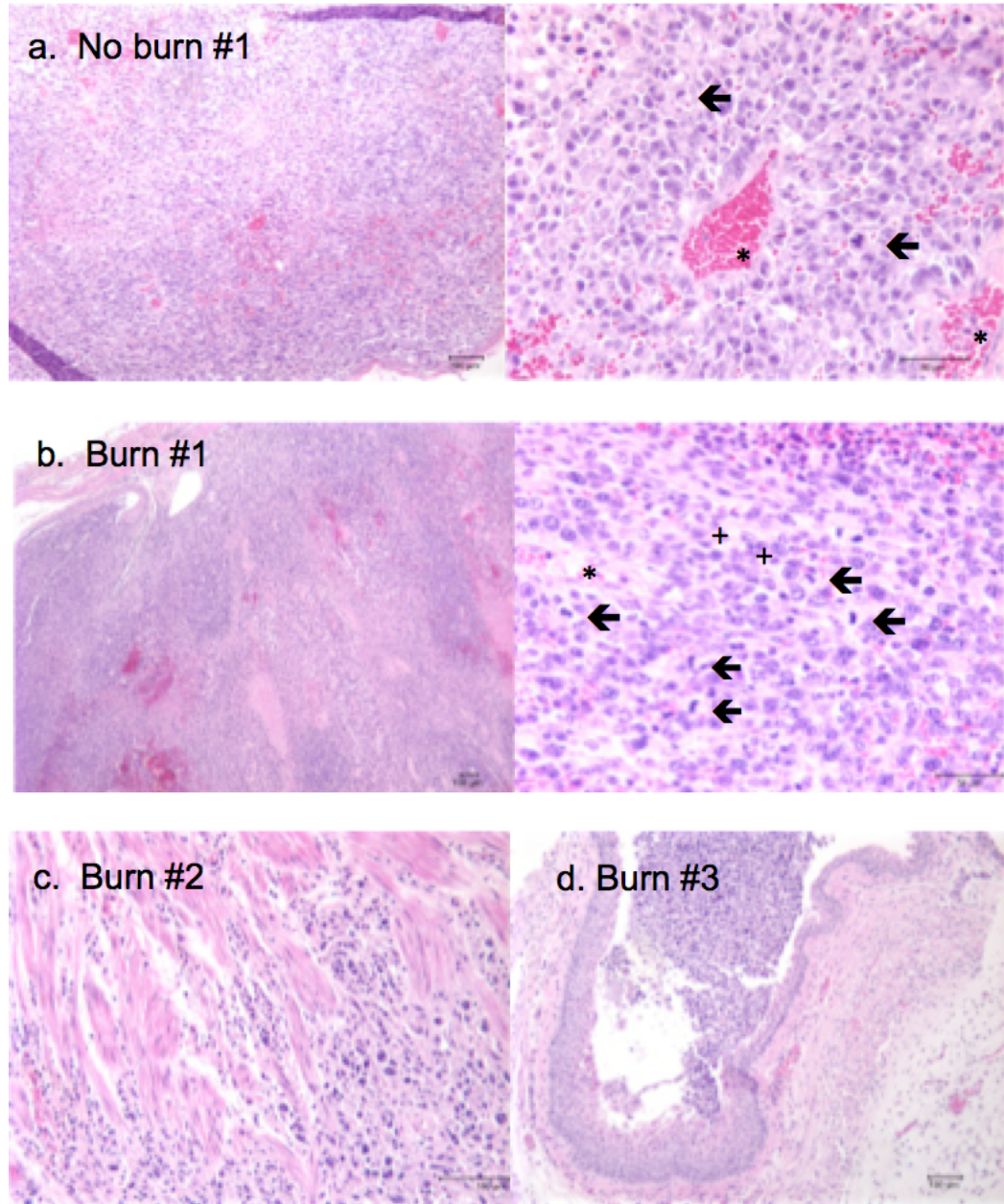


**Figure 2.5.** H&E staining on bladder tumor tissues from a) an unburned bladder, b) a burned bladder (#1), c) a burned bladder (#2) in which neoplastic cells invaded into the muscle layer and d) a burned bladder (#3) showing severely expanded bladder wall. “\*” indicates hemorrhage. “+” indicates neoplastic cells arranging in bundles. “◀” indicates a cell in the metaphase of cell cycle. Unburned #1 mouse was sacrificed at Day 12 post-tumor implantation. Burned #1 mouse was sacrificed at Day 15 post-tumor implantation. Burned #2 mouse was dead at Day 15 post-tumor implantation. Burned #3 mouse was dead at Day 9 post-tumor implantation.

## 2.4. Discussion

The orthotopic murine model utilized exposure of the bladders of mice to a suspension of MB49 cells. In similar models, pretreatment of the urothelial surface prior to exposure to tumor cells utilizes electrocautery (Lodillinsky et al., 2009, Wu et al., 2004, Wu et al., 2003b, Jurczok et al., 2008) or exposure to chemicals such as hydrochloric acid, (Lee et al., 2012, Chin et al., 1996) trypsin, (Kasman and Voelkel-Johnson, 2013, Chan et al., 2009b) or poly(L-lysine) (Chan et al., 2009b, Zaharoff et al., 2009). The purpose of these pretreatments is to remove part of the glycosaminoglycan(GAG) layer to allow for cellular attachment, therefore increasing the success rate of tumor implantation (Lee et al., 2012). However, few published studies have investigated the effects of the different pretreatment approaches on subsequent gene delivery. Here we attempted to instill  $10^5$  cells transurethrally into murine bladders without traumatizing the urothelial surface, with incubations to allow for tumor cell attachment lasting 1.5 hours. This group (n=6) had a 100% tumor-take rate, with an average bladder mass of  $(94.2 \pm 32.4 \text{mg})$ . In parallel, we infused  $10^5$  cancer cells into a separate group of mice having received two pulses of 2.5W electrocautery. This group (n=6) also had a 100% tumor-take rate, but the average bladder masses increased dramatically to  $(206.7 \pm 131.3 \text{mg})$ . With respect to tumor-take rates, it would seem unnecessary to perform the burn pretreatment.

Interestingly, electrocautery pretreatment decreased levels of G.LUC in both tumor-bearing and tumor-free mice (*fig.2.2* and *fig.2.3*). Possible factors that may have contributed to the observation are as follows: First, although a low wattage was used (2.5

W) for electrocautery, it was unavoidable that some urothelial cells beneath the GAG layer of the bladder luminal surface were also damaged during the procedure. Edema in the lamina propria and muscle layer have been observed in bladders which had been burned (Wu et al., 2003b). This was also observed in our laboratory in groups having received burns. It may have followed that levels of pro-inflammatory cytokines, such as tumor necrosis factor (TNF)-alpha in wound fluid (Yilmaz et al., 2011) or damaged tissues (Barada et al., 2015), were elevated due to early-stage wound healing. Published studies have demonstrated that TNF-alpha and other cytokines are able to inhibit the expression of transgenes driven by viral promoters such as the  $P_{cmv}$  used in the present experiments (Qin et al., 1997). A second possible factor for the lowering of G.Luc levels in bladders pre-treated with burn injuries is the infiltration of fibroblasts into the wound site, followed by collagen and proteoglycan synthesis (Schultz GS, August 2005). The newly synthesized sulfated proteoglycans are negative-charged, which may have posed a roadblock to transfection via cationic gene delivery complexes.

## 2.5. Conclusion

Exogenous gene expression was evaluated in both tumor-bearing mice and healthy mice, either operated with electrocautery or not. Secreted reporter levels were not significantly higher in healthy burned mice that were transfected with  $P_{cmv-G.luc}$  than those treated with pUC19. Instead, if electrocautery was not performed,  $P_{cmv-G.luc}$ -treated healthy mice could secrete significantly higher levels of reporters than pUC19-treated mice the next day after every transfection. Though  $P_{cmv-luc}$ -treated tumor-bearing mice, no matter whether electrocautery was performed, could secrete higher

concentrations of G.Luc than those transfected with pUC19 at 24 hours after the third transfection, *P<sub>cmv-luc</sub>*-treated tumor-bearing unburned mice can produce higher levels of G.LUC than their burned counterparts at that time point. Therefore, electrocauterization was considered to have a negative effect on exogenous reporter gene expression.

All of mice that received MB49 cells implantation both in burned group (6/6) and unburned group (6/6) got tumors. Though there was no significant difference between bladder weights from burned tumor-bearing group and those from unburned tumor-bearing group, the former group had bladder weights with larger standard deviation.

Compared to electrocauterized bladder tumor mode, the advantages of non-pretreated bladder tumor model include: 1) comparably high tumor take-rate; 2) transfection efficiency is not lost; 3) less muscle-invasive, which is more like clinical cases. Considering these advantages, we used non-pretreated bladder tumor model for the following studies.

## **Chapter 3. Non-invasive Detection of Bladder Cancer via Expression-targeted Gene Delivery**

### **3.1. Introduction**

In 2015, bladder cancer was the ninth most common cancer worldwide, with approximately 74,000 new cases diagnosed and an expected 16,000 deaths in the United States alone (American Cancer Society). Of the bladder cancers, over 90% were urothelial carcinomas. At the time of diagnosis, ~ 60% of bladder cancers are non-invasive papillary tumors, while ~ 20% have developed into muscle-invasive bladder cancers (Knowles and Hurst, 2015).

One of the most prevalent methods for diagnosing bladder cancer is via cystoscopy, in which a small camera is inserted into the bladder through the urethra to allow the physician to observe the luminal surface of the bladder. Because of the discomfort experienced by some patients, local anesthesia may be used in this minimally invasive procedure. Other imaging techniques, including intravenous pyelogram, computed tomography scan, magnetic resonance imaging, and ultrasound rely on expensive equipment or facilities that may not be readily available to all patients, such as in rural areas or underdeveloped countries.

There is a need for a simple and sensitive means of tumor detection, such as via the analysis of urine. Cytology is a common means of bladder cancer diagnosis, but the technique is limited to high-grade tumors (Lokeshwar and Soloway, 2001). A small number of commercial assays for urinary tumor markers has been developed, including tests for nuclear mitotic apparatus protein 22 (NMP22) and bladder tumor-associated antigen (BTA), but these assays are marred by low sensitivity and high cost per test (Cheung et al., 2013b). The discovery of additional biomarkers would be important for improving sensitivity or lowering the cost of this non-invasive approach to tumor detection. However, due to the strict requirements for clinically available biomarkers (such as high sensitivity and specificity), few biomarker assays receive FDA approval (Brooks, 2012). Current urinalysis methods for tumor detection do exist in the form of BTA and NMP assays, marketed as BTA stat<sup>TM</sup> and BTA TRAK<sup>TM</sup> (Polymedco Inc. Cortlandt Manor, NY, USA), and the NMP22<sup>®</sup> Bladder Cancer ELISA Test Kit and NMP22<sup>®</sup> BladderChek<sup>®</sup> point-of-care tests (Alere Scarborough, Inc. Waltham, MA) (Miyake et al., 2012).

Rather than look for novel biomarkers, the strategy employed in the work presented here utilized the delivery of genes encoding a secretable form of the luciferase reporter to cells lining the luminal surface of the urinary bladder. The transgenes used were under the control of promoters that are specifically active in cancer cells, leading to reporter expression that was limited to cancer cells in both *in vitro* and *in vivo* experiments. This technique is known as expression-targeted gene delivery. In the described experiments, two promoters were investigated for their specificity and utility in driving the expression

of genes encoding *Gaussia* luciferase in carcinoma cells. The promoters were derived from the cyclooxygenase-2 ( $P_{cox2}$ ) and osteopontin ( $P_{opn}$ ) genes. Reporter levels were detected in cell media *in vitro*, and in urine samples in murine experiments.

COX2 is an enzyme in the cyclic arm of the arachidonic acid cascade, which is responsible for prostaglandin and thromboxane production. This isoform, as opposed to cyclooxygenase type 1, is known for being inducible, especially as part of the inflammatory response. COX2 levels are low-to-undetectable in most normal tissues in the absence of cytokines, mitogens, and other pro-inflammatory factors (Godbey and Atala, 2003). However, *cox2* is overexpressed in many carcinomas, including gastric (Lim et al., 2000, Ristimaki et al., 1997), lung (Wolff et al., 1998), hepatocellular (Koga et al., 1999), prostate (Yoshimura et al., 2000), ovarian (Denkert et al., 2002) and colon (Yamamoto et al., 2001b) carcinomas. While *cox2* is not typically expressed in normal urinary bladder, Mohammed *et al.* found that roughly 86% of invasive transitional cell carcinomas of the urinary bladder were COX2-positive (Mohammed et al., 1999). COX2 expression is also associated with the stage of pathology in urologic tumors (Shariat et al., 2003, Margulis et al., 2007). Within the *cox2* gene, a series of positive regulatory elements in the promoter – such as the E-box and the nuclear factor IL 6 site (where stimulatory factors and CCAAT/enhancer-binding proteins bind) – contribute to the promoter activation (Kim and Fischer, 1998). Effective targeting of numerous types of *cox2*-overexpressing cancers has been achieved using  $P_{cox2}$ -driven plasmids (Godbey and Atala, 2003).

OPN is a phosphorylated glycoprotein that is produced by many cell types and tissues including epithelial cells on the luminal surfaces of the gastrointestinal, urinary, and reproductive tracts, the gall bladder, pancreas, lung bronchi, lactating breast, salivary glands, and sweat ducts (Brown et al., 1992), as well as by bone cells (Oldberg et al., 1986), and in activated macrophages, leukocytes, and T lymphocytes (Rodrigues et al., 2007). OPN acts through phosphorylation to activate various kinases which, in turn, activate many transcription factors. In terms of cancer, OPN helps with the activation of genes that are involved with the synthesis of matrix-degrading proteases, thus contributing to cancer cell motility and tumor metastasis (Rangaswami et al., 2006). OPN is overexpressed in cancers of the breast (Rudland et al., 2002), ovary (Tiniakos et al., 1998, Kim et al., 2002), colon (Agrawal et al., 2002), stomach (Higashiyama et al., 2007), lung (Hu et al., 2005), and pancreas (Koopmann et al., 2004). Previous work by our laboratory has shown that the  $P_{opn}$  can be used to yield targeted expression of the green fluorescent protein (Chen and Godbey, 2015). The present work extends the findings to a system involving secreted luciferase *in vivo*.

The following experiments used a luciferase gene from the copepod marine organism *Gaussia princeps* as a reporter. The humanized form of *Gaussia* luciferase (*G.luc*) is efficiently secreted by mammalian cells (Tannous et al., 2005), and is therefore of interest for both these initial murine investigations as well as possible future applications in higher mammals including humans. Gene delivery, with transcription of transgenes being controlled via  $P_{cox2}$  or  $P_{opn}$ , was used to successfully induce bladder cancer cells

to express *G.luc*. Detected signals from both cell supernatants and urine samples serve as a proof-of-concept for a possible urine-based regimen for cancer detection.

## 3.2. Materials and Methods

### 3.2.1. Plasmid Construction

The *G-luc* exon was originally amplified via traditional PCR upon the plasmid <sup>P</sup>*cmv-Gaussia luc* (Thermo Scientific, Rockford, IL, USA) using the following set of primers. Forward: 5'- TGATGTGAATTCGCCACCATGGGAGTCA-3' (inserted EcoRI is underlined); Reverse: 5'- AGGTTTGGTACCTTAGTCACCACCGGCC-3' (inserted KpnI is underlined). The amplicons thus obtained were used to replace the *psa* exons in the intermediate plasmids – <sup>P</sup>*cmv-psa*, <sup>P</sup>*cox2-psa* and <sup>P</sup>*opn-psa* – via the EcoRI and KpnI restriction sites to form <sup>P</sup>*cmv-G.luc*, <sup>P</sup>*cox2-G.luc* and <sup>P</sup>*opn-G.luc*, respectively. Construction of <sup>P</sup>*cmv-psa*, <sup>P</sup>*cox2-psa* and <sup>P</sup>*opn-psa* was described in detail in section 4.2.2.

### 3.2.2. In vitro transfections

The murine transitional cell carcinoma cell line MB49 and the murine fibroblast cell line MF (low passage cells, derived in-house via explant) were cultured in Dulbecco's modified Eagle's medium (DMEM) (Invitrogen, Carlsbad, CA, USA) supplemented with 10% fetal bovine serum (Gemini Bio-Products, West Sacramento, CA, USA), 100U/ml penicillin and 100U/ml streptomycin (Invitrogen), and collected in the late-log phase (confluence of ~70-80%). A total of 10<sup>5</sup> cells per well were seeded into 6-well plates

containing 2ml of growth medium per well, at 16 hours prior to transfection. The 25kDa (weight-average) polycation poly(ethylenimine) (PEI) (Sigma-Aldrich, St. Louis, MO, USA) was diluted, titrated to pH = 7.0, and complexed with 3.6 $\mu$ g of plasmid DNA (pUC19, <sup>P</sup>*cmv-GLuc*, <sup>P</sup>*mCox2-GLuc* and <sup>P</sup>*hOPN-GLuc*) at a N:P ratio of 7.5:1 and a total volume of 100  $\mu$ l per dose (Dobek et al., 2011). The non-coding vector pUC19 (New England Biolabs) was used as a negative control in transfection experiments. At the time of transfection, growth media were replaced with 2 ml FBS-free medium plus 100  $\mu$ l of gene delivery complexes. Transfections were allowed to proceed at 37°C for 2 hours, after which the transfection media were replaced with 1 ml of fresh growth medium (DMEM containing 10% FBS and 100 U/ml of Penicillin/Streptomycin). In the time course experiments, fresh growth medium was renewed every six hours.

### 3.2.3. *Murine orthotopic tumor model*

All experiments were performed with the approval of the Tulane University Institutional Animal Care and Use Committee. Female, 4- to 6-week-old C57Bl/6J mice (Jackson Laboratories, Bar Harbor, ME) were randomly assigned to treatment or control groups. Sample size was determined via power analysis (software G\*Power 3.1) based on preliminary results shown in fig.2.3 (log-transformed luciferase level in pUC19 group: 1.7266 $\pm$ 0.064; <sup>P</sup>*cmv-GLuc* group: 2.6041 $\pm$ 0.2353;  $\alpha$ =0.05, power = 0.8). Power analysis result indicated that at least three mice were required in each group. 1 $\times$ 10<sup>5</sup> MB49 cells (100  $\mu$ l of cells at a concentration of 10<sup>6</sup> cells/ml) were delivered into the bladders of mice via transurethral catheterization and allowed to incubate for 90 minutes. Details of the procedure can be seen in our previous study (Dobek and Godbey, 2011).

### 3.2.4. *In vivo transfections*

Mice were anesthetized via isoflurane and urine in each bladder was drained via transurethral catheterization. A 100ul suspension of plasmid ( $pUC19$ ,  $P_{cmv-luc}$ ,  $P_{cox2-luc}$  or  $P_{opn-G.luc}$ ) /PEI complexes was delivered into each bladder via transurethral catheterization. Transfection was allowed to proceed for 120 minutes, followed by catheter removal and animal revival.

In the experiments designed to investigate the specificity of cancer-associated promoters, transfections were repeated every three days on healthy mice, with a total of 3 transfections per mouse. Urine was collected at 24h and 48h after each transfection.

In the time-course experiments, designed to determine the expression patterns of the delivered genes following transfection, only one transfection was conducted on mice. The transfection took place on day 8 after tumor inoculation to allow for the establishment of a larger tumor mass. Urine was collected every 6 hours, starting at 12 hours and continuing through 72 hours post-transfection. Urine was obtained by placing each mouse in an individual cage without bedding for up to 3 hours. Urine samples were collected as the mice urinated until either the required quantity of urine had been collected (20-100  $\mu$ l, depending upon the assay) or 3 hours had passed, whichever occurred first. Urine samples were then centrifuged at 1,000 x G for 10 minutes to remove larger debris, such as red blood cells due to hematuria. G.LUC expression was measured using 20 ul urine samples, using *Gaussia* Luciferase assay kits (New England BioLabs).

### 3.2.5. *In vitro serum deprivation and shock*

MB49 Cells were trypsinized in the late-log phase (confluence of ~70-80%). On day 0, a total of  $1 \times 10^5$  cells per well were seeded into 6-well plates containing 2 ml of FBS-free DMEM per well. This was 48 hours prior to serum shock. On day 2, the FBS-free medium was replaced with DMEM containing 50% horse serum. Cells were allowed to incubate under serum shock for 2 hours, followed by replacement of the shock medium back to FBS-free DMEM. On day 3, a second serum shock was performed and cells were transfected as described above immediately after the 2-hour shock. Cells were incubated in the serum-free transfection medium for 2 hours. Following transfection, the medium was replaced every 6 hours. Detection of G.LUC was performed within one hour of each medium collection. As a negative control, cells that did not receive the serum shock received the same serum-free medium changes.

### 3.2.6. *Identification of signal inhibitors in urine*

Experiments were performed to explore the possibility of urine-borne factors inhibiting the detection of G.LUC, to explain the apparent circadian pattern of G.LUC detection *in vivo*. Urine was collected at 6:00 pm on day 7 after tumor instillation, and again at 6:00 am the next morning, to correspond with the end of the mouse night (6:00 pm, mice being nocturnal) and day. Urine from normal, untreated mice, collected at the same times, was used as controls. The weights of a urine sample and water with an equal volume were measured respectively and specific gravity of urine samples was the ratio of the weights of urine and water. For each test, 5 ul of G.LUC-positive (*in vitro*) cell

supernatant was mixed with 15 ul of one of the urine samples, with G.LUC being detected via *Gaussia* Luciferase assay kit (New England BioLabs).

### 3.2.7. *Statistics*

Luciferase activity data were log transformed to put them in the form of a normal distribution. Student's t-test was used to compare differences between group pairs.  $P < 0.05$  was used to define differences as significant.

## 3.3. **Results**

### 3.3.1. *In vitro transfections*

Cells were transfected with plasmids containing the *G.luc* exon, driven by either the  $P_{cmv}$  (a ubiquitously strong promoter, used as a positive control),  $P_{opn}$ , or  $P_{cox2}$ . The empty vector pUC19 was used as a negative control to verify that the act of transfection did not induce detectible luminescence, and sham-treated cells receiving normal saline as the transfection solution served as the baseline negative control. G.LUC intensity of all groups was normalized to cells of the same type receiving transfections with the positive control to address differences in transfectability between cell lines. The cell lines were normal murine fibroblasts ("MF") and MB49 cells from murine bladder carcinoma. While both cell types expressed ample reporter when transfected with the  $P_{cmv}$ -driven plasmids, the  $P_{cox2}$ - and  $P_{opn}$ -driven plasmids were only effective in the carcinoma cells tested. These observations are reflected in Figure 3.1, which shows the ratio of targeted gene expression to that of the positive control in each cell type 48 hours after transfection. The supernatants of MB49 cells transfected with  $P_{cox2}$ -*G.luc* contained

significantly more G. luciferase versus identically treated normal fibroblasts ( $p < 0.005$ ). Secreted G.LUC levels in the supernatants of MB49 cells transfected with  $P_{opn-G.luc}$  were also significantly higher versus identically treated normal fibroblasts ( $p < 0.05$ ). The degree of specificity was higher for the trials using the  $P_{cox2}$ .

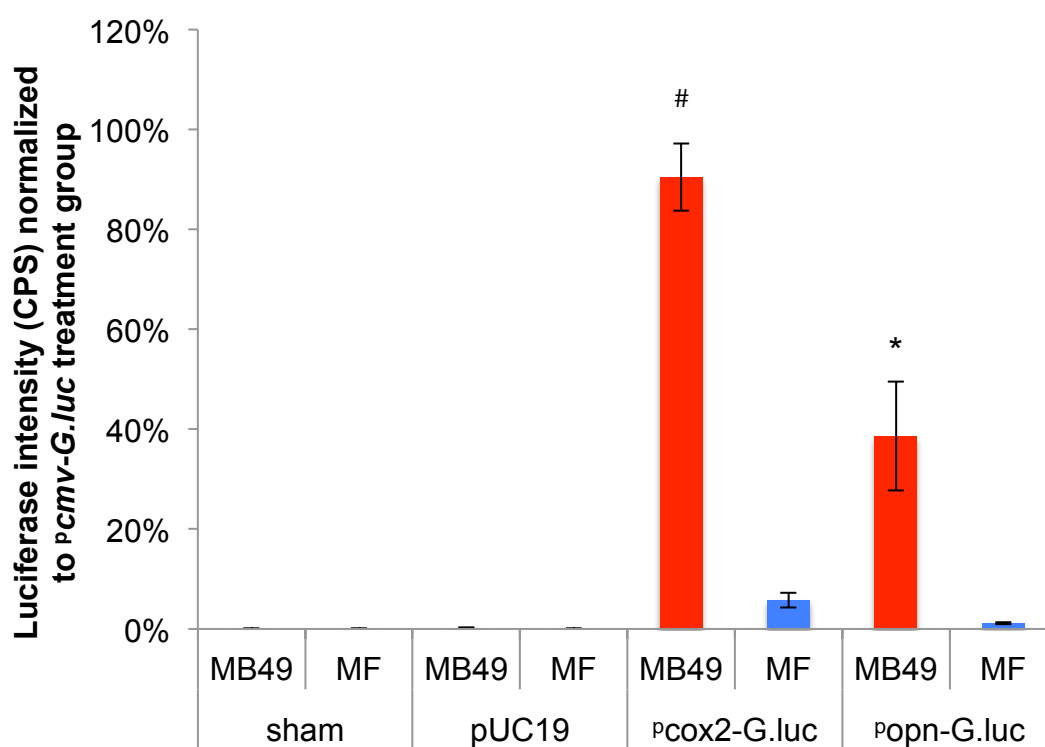


**Figure 3.1.** Secreted G. luciferase levels, measured as intensity (counts per second), of the supernatants of transfected of MF cells or MB49 cells. All values have been normalized to positive controls (cells transfected with  $P_{cmv-G.luc}$ ). “\*” and “#” indicate a significant differences between normal MF cells and MB49 carcinoma cells for transfections with the indicated plasmid (t-test,  $n=3$ , “\*”:  $p < 0.05$ , “#”:  $p < 0.005$ ).

Since the cancer-specific *cox2* and *opn* promoters were to be used to drive reporter expression as a cancer diagnostic, determining the kinetics of transgene expression for each plasmid was of necessary importance to determine the best time to perform future detection assays. It was found that the time of maximal gene expression differed between the strong  $P_{cmv}$  and the more specialized  $P_{cox2}$  and  $P_{opn}$  (fig. 3.2). In terms of the expression profiles, transfections of MB49 cells with plasmids utilizing the *cmv* promoter yielded strong reporter expression by 12 hours post-transfection, with a consistently strong expression lasting for at least 18 hours.  $P_{cox2}$  and  $P_{opn}$  yielded the strongest expression later, at 36 hours post-transfection. The time span of strongest expression (mean values > 80% of maximal values) for these two promoters was approximately 12 hours (spanning 30 to 42 hours post-transfection)

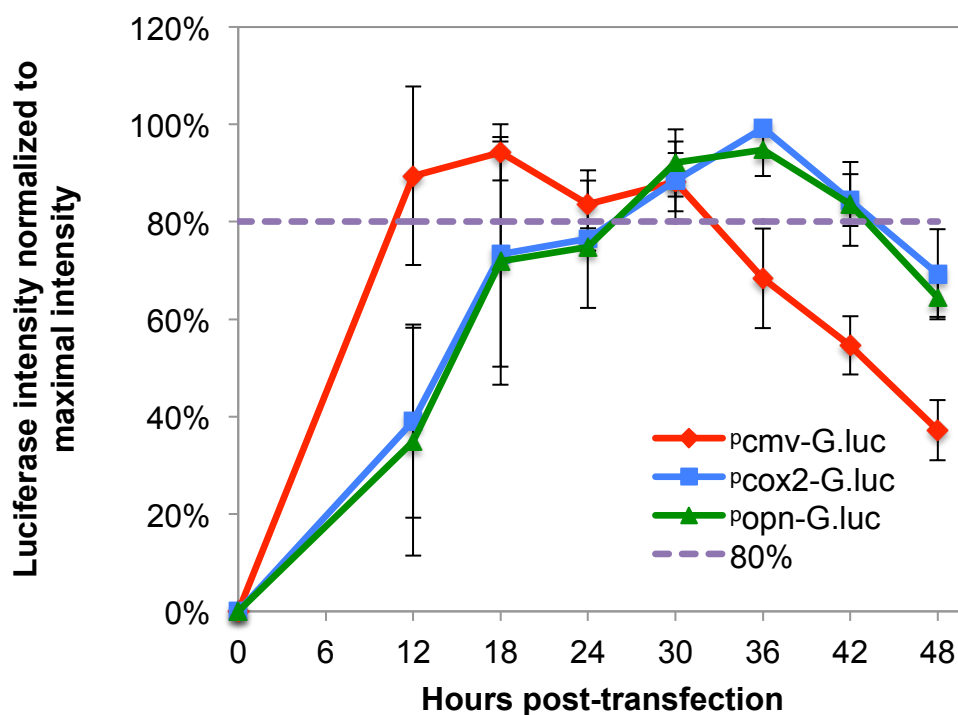


**Figure 3.2.** Luminescence intensities of supernatants of MB49 cells treated with  $P_{cmv}$ -G.luc (red line),  $P_{cox2}$ -G.luc (blue line), or  $P_{opn}$ -G.luc (green line). Cell media were changed at the indicated time points, then samples were collected one hour later.

### 3.3.2. *In vivo transfections*

The feasibility of using  $P_{cox2}$  and  $P_{opn}$  for detection of tumor cells in an orthotopic tumor model was first tested in normal bladders. As with the *in vitro* experiments, the strong  $P_{cmv}$  was used as the positive control. It was found that, in normal bladders, the two promoters being tested for cancer specificity yielded luminescence that was indistinguishable from background levels obtained from transfections with an empty vector (*fig. 3.3*). This experiment was designed to address the possibility of false-positive results.

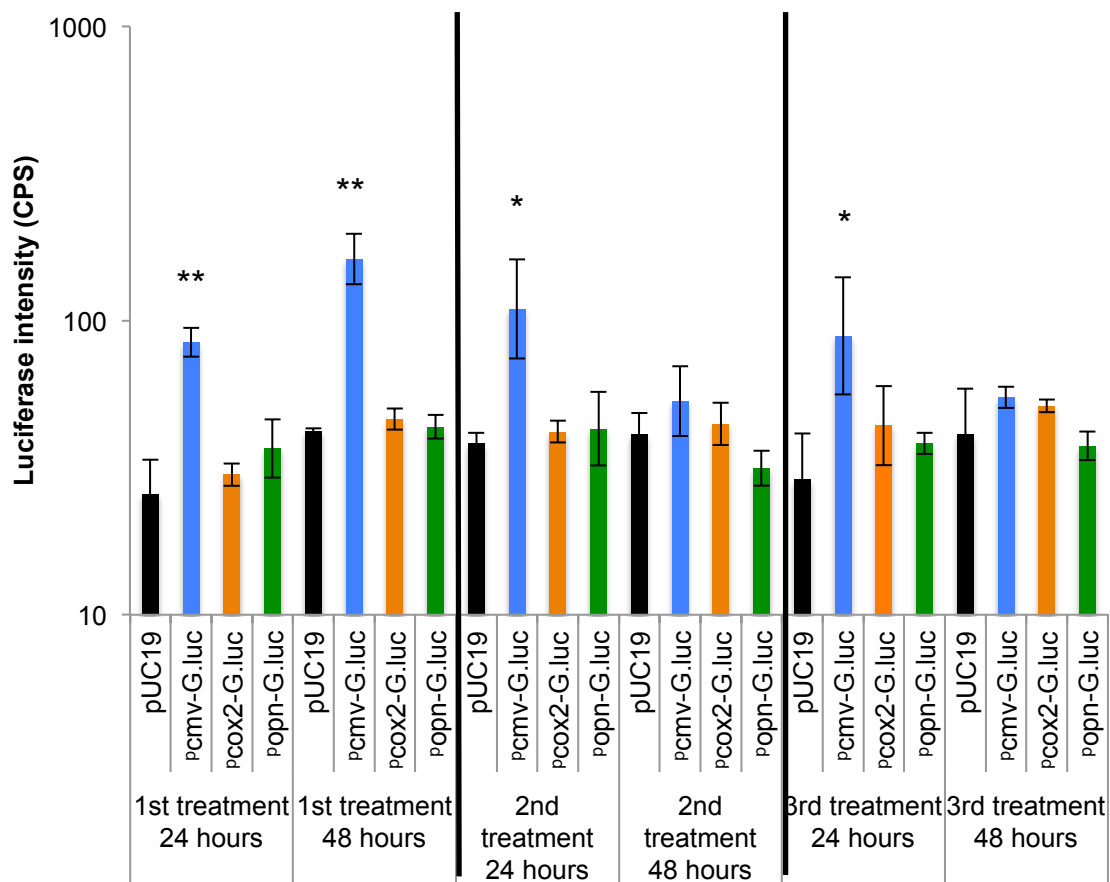


**Figure 3.3.** Reporter luminescence in urine following transfection with the indicated plasmids. Mice bearing no tumors underwent transfections every three days for a total of three treatments. 24- and 48-hours after each treatment, each mouse was assigned in an individual cage and stayed there about 2 hours. 2-hour urine was collected using a pipet. Data are presented on a log scale. “\*” and “\*\*” indicate significant differences between the indicated treatment group and negative control [ANOVA followed by post hoc test, n=3 (each group has three mice),  $p < 0.05$  (\*) or  $p < 0.01$  (\*\*)].

Moving on from the tumor-free control experiment, luminescence was next examined in mice bearing MB49 tumors using the same transfection technique that was used for tumor-free mice, with urine being collected every six-hours beginning 12 hours post-transfection. During the 18-72 hour time period following transfection, urine samples from <sup>P</sup>*cox2-G.luc*-treated mice bearing tumors contained significantly more G.LUC than those from pUC19-treated negative controls (*fig. 3.4a*). The same encouraging results were not obtained in <sup>P</sup>*opn-G.luc*-treated mice, as the generally higher secretion of G.LUC was not significantly different from mice treated by pUC19 (*fig3.4b*).

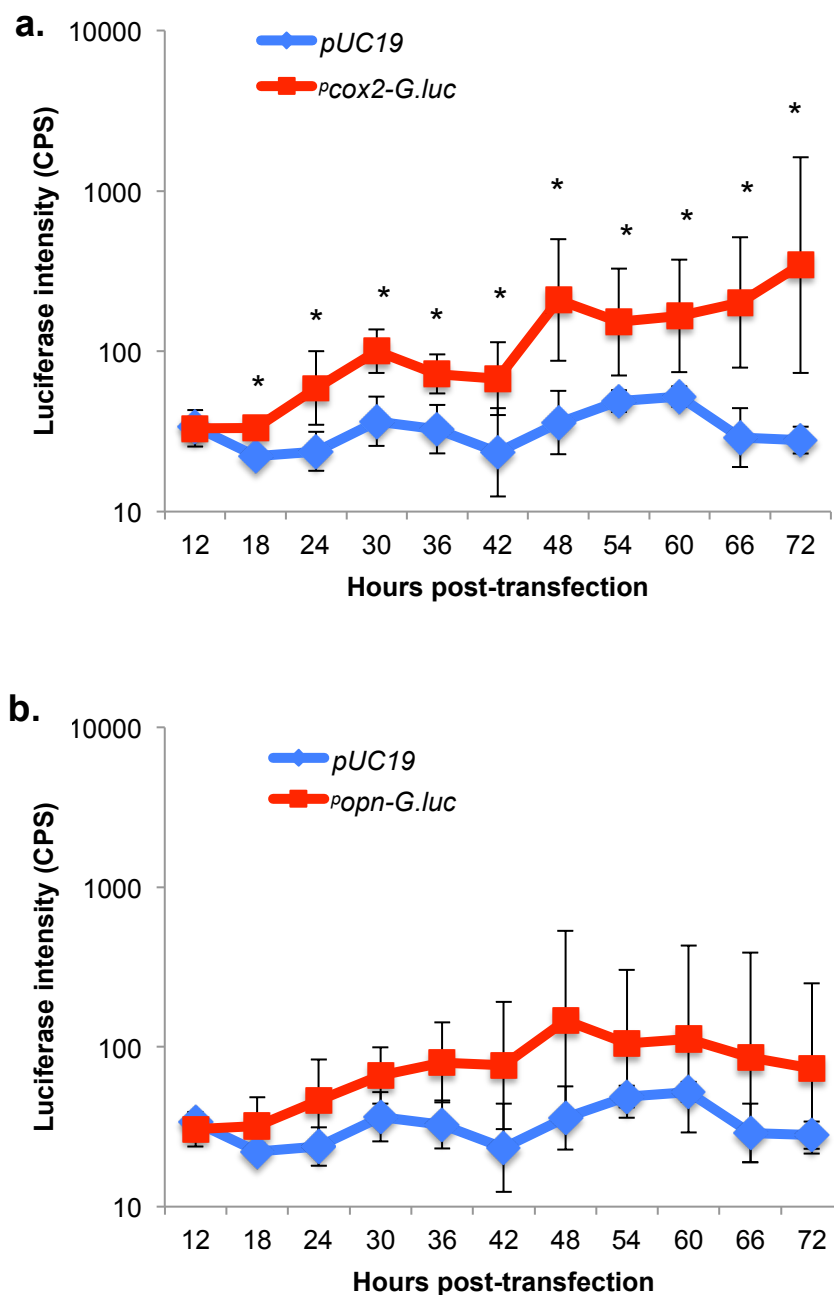
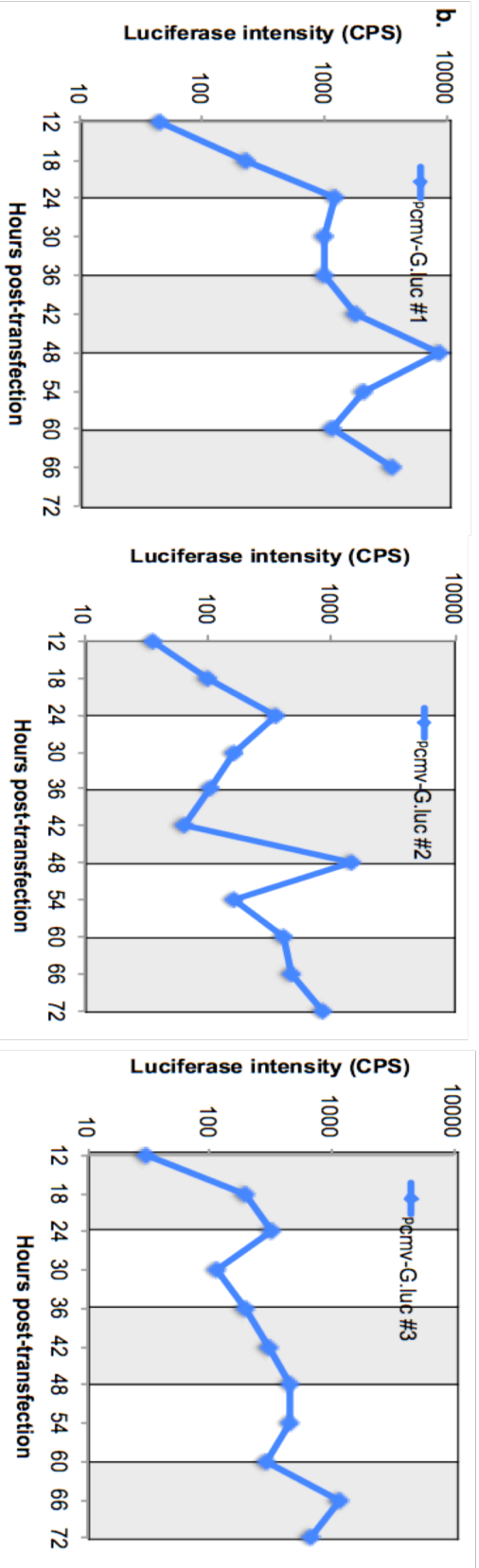
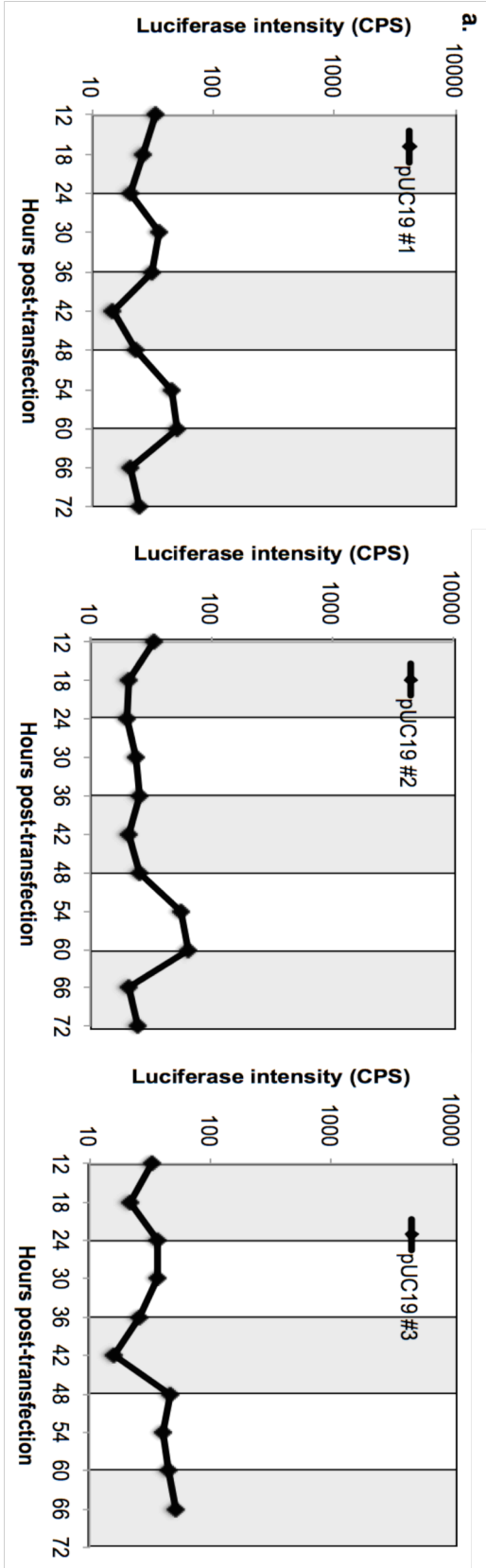


**Figure 3.4.** Reporter luminescence in urine following transfection with the indicated plasmids. Mice received only one transfection at Day 8 (Day 0 was the tumor implantation day). Since 12 hours post-transfection, each mouse was assigned in an individual cage every six hours and stayed there for about one hour. Urine was collected using a pipet. Luciferase levels detected in urine samples from tumor-bearing mice that were treated with the null vector pUC19 (blue line) (n=4) and *G.luc*-containing plasmids (red lines): **a)** Luciferase activities in the urine of mice

treated with  $P_{cox2-G.luc}$ . “\*\*” indicates a significant difference between the two groups at that time point (t-test, n=5, p<0.05). **b)** Luciferase activities in the urine of mice treated with  $P_{opn-luc}$ . Although the mean levels of G.LUC were higher versus negative controls, the differences in the means were not considered significant (t-test, n=5 [except for 72 hours, where n=4], p<0.05).

### 3.3.3. *Establishing the best time to collect urine for analysis*

Expression profiles for the different promoters were next established in the *in vivo* model. With the goal of being able to detect tumors with a single urine-based assay, the optimal time for reporter detection had to be established. The pUC19 negative controls showed a relatively constant background with the maximal value of 64 CPS. Looking at the  $P_{cmv}$ -driven positive controls, a periodicity of expression that was possibly circadian was noted (*fig. 3.5b*). Expression profiles revealed small local maxima at 24 hours and stronger peaks 48 hours post transfection, which occurred at 6:00 pm (one hour before the end of the murine inactive cycle, which we are defining as the murine “night” for these nocturnal animals. Vivarium lights were on from 7:00am to 7:00 pm.) A similar pattern of expression, especially with peaks at 48 hours post-transfection, was seen in mice treated with  $P_{cox2-g.luc}$  and  $P_{opn-g.luc}$  (*fig. 3.5c, d*).



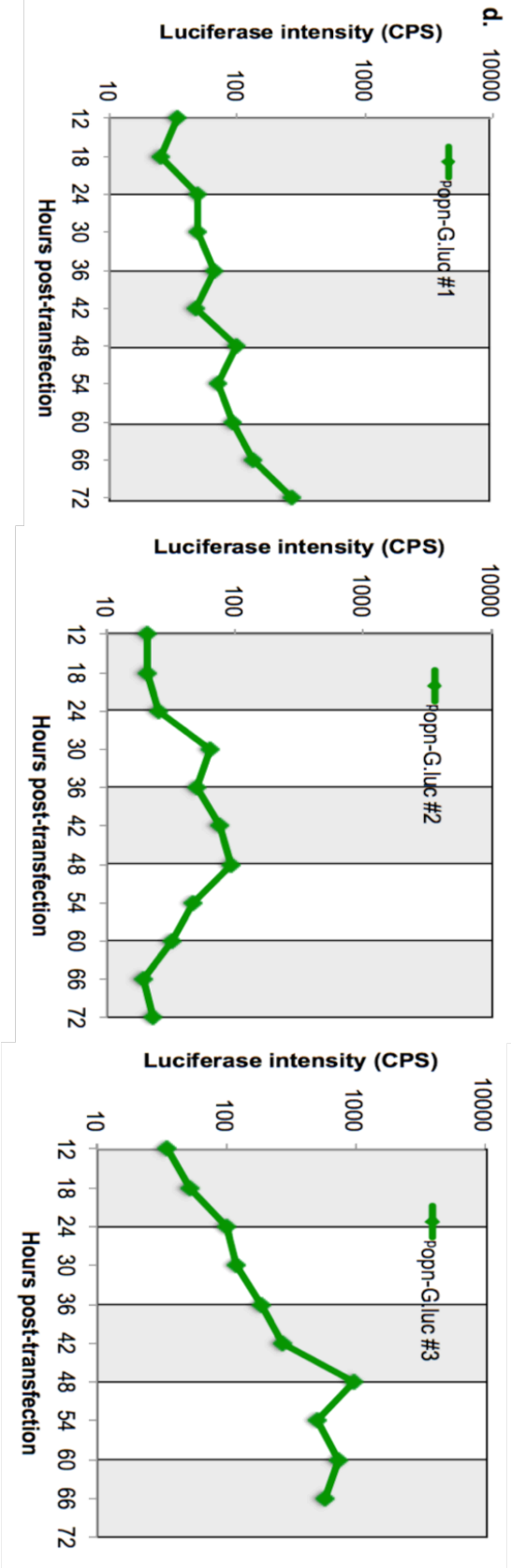
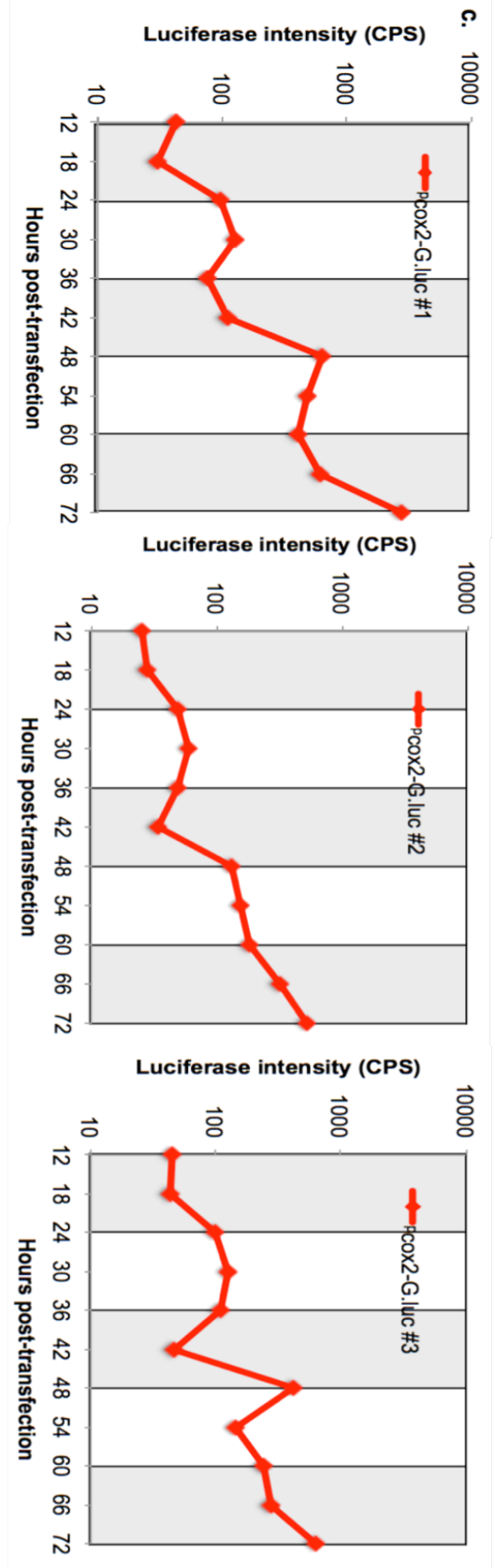


**Figure 3.5.** Profiles of G.LUC intensities in the urine of mice bearing bladder tumors and transfected once with a) pUC19; b)  $P_{cmv-luc}$ ; c)  $P_{cox2-luc}$ ; d)  $P_{opn-luc}$  on Day 8 (Day 0 was the tumor implantation day). Every six hours since 12-hour post-transfection, each mouse was assigned in an individual cage and stayed there for about one hour. Urine was collected using a pipet.

The periodicity seen in G.LUC detection was counterintuitive because implanted tumor cells were not expected to preferentially express transgenes based upon the time of the circadian day for the three non-circadian promoters used. Even if circadian transgene expression were present, one might not expect it to be greatest at the end of the sleep cycle, when urine production is slowed. (Anti-diuretic hormone (vasopressin), secreted by the pituitary gland, increases water permeability of the renal collecting ducts, thus allowing more water to be moved from the urine back into the blood via collecting duct cells (Nielsen et al., 1995). Levels of anti-diuretic hormone are normally elevated during sleep in mammals, thereby decreasing the amount of urine production as an animal sleeps (Trudel and Bourque, 2010).

To determine whether the observed periodicity was circadian, as opposed to occurring at a strict number of hours post-transfection, an additional experiment was run with the positive-control <sup>P</sup>*cmv-G.luc* plasmids, this time with transfections taking place at 6:00 am, an hour before the end of the murine “day” in tumor-bearing mice. While the location of the peaks of luciferase detection varied, it was noted that the peaks at 24- and 48-hours post transfection were shifted by 6-hours in one direction or the other. Representative profiles are shown in Figure 3.6. This indicated that periodicity in G.LUC detection was not due to a fixed amount of time following transfection, but rather some other factor that involved either the time of day or the activity levels (cellular or whole organism) of individual mice.

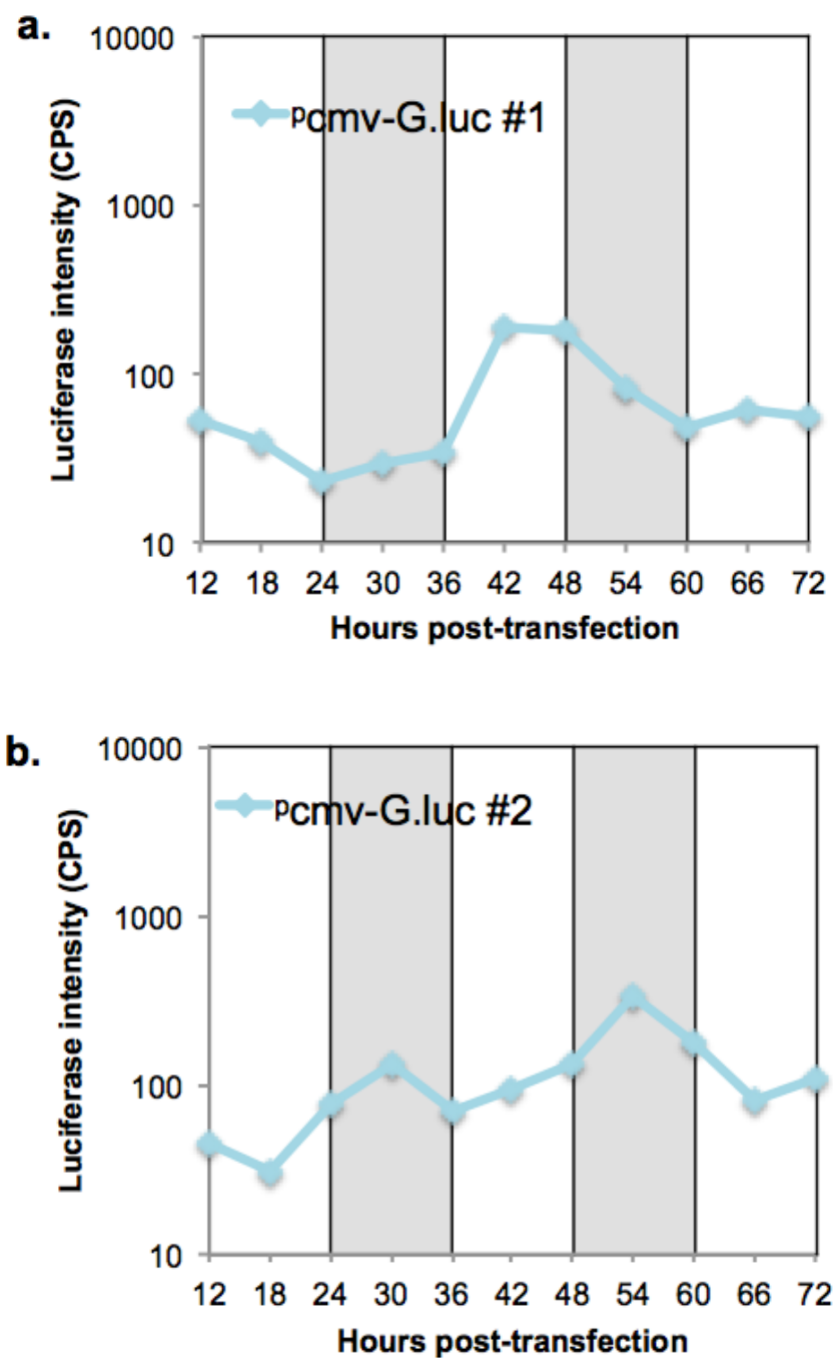


**Figure 3.6.** Representative profiles of G. luciferase intensities in the urine of tumor-bearing mice transfected with  $P^{cmv}$ -luc. All transfections were performed at 6:00 am, an hour before the end of the murine “day”.

#### 3.3.4. *In vitro time course secreted gaussia luciferase assay*

A trial of serum shock experiments was carried out in MB49 cells *in vitro* in an attempt to generate the periodicity seen in the *in vivo* experiments. The cells were grown in serum-free medium, and exposed to a series of four serum shocks (exposure to 50% horse serum in DMEM for two hours) every 24-hours (Balsalobre et al., 1998). The purpose of growing the cells in serum-free medium was to stall them in G<sub>0</sub>/G<sub>1</sub> of the cell cycle, with a synchronized release from the stall occurring during the serum pulse (Langan and Chou, 2011). The series of stall/shock was repeated twice before transfection, with an additional 2 serum pulses being administered after transfection to keep the cells synchronized. In all, the pulses commenced at [-26, -2, +22, and +46] hours, with the 0-hour being defined as when transfection was started. Cells grown in serum-free medium, without serum shocks, were used as controls.

#### 3.3.5. *In vitro serum deprivation and shock*

In the absence of serum shock, <sup>P</sup>*cmv-g.luc*-treated MB49 cells showed high G.LUC levels at 12 hours and 18 hours post-transfection and levels decreased after 42 hours post-transfection. G.LUC that was secreted from <sup>P</sup>*cox2-luc*-treated MB49 cells reached a plateau during 30 to 48 hours post-transfection and gradually went down after then. Secreted luciferase from <sup>P</sup>*opn-luc*-treated MB49 cells also showed high levels during 30 to 48 hours after transfection. Kinetics profiles of each promoter in MB49 cells cultured in DMEM without serum were similar as shown in fig.3.2. However, if MB49 cells received a serum shock at an interval of 24 hours, G.LUC levels were elevated right after

each serum shock and declined sharply 6 hours later. This phenomenon existed among all of three promoters (*fig 3.7. (b) (d) (f)*). Moreover,  $P_{cmv}$ -driven luciferase expression under stimulus showed a distinguishable peak at 24h post-transfection and a less apparent peak at 48 hours post-transfection. However, less than 20% of maximal luciferase intensity was observed at 48 hours post-transfection. For  $P_{cox2}$ -driven luciferase expression after serum shock, the expression peak at 24 hours post-transfection was dominating while the peak at 48 hours post-transfection was also demonstrable. The  $P_{opn}$ -driven luciferase expression displayed the strongest peak at 48 hours and local maxima at 24 hours was very strong, showing about 80% of maximal luciferase intensity. The difference of strongest peak locations of three promoters under a periodic stimulation can be explained by their original difference of working time. As a universally strong promoter,  $P_{cmv}$  showed its strength at an early stage after transfection. However, cancer-specific promoters like  $P_{cox2}$  and  $P_{opn}$  showed their strength later than  $P_{cmv}$ . Serum shock helped cells to get rid of G0 phase and provided them sufficient sources to transcribe and translate genes. Therefore,  $P_{cmv}$ -driven luciferase expression showed the strongest peak right after the first serum shock after transfection while  $P_{opn}$ -driven luciferase expression showed it after the second serum shock after transfection. Though we attempted to imitate the periodicity observed *in vivo* by stimulating cells with nutritional factors at an interval of 24 hours,  $P_{cmv}$  and  $P_{cox2}$  did show the strongest peak at the same time point as they did *in vivo*.

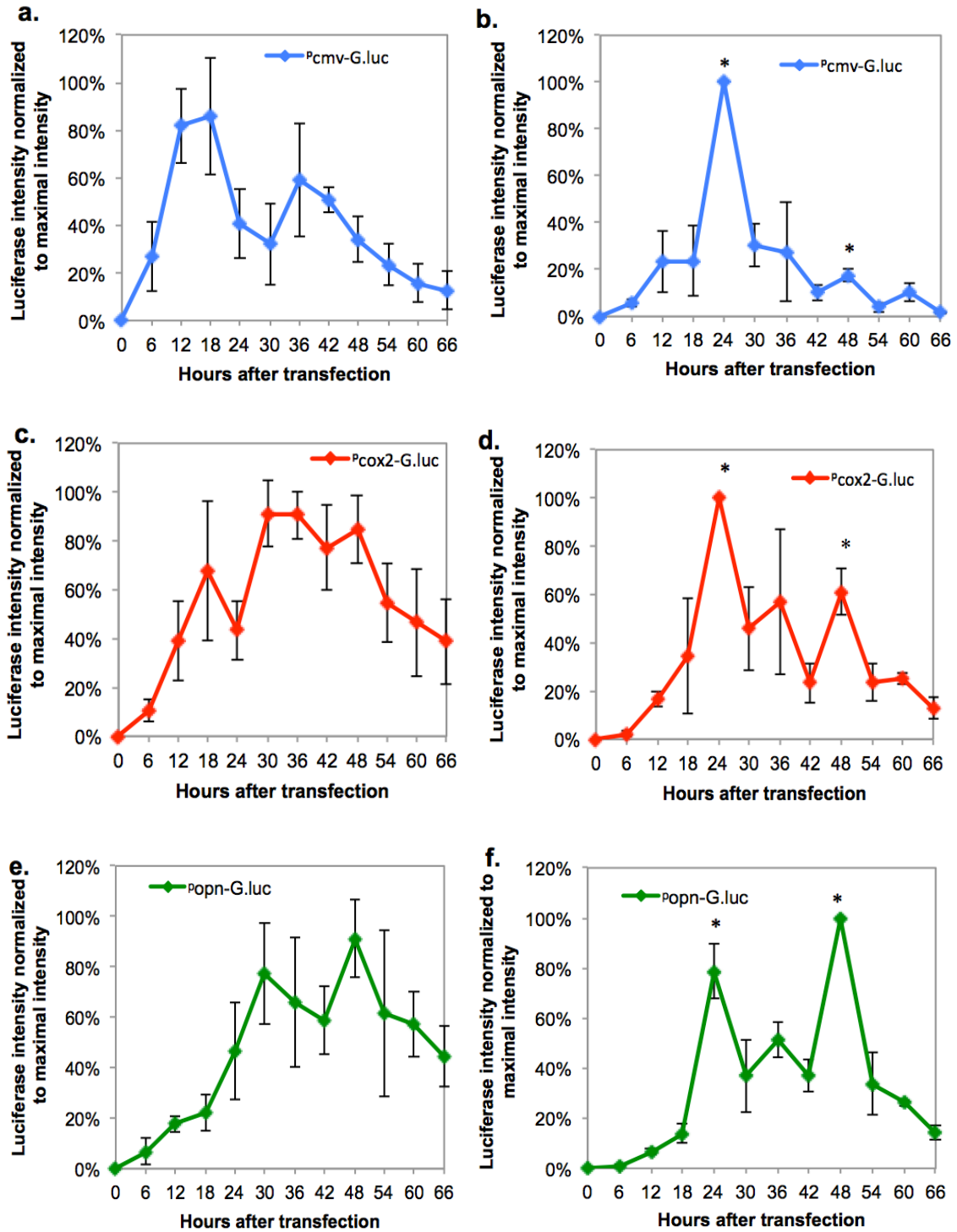


**Figure 3.7** Luciferase intensity normalized to maximal intensity tested during 66h after transfection on MB49 cells that were transfected with  $P_{cmv}$ -luc (a) (b),  $P_{cox2}$ -luc (c) (d) and  $P_{opn}$ -

*luc* (e) (f). The time point when transfection was started was defined as 0. MB49 cells received 50% horse serum shock at -26h, -2h, 22h and 46h (b) (d) (f) while their counterparts (the controls) received DMEM medium containing no serum at given time points above (a) (c) (e). \* indicated that the normalized luciferase intensity percentage at this time point was significantly higher than those at 6 hours before and 6 hours after this time point (t-test, n=3, p<0.05).

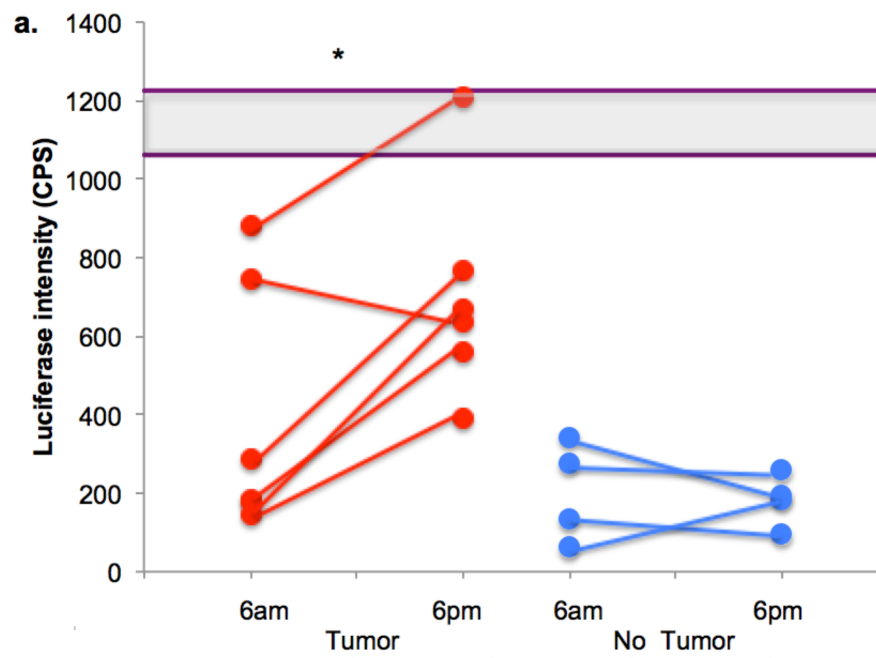
### 3.3.6. *Presence of a Masking Factor?*

One hypothesis to explain the periodicity observed in G.LUC detection was that some factor was being excreted from the body in a periodic nature, and this factor could be serving to mask the G.LUC signal. To test this hypothesis, MB49 cells were transfected in vitro with the positive-control vector  $P_{cmv-g.luc}$ . Supernatants were collected and mixed with urine that had been collected at either 6:00 am or 6:00 pm from untransfected, tumor-bearing mice. It was found that G.LUC luminosity was significantly higher in the samples diluted with the 6:00 pm urine (from the end of the mouse “night”) (paired t-test, n=6, p < 0.025) (*fig. 3.8a*). These results were consistent with the local maxima observed at 48 hours in figures 3.4 and 3.5.

The experiment was repeated using urine from untransfected, non-tumor-bearing mice. Without tumor cells present, there was little difference in G.LUC signal whether the cell supernatants were diluted with urine from the morning or night.

In addition, specific gravity did not show a significant difference between urine from morning and that from evening from both untransfected tumor-bearing mice and non-tumor-bearing mice (Table 3.1). Therefore, if diluted G.LUC signal was normalized to

specific gravity of urine sample that was used to dilute signal, the normalized luminosity was still significantly higher in the samples diluted with the 6:00 pm urine than those diluted with the 6:00 am urine in tumor-bearing mice (paired t-test,  $n=6$ ,  $p < 0.025$ ) (fig. 3.8b). Little difference in normalized luminosity was seen between the cell supernatants diluted with morning urine and those diluted with evening urine in non-tumor-bearing mice.



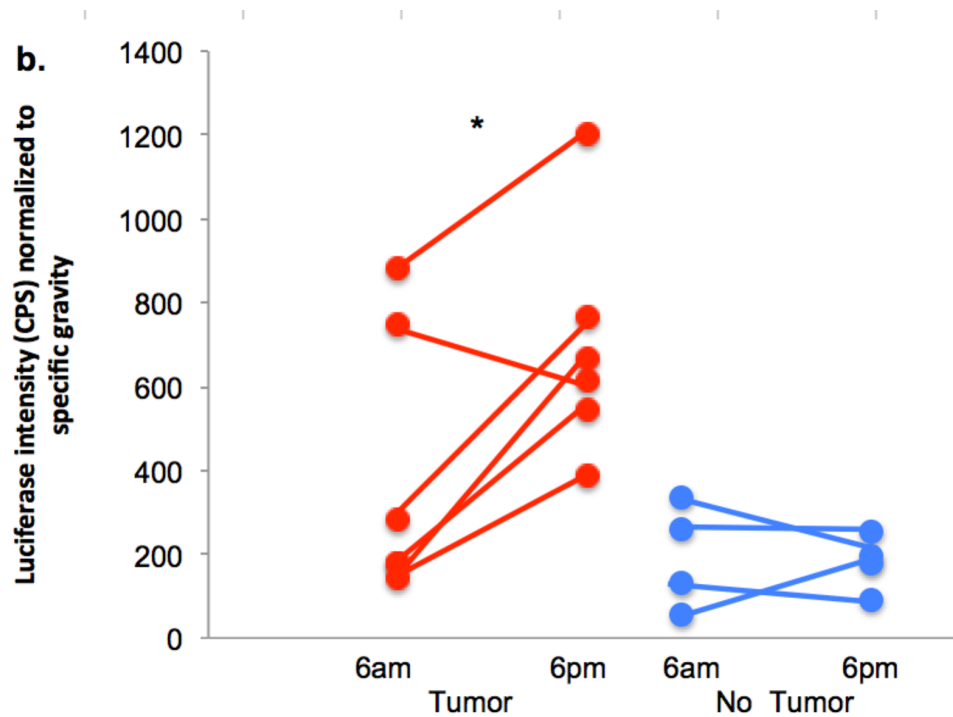


**Figure 3.8.** Luciferase intensities detected in luciferase-positive cell supernatants that had been diluted with urine collected from mice at either 6:00 am or 6:00 pm (a). Specific gravity-adjusted luminosities in luciferase-positive cell supernatants that had been diluted with urine collected from mice at either 6:00 am or 6:00 pm (b). Each supernatant was split into two vials, allowing for paired analysis. Paired data are indicated with lines. “\*” indicates a significant difference between the average luminosities of samples diluted with evening versus morning urine (paired t test,  $n = 6$  pairs,  $p < 0.025$ ). The shaded area indicates the luciferase intensity of G.LUC-positive supernatants that had been diluted with FBS-free DMEM medium.

**Table 3.1. Specific gravity of urine samples collected at 6am and 6pm from tumor-bearing mice and normal mice.**

Tumor-bearing mice	6am urine specific gravity	6pm urine specific gravity
1	1.002	1.003
2	1.002	1.028
3	1.001	1.001
4	1.054	1.034
5	1.004	1.004
6	1.002	1.003
Normal mice	6am urine specific gravity	6pm urine specific gravity
1	1.048	1.006
2	1.056	1.023
3	1.014	1.002
4	1.001	1.003

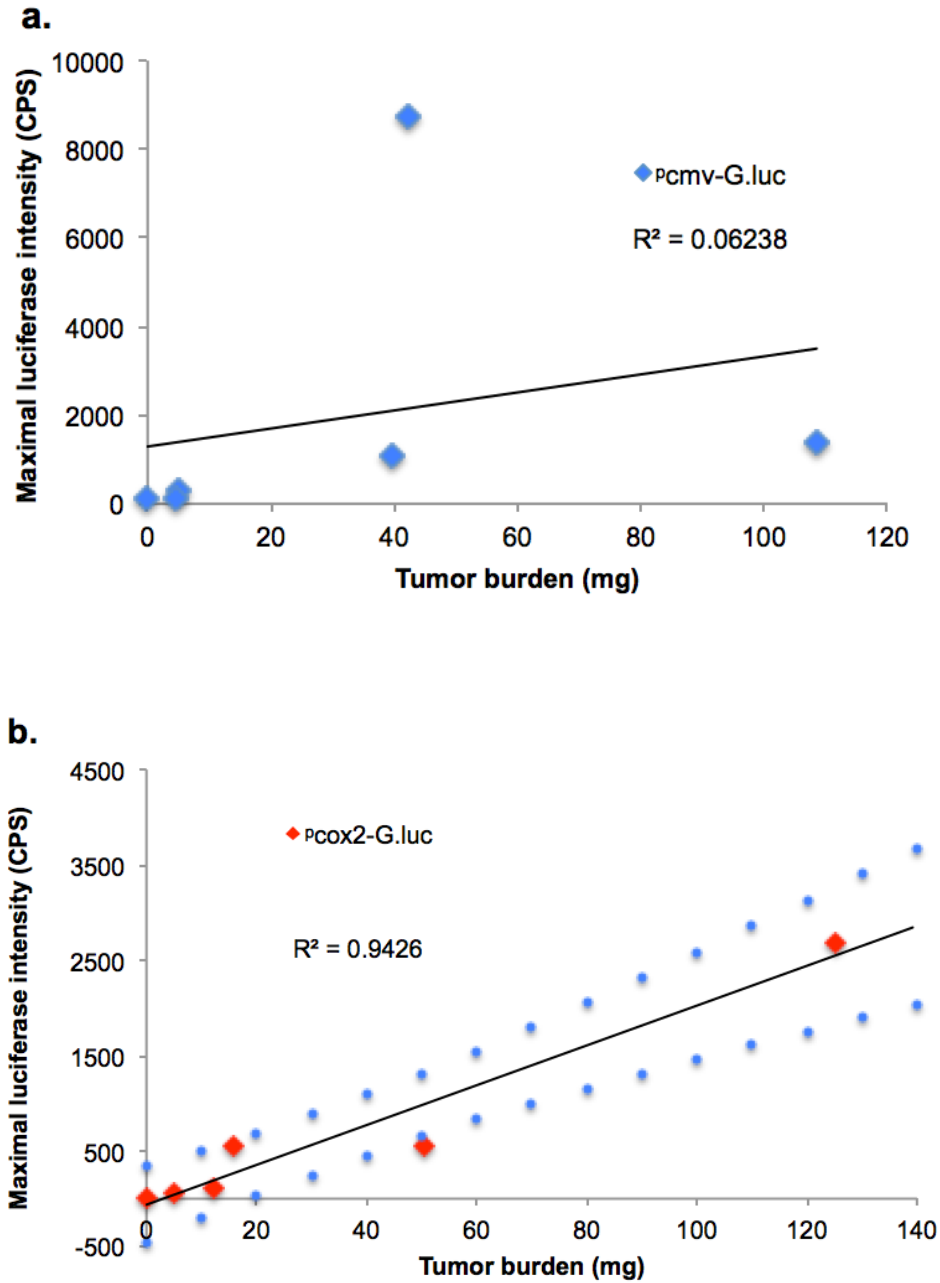
### 3.3.7. Correlation between *G.LUC* levels and tumor burden

Figure 3.9 attempted to establish the relationship between detected luciferase signals and tumor burden of mice that were treated by pUC19,  $P_{cmv-luc}$ ,  $P_{cox2-luc}$ , or  $P_{opn-luc}$ . Mice were sacrificed after urine collection was finished and the bladder of each mouse was extracted and weighed. The maximal luciferase intensity was the highest signal we obtained during the 72 hours urine collection for individual mouse. The bladder weight of mice at the point where the maximal luciferase intensity was obtained was extrapolated by the following equation (published for MB49 cells in the same C57 orthotopic model (Zhang and Godbey, 2011a)):

$$Tumor\ weight\ (mg) = 20.088 e^{0.1294 t}, \text{ where } t = \text{days post instillation.} \quad (3.1)$$

The maximal luciferase levels from urine samples of pUC19-treated mice was relatively constant at  $56 \pm 6$  CPS, regardless of bladder tumor weight.

The group treated with  $P_{cmv}\text{-}G.\text{Luc}$  failed to produce a reliable correlation between G.LUC levels and tumor burden. That may have resulted from the fact that both MB49 cells and normal urothelial cells could be transfected by  $P_{cmv}\text{-}G.\text{Luc}$ . However, a correlation between luciferase intensity and bladder weight ( $R^2=0.9426$ ) was seen in mice treated with  $P_{cox2}\text{-}G.\text{Luc}$ . The  $P_{opn}\text{-}G.\text{Luc}$ -treated group did not produce a reliable correlation, perhaps because of the weak expression of G.LUC (not shown).



**Figure 3.9.** The relationship between maximal luciferase intensity detected in urine samples and at that times the tumor burden of tumor-bearing mice that were transfected by (a)  $P^{cmv}$ -G.luc or (b)  $P^{cox2}$ -G.luc. Mice were sacrificed after urine collection was finished and the bladder of each mouse was extracted and weighed. The maximal luciferase intensity was the highest signal we obtained during the 72 hours urine collection for individual mouse. The bladder weight of mice at

the point where the maximal luciferase intensity was obtained was extrapolated by the equation (3.1) mentioned in the text. Tumor burden was obtained by subtracting an average normal bladder weight (19.6mg) from the total bladder weight. The black line was a trend line based on a linear model ( $y=20.883x - 62.973$ ). Blue dotted curves show the 95% confidence interval around the linear regression to the data. The intercept of the upper blue dotted curve is 335.885 CPS. From the equation of the trend line, the extrapolated value for the sensitivity of the  $P_{cox2-G.luc}$  based assay can be determined. The assay can detect bladder tumors, which are larger than 19.1 mg.

### 3.4. Discussion

The purpose of this work was to demonstrate that expression-targeted gene delivery could be used to selectively induce cancer cells to produce a secreted reporter molecule, with the long-term aim of development of a urine-based assay for cancer detection. It was shown that the two investigated promoters,  $P_{cox2}$  and  $P_{opn}$ , both demonstrated specificity for the bladder cancer cell line MB49 versus normal fibroblasts. Direct comparison of the two promoters revealed that  $P_{cox2}$  yielded a higher degree of specificity and intensity than did  $P_{opn}$  in *in vitro* transfections of cancer cells.

With the ultimate goal of producing a urine-based test for cancer detection, the optimal time for urinalysis had to be determined to eliminate the need for multiple detection assays following transfection. Interestingly, different promoters were expressed via different kinetics. The promoter  $P_{cmv}$ , a strong promoter used throughout gene delivery for its ability to ensure relatively large amounts of transcription for virtually all cell types at all stages of the cell cycle, yielded strong expression ( $\geq 80\%$  of

maximal expression) by 12 hours post-transfection, lasting for a period of at least 18 hours. The cancer-specific promoters did not yield their strong expression until 36 hours post-transfection, and the period lasted 12 hours. It is evident that observation times for each promoter used for expression-targeting must be fine-tuned when the expression level of the driven gene is important.

Similar trials performed *in vivo* yielded different results. While the cancer specificity of <sup>P</sup>*cox2* and <sup>P</sup>*opn* was again confirmed, and while the utility of the <sup>P</sup>*cox2* versus the <sup>P</sup>*opn* was again demonstrated, the expression patterns resulting from the use of all three promoters differed in the orthotopic model versus what was observed *in vitro*. For example, <sup>P</sup>*cmv-G.luc*-treatments yielded strong G.LUC expression at 12 hours post-transfection *in vitro*, but the same trials failed to produce significant expression at 12 hours *in vivo*. It is no surprise that transgene expression characteristics *in vitro* differ from their *in vivo* counterparts.

Non-tumor-bearing mice receiving three deliveries of <sup>P</sup>*cmv*-driven reporter genes yielded an interesting result: at the 48-hour time point following the first transfection, there was a significant elevation of G.Luc expression versus controls, but the 48-hour elevation was not present following the second and third transfections. That may result from the secretion of some cytokines due to immune response in immune-competent mice, which was triggered by the expression of non-murine protein (G.Luc). Cytokines such as interferon-gamma and tumor necrosis factor-alpha could attenuate viral promoters/enhancers including <sup>P</sup>*cmv* (Qin et al., 1997). The result had no bearing on the

data presented in the subsequent figures of this report, as single transfections were used for the remaining studies. However, the observation may provide an interesting aside for those working with viral promoters *in vivo*.

One of the most striking results of gene delivery to tumor-bearing mice was an apparent periodicity in gene expression. While a minor local maximum in expression was observed 24-hours after transfection, all three promoters also generated a more striking expression spike at 48 hours post-transfection. Altering the time of transfection by 12 hours produced a shift in the local maxima by 6 hours (in either direction), indicating that both the time of transfection and some other rhythmic physiological factor were at play in the murine model. We hypothesize that one or more circadian-related factors was involved with masking the detection of G.LUC during the assay procedure. Results from an experiment that mixed aliquots of G.LUC-positive cell medium with urine collected at a morning versus nighttime hour revealed a significant amount of G.LUC signal masking resulting from exposure to urine collected at 6:00 am. However, the masking was also observed with urine collected at 6:00 pm in non-tumor-bearing mice. Of the four urine classes collected, it was the urine collected at 6:00 pm in tumor-bearing mice showed a greatly reduced masking effect, demonstrating that the tumors themselves are responsible, at least in part, for the magnitude of the masking effect observed. Perhaps they secrete a factor that interacts with the masking agent secreted by healthy cells.

Relevant studies have shown that circadian rhythms in tumors affect growth, DNA synthesis, and mitosis (Wood et al., 2006). For instance, the cosine simulation plot from Wood *et al.* showed that thymidylate synthase activity was higher in mice sacrificed at the time of light versus those sacrificed at the time of lights-off (Wood et al., 2006). Furthermore, mice sacrificed 2 hours before lights-on contained the largest-sized tumors (Wood et al., 2006). Numerous proteins, including thymidylate synthase and vascular endothelial growth factor, affect tumor growth in a circadian manner. Such proteins, along with other tumor-produced products, could account for the differences observed in G.LUC detection when samples were exposed to different urines. To explain the spikes in G.LUC detection seen at 48-hours post-transfection, we propose that G.LUC was not necessarily being expressed more at 48 hours, but it was being masked less.

Mammalian circadian rhythms are controlled by a series of endogenous biological oscillators which participate in positive and negative transcriptional-translational feedback loops of clock genes. The core oscillatory machinery has been shown to be present in the urinary bladder through the expression of the circadian clock genes *clock*, *bmal1*, *cry1*, *per1*, and *per2* (Negoro et al., 2012). Moreover, Changhao *et al.* demonstrated interactions between receptors and peripheral clock existed in the urinary bladder (Wu et al., 2014). In our case, it is possible that infused MB49 cells synchronized to the peripheral clock of the urinary bladder. Shaojin *et al.* showed that tumor growth followed a significant circadian rhythm in a syngeneic model of estrogen binding in mammary tumors, which was reflected by circadian organized tumor growth rates, tumor

mitotic index, and G<sub>1</sub>/S phase-regulated expression of cyclin E and *bmal1* (You et al., 2005).

The sensitivity of the tumor-detection method was addressed via correlations between G.LUC signal and tumor burden. Although *in vivo* gene delivery is affected by many complicating factors, the <sup>P</sup>*cox2-G.luc*-treated animals in this investigation displayed a reasonable correlation between detected G.LUC and tumor size, demonstrating the potential of the procedure for cancer diagnosis. Controls involving transfections with <sup>P</sup>*cmv-G.luc* had G.LUC expression occurring in both untransformed bladder cells and infused MB49 cells, so detected signals did not correlate with tumor burden. Limited by strength of the <sup>P</sup>*opn*, the G.LUC signals produced in the animals transfected with <sup>P</sup>*opn-G.luc* did not correlate well with bladder.

Previous studies have looked at using urine-borne G.LUC for reporter assessment, and concluded that the use of urine for tumor assessment was not as good as using blood samples (Chung et al., 2009). There was a major difference between that report and the present studies in that the previous studies infused G.LUC-positive cancer cells into animals, while the present work used gene delivery to tumors in an orthotopic model to detect whether the tumors were present. In the former studies, the gene-containing viral RNA copy of *G.luc* was inserted into the host genome via viral vectors to form a stable G.LUC-expressing cell line. The present studies sought to detect growing tumor masses through the delivery of a temporary signal. Without using a viral delivery vector, the detection test could be repeated in a patient many times, such as during annual checkups.

### 3.5. Conclusion

Expression-targeted gene delivery was used to detect the presence of bladder cancer cells via the detection of G.LUC reporters in the urine. The approach was of interest because detection did not rely upon typical endogenous biomarkers, but rather produced biomarkers based upon gene expression patterns occurring within cells. *In vitro* studies implicated that both cancer-specific promoters ( $P_{cox-2}$  and  $P_{opn}$ ) could drive significant expression of G.LUC in bladder carcinoma cells, and that the expression was absent in untransformed cells. *In vivo* experiments in an orthotopic model of transitional cell carcinoma demonstrated that delivery of  $P_{cox2}$ -*G.luc* plasmids into the bladders of tumor-bearing mice yielded detectable levels of the reporter protein in the urine, and that the excreted levels were significantly higher versus negative controls and non-tumor-bearing mice at 48-hours post-transfection. It was found that tumor-bearing mice excreted G.LUC with an apparent 24-hour periodicity, and that urine collected at the end of the mouse “night” (lights-on) had a lower amount of G.LUC signal masking. The detection system, having shown tumor specificity, and having been calibrated to circadian expression patterns, shows great promise for future investigation of tumor presence both in the urinary bladder and other models of cancer.

## **Chapter 4. Cancer Detection Using Expression-targeted Gene Delivery to Drive Expression of Urine-borne Reporters**

### **4.1. Introduction**

Early cancer detection is of key significance to the survival of affected patients. Methods used for clinical screening and diagnosis for cancer include an array of imaging tests including mammography, CT, MRI, and ultrasound, each of which are associated with expensive equipment and facilities. Laboratory tests have been developed to analyze patient samples, such as tissue biopsies, blood, or urine. While promising, detection via cancer biomarkers is limited by a relatively small set of known markers. HER2 (breast cancer) (Ross, 2009), Cancer antigen 125 (ovarian cancer) (Moore et al., 2012), and carcinoembryonic antigen (colon) (Tiernan et al., 2013) to name a few.

One of the greatest challenges for both cancer detection and therapy is the ability to differentiate between transformed and untransformed cells. It has been shown that the technique of expression-targeting can be used to distinguish cells via the use of specific DNA entities that control the transcription of genes. If a cancer cell expresses more of a certain gene because it has transcription factors that bind to a specific DNA sequence

(promoter element), then using this DNA sequence to control the transcription of a delivered transgene should limit gene expression to that type of cancer cell. In the application described here, cancer cells were targeted via the use of promoters / promoter elements associated with the cyclooxygenase type-2 and osteopontin genes ( $P_{cox2}$  and  $P_{opn}$ , respectively). The promoters were used to drive the expression of exons that encoded proteins that are both secreted by cells and are easily detectable in the urine. It is important to note that tumor-specific promoters and urinary reporter proteins make up two independent components of this investigation.

### *The promoters*

There are a number of tumor-specific promoters that make expression-targeting of cancer cells possible. In the past, the alpha-fetoprotein promoter has been used to target hepatocellular carcinoma (Takahashi et al., 2002), and the carcinoembryonic antigen promoter has been applied to targeting lung and colorectal cancers (Osaki et al., 1994, Richards et al., 1995). Here we present the *cox2* and *opn* promoters as DNA regulatory units that can be used to target cells from bladder and colon carcinomas.

The Cox-2 protein is a key enzyme in the cyclic arm of the arachidonic acid cascade. Its expression is low-to-nonexistent in most untransformed cells and tissues when not stimulated by (pro-inflammatory) signaling molecules (Godbey and Atala, 2003, Wardlaw et al., 2002, Turini and DuBois, 2002). Overexpression of Cox-2 is correlated with tumor development and is commonly found in many different types of carcinomas, including those of colorectal, prostate, breast, lung, skin, pancreatic, and bladder origin

(Zha et al., 2004). The murine <sup>P</sup>*cox2* contains several positive regulatory elements such as an E-box enhancer element and a nuclear factor IL6 binding site, which play important roles in recruiting transcription factors that might be expressed differently in transformed versus normal cells (Kim and Fischer, 1998).

OPN is an acidic protein that is expressed at high levels in bone (Mazzali et al., 2002). It is also expressed in immune cells such as macrophages and T cells, as well as in non-immune cells such as endothelial and epithelial cells (O'regan and Berman, 2000). Overexpression of OPN, to a degree much higher than in normal cells, is very common in a series of malignancies such as carcinomas of the lung (Hu et al., 2005), breast (Rudland et al., 2002), cervix (Song et al., 2009), ovary (Kim et al., 2002), colon (Agrawal et al., 2002), and pancreas (Koopmann et al., 2004). More importantly, in terms of disease state, increased tumor expression of OPN is associated with enhanced invasiveness and metastatic potential (Rodrigues et al., 2007). In humans, <sup>P</sup>*opn* has the multiple actions as a positive regulatory sequence (RE-1) for the binding of the transcription factors Sp1, Myc, and Oct-1, which could act in a synergistic manner to enhance the transcription of downstream genes (Denhardt et al., 2003). The promoter also contains a Ras-activated enhancer, which is bound by the Ras-response factor to stimulate transcription of *opn*, which in turn strengthens the metastatic potential of tumor cells (Denhardt et al., 2003). Early identification of such cells would be very important for the prevention of metastatic disease.

*The reporters*

In addition to looking at the utility of <sup>P</sup>*cox2* or <sup>P</sup>*opn* for use in targeting the expression of delivered genes to cancer cells, the experiments described here investigated the use of reporter proteins that were identified because of their secretion from cells as well as their detectability in the urine. Candidates were selected according to the following criteria: 1) proteins that are detectable in human urine but with low basal levels since it is undesirable if a large amount of the urinary protein being used as a reporter is present before transfection; 2) reporters for which commercial quantitative immunoassays are currently available are the most desirable to use at this stage, to avoid the expense of raising antibodies for novel detection kits; 3) efficient excretion ability is preferable since reporters require to be filtered through the glomerulus given that expression-targeted gene delivery may be administered systemically in the future. Proteins and polypeptides with molecular weights smaller than 30kDa are more easily filtered by the glomerulus while large molecular weights (>60kDa) can prevent a protein from glomerular filtration (Verbeeck and Musuamba, 2009, Nagaraj and Mann, 2011). A good excretory reporter should have high urine:serum ratio, indicating efficient filtration by kidney.

As such,  $\beta$ 2 microglobulin ( $\beta$ 2m), the  $\beta$  subunit of human chorionic gonadotropin ( $\beta$ hCG), prostate specific antigen (PSA), and secreted embryonic alkaline phosphatase (SEAP) were chosen as candidate reporters. It is important not to confuse, for example, the detection of a marker such as PSA with the detection of prostate cancer in this system. These proteins are being used as reporters to mark a positive match to a cellular behavior via expression-targeted gene delivery.

$\beta$ 2m is a small extracellular protein with a molecular weight of 11.8 kDa. It is a component of the major histocompatibility complex Class I. Since molecular weights smaller than 30kDa are more easily filtered by the glomerulus (Verbeeck and Musuamba, 2009, Nagaraj and Mann, 2011),  $\beta$ 2m could be expected to appear in urine samples due to its small size. Low levels of  $\beta$ 2m ( $\leq 300\mu\text{g/L}$  for male;  $\leq 183\mu\text{g/L}$  for female) are present in urine samples from healthy individuals (Chan et al., 2012). While  $\beta$ 2m levels are elevated in renal maladies such as membranous nephropathy and glomerular injury, in a clinical setting such conditions would be screened for before the described cancer-detection procedure would be performed.

hCG is a glycoprotein hormone that is primarily produced during pregnancy by syncytiotrophoblast cells of the placenta. It plays an active role during pregnancy in the development of the corpus luteum, which secretes progesterone to aid with the development of the uterus and placenta for fetal development (Glick, 1991). The hCG hormone consists of an  $\alpha$  subunit, which is also used in pituitary gonadotropins, and a  $\beta$  subunit that is unique to the hormone (de Medeiros and Norman, 2009). In urine samples from healthy males and non-pregnant females, hCG levels are commonly lower than 5 mIU/ml, which would yield a negative result from a standard home pregnancy test (levels over 25 mIU/ml indicate pregnancy) (Chard, 1992). This implies that  $\beta$ hCG could serve as a reporter candidate in the present system for the detection of cancers in healthy males and non-pregnant females.

PSA is a 34 kDa serine protease that is secreted by epithelial cells of the human prostate, and is considered as a tumor marker associated with the risk of prostate cancer (Stephan et al., 2014). Being fairly unique to the urine of males, PSA could serve as an excellent reporter for the described detection system in female subjects. In a study involving 50 healthy females, it was found that the PSA concentration in all serum samples was lower than 0.06 ng/ml, and that 80% of the associated urine samples tested PSA positive with a mean  $\pm$ SE of (0.038 $\pm$ 0.005) ng/ml (Mannello et al., 1998). PSA-expressing MB49 cells have been implanted into mice, with urinary PSA production increasing in parallel to tumor growth, which allows PSA a potentially good reporter for bladder cancer study (Luo et al., 2004). The tumor volume was correlated well with PSA production in the subcutaneous cancer model using MB49-PSA<sup>+</sup> cells and PSA secretion in mouse serum and urine were also assayed in the orthotopic model to reflect tumor response to anticancer therapy (Wu et al., 2003b).

Secreted alkaline phosphatase (SEAP) is very useful as a reporter protein. It can be secreted by cells into culture media *in vitro* or body fluids *in vivo*, with cellular secretion being proportional to the up-regulation of intracellular *seap* mRNA (Cullen and Malim, 1992). SEAP activity can be directly assayed via cell supernatants (as opposed to cell lysates). Although endogenous alkaline phosphatase is typically present where there are viable cells, SEAP is easily differentiated from its endogenous counterpart via its heat stability and resistance to L-homoarginine. In addition, SEAP activity can be accurately measured by sensitive chemiluminescent assays. All of these properties make SEAP a desirable reporter protein for monitoring *in vitro* and *in vivo* processes (Hiramatsu et al.,

2005). SEAP has been used as a soluble marker for non-invasively measuring tumor burden *in vivo*. SEAP levels in plasma samples correlated very well with tumor volume after stably  $P_{cmv-seap}$ -transfected OCC1 ovarian carcinoma cells (Nilsson et al., 2002) or  $P_{cmv-seap}$ -transfected A2780 ovarian cancer cells (Bao et al., 2000) were implanted into mice. A2780 cells that were stably transfected with cancer-specific promoter  $P_{survivin}$ -driven *seap* were implanted into the intrabursal cavity of mouse ovaries, producing plasma SEAP activity that is reflective of tumor growth (Bao et al., 2002).

In the work presented here, both  $P_{cox-2}$  and  $P_{opn}$  were used to drive the expression of  $\beta 2m$ ,  $\beta hCG$ , PSA, and SEAP reporter proteins in cancer cells (versus normal cells). Application of the expression-targeted cancer detection system was investigated *in vitro*, and *in vivo* in an orthotopic model of murine bladder carcinoma where cells were transfected by transurethral intravesical gene delivery.

## 4.2. Materials and Methods

### 4.2.1. Cells

Carcinoma cells were represented by the murine transitional cell carcinoma MB49 and the murine colon carcinoma cell line CT26.CL25. Normal cells were represented by a fibroblast cell line derived in-house via explant of tissue from a normal mouse and designated “MF”. MB49 and MF cells were maintained in Dulbecco’s modified Eagle’s medium (Invitrogen, Carlsbad, CA, USA) supplemented with 10% fetal bovine serum (Gemini Bio-Products, West Sacramento, CA, USA), 100 U/ml penicillin, and 100 U/ml streptomycin (Invitrogen). CT26.CL25 cells were cultured in Roswell Park Memorial

Institute (RPMI) 1640 medium (Invitrogen) supplemented with 10% fetal bovine serum, 100 U/ml penicillin, 100 U/ml streptomycin, and a solution of minimum essential medium non-essential amino acids (Invitrogen, catalogue #11140-050). All cells were grown in 25-cm<sup>2</sup> culture flasks in a humidified incubator held at 37°C and containing 5% CO<sub>2</sub>.

#### 4.2.2. Plasmid construction

<sup>P</sup>*cmv-βhCG*: The *βhCG* exon was originally amplified via traditional PCR upon whole-cell genomic extracts. The amplicons thus obtained were inserted into the vector pEGFP-N1 (Clontech/Takara Bio Co., Mountain View, CA, USA) via the BglII and SalI restriction sites. The original reporter sequence that encodes an enhanced green fluorescent protein was later excised.

<sup>P</sup>*opn-βhCG*: The <sup>P</sup>*opn* promoter from -134 to +125 was amplified via PCR performed on a whole-genome extract of human foreskin fibroblasts (HFF-1, ATCC, Manassas, VA) using the following set of primers: Forward: 5'-AAGATCGATTAATAAAACCAGAGGGG-3' (inserted AseI site is underlined); Reverse: 5'-TCATAGGCTAGCTGAATGCACAA-3' (inserted NheI site is underlined). The <sup>P</sup>*cmv* promoter in the pEGFP-N1 plasmid was replaced by the <sup>P</sup>*opn* promoter via AseI and NheI. The reporter sequence of *βhCG* was extracted from the <sup>P</sup>*cmv-βhCG* plasmid just described, via EcoRI and DraIII, then inserted into the <sup>P</sup>*opn-gfp* plasmid after the *gfp* sequence had been removed as described.

*<sup>P</sup>cox2-βhCG*: The murine promoter sequence *<sup>P</sup>cox2* (also known in the literature as TIS10) was extracted from a plasmid originally provided by Carol Pilbeam (University of Connecticut Health Center, USA) (Fletcher et al., 1992, Choudhary et al., 2004). The *<sup>P</sup>cmv* was removed from the pEGFP-N1 vector with AseI and BglII, followed by insertion of *<sup>P</sup>cox2* promoter using the same sticky ends to form *<sup>P</sup>cox2-gfp*. The reporter sequence *βhCG* was extracted from *<sup>P</sup>cmv-βhCG* (see above) via EcoRI and DraIII, then inserted into the *<sup>P</sup>cox2-gfp* after the *gfp* exon had been removed using the same restriction sites.

*<sup>P</sup>cmv-β2m*, *<sup>P</sup>cox2-β2m*, and *<sup>P</sup>opn-β2m*: The reporter sequence of β2m was amplified on the basis of the plasmid pBJ1-β2m (Addgene plasmid 12099, Bjorkman PJ, CIT, CA, USA) via PCR using the following set of primers: Forward: 5'-ATATGTCTGACTGTTCTGCGCCGTTACAG-3' (Sall site underlined); Reverse: 5'-GGCGGACCGATAAGCTTGATATCGAATTC-3' (a NotI site, used to modify the amplicons, was already present in the amplified portion of the pBJ1-β2m plasmid). To construct *<sup>P</sup>cmv-β2m*, the EGFP exon in pEGFP-N1 was replaced by the amplified β2m exon sequence via Sall and NotI digestion. Similarly, construction of *<sup>P</sup>cox2-β2m*, and *<sup>P</sup>opn-β2m* was achieved by substituting the EGFP exon in *<sup>P</sup>cox2-gfp* and *<sup>P</sup>opn-gfp*, respectively, with the β2m exon via digestion with Sall and NotI.

*<sup>P</sup>cmv-psa*, *<sup>P</sup>cox2-psa*, and *<sup>P</sup>opn-psa*: The reporter sequence of prostate specific antigen (psa) was amplified via tradition PCR upon whole-cell genomic extracts using the following primers: forward: 5'-CTAGTA GAATTC CGCCACC ATGTGGGTCCCGGTT-3' (inserted EcoRI is underlined); reverse: 5'-ATTATT

GGTACC TCAGGGG TTGGCCACGATGGTG-3' (inserted KpnI is underlined). To construct *<sup>p</sup>cmv-psa*, the *βhCG* exon in *<sup>p</sup>cmv-βhCG* was replaced by the amplified *PSA* exon sequence via restriction sites EcoRI and KpnI. Similarly, construction of *<sup>p</sup>cox2-psa*, and *<sup>p</sup>opn-psa* was completed by substituting the *βhCG* exon in *<sup>p</sup>cox2-βhCG* and *<sup>p</sup>opn-βhCG*, respectively, with the *PSA* exon via digestion with restriction sites EcoRI and KpnI.

*<sup>p</sup>cmv-seap*, *<sup>p</sup>cox2-seap*, and *<sup>p</sup>opn-seap*: The reporter sequence of secreted embryonic alkaline phosphatase (*seap*) was amplified via traditional PCR on the basis of the plasmid *<sup>p</sup>cmv-seap*, a gift from Alan Cochrane (Addgene plasmid #24595) using the following primers: forward: 5'- ATTTAT GAATTC GCCACCATGCTGGGGCC-3' (inserted EcoRI underlined) ; reverse: 5'- ATTTTT GGTACC TTAACCCGGGTGCGCGG-3' (inserted KpnI underlined). To construct *<sup>p</sup>cmv-seap*, *<sup>p</sup>cox2-seap*, and *<sup>p</sup>opn-seap*, the *seap* exon was substituted for the *seap* exon via EcoRI and KpnI digests of *<sup>p</sup>cmv-psa*, *<sup>p</sup>cox2-psa*, and *<sup>p</sup>opn-psa*, respectively.

All of the sequences described above were verified by DNA sequencing (Integrated DNA Technologies, Coralville, IA). The non-coding vector pUC19 (New England Biolabs) was used as a negative control in transfection experiments.

#### 4.2.3. *In vitro* transfections

Cells were collected in the late-log phase (confluence of ~70-80%). A total of 10<sup>5</sup> cells per well were seeded into 6-well plates containing 2 ml of growth medium per well,

at 16 hours prior to transfection. The 25 kDa polycation poly(ethylenimine) (PEI) (Sigma-Aldrich, St. Louis, MO, USA) was diluted, titrated to pH = 7.0, and complexed with 3.6 µg of plasmid DNA at a N:P ratio of 7.5:1 in a total volume of 100 µl per dose (Dobek et al., 2011). At the time of transfection, growth media were replaced with 2 ml FBS-free medium plus 100 µl of gene delivery complexes. Transfections were allowed to proceed at 37°C for 2 hours, after which the transfection media were replaced with 1 ml of fresh growth medium.

#### 4.2.4. *Real-time quantitative PCR*

24 hours after transfection, cells were lysed and total RNA was extracted using RNeasy mini kits (Qiagen Inc., Valencia, CA, USA). RNA was reverse-transcribed into cDNA using the High Capacity cDNA Reverse Transcription Kit (Applied Biosystems, Carlsbad, CA). Real-time qPCR was carried out via iCycler (Bio-Rad, Hercules, CA). The total volume for each reaction was 25µl, which included 12.5 µl SYBR green supermix (Bio-Rad), 200 nM each of forward and reverse primers (Integrated DNA Technologies), 1µl cDNA template, and water. The qPCR was performed using 95°C for 3 minutes, a loop of 95°C for 10 seconds (melt), 54.2°C—59.4°C (depending upon the specific primers being used) for 30 seconds (anneal), and 72°C for 20 seconds (extend). The loop was repeated for a total of 40 cycles. The housekeeping gene 18s rRNA was used as an internal reference. The primer sequences used for 18s rRNA (locus: NR\_003286, accession: NR\_003286) were: forward: 5'-TCAATCTCGGGTGGCTGAACGC-3', reverse: 5'-CGGACACGGACAGGATTGACAGAT-3'. The primer sequences used for human  $\beta 2m$  (locus: NM\_004048, accession: NM\_004048) were: forward: 5'-

GGTTTCATCCATCCGACATT-3', reverse: 5'-ACGGCAGGCATACTCATCTT-3'.

The primer sequences used to detect *βhCG* (locus: NM\_000737.3, accession: NM\_000737.3) were: forward: 5'-GATGTTCCAGGGGCTGCT-3', reverse, 5'-GCACAGATGGTGGTGTGAC-3'. The primer sequences used to detect *psa* (locus: NM\_001030047, accession: NM\_001030047) were: forward: 5'-CGCAAGTTCACCCTCAGAA-3'; reverse: 5'-GCACACCATTACAGACAAGTGG-3'.

All PCR data were analyzed using the Pfaffl method (Pfaffl, 2001), where

$$ratio = \frac{(E_{target})^{\Delta Ct(control-treatment)}}{(E_{ref})^{\Delta Ct(control-treatment)}}$$

The ratio is a normalized expression ratio, reflecting the fold change of the target gene (*β2m*, *psa* or *βhCG*) in treated samples relative to control samples under the condition of being normalized to the expression of a reference gene (18s rRNA).  $E_{target}$  and  $E_{ref}$  correspond to efficiencies of primers toward the target gene and the reference gene respectively.

It is common for users of PCR to use the  $2^{-\Delta\Delta Ct}$  method (Livak and Schmittgen, 2001) in determining up- or down-regulation of transcription. Considering that method for a moment, it should be noted that the ratio of gene upregulation ( $2^{-\Delta\Delta Ct}$ ) does not follow a normal distribution. It has therefore been suggested that statistical analyses be performed on  $\Delta\Delta Ct$  as opposed to  $2^{-\Delta\Delta Ct}$  (Yuan et al., 2006). The Pfaffl method was chosen for use in these experiments over the  $2^{-\Delta\Delta Ct}$  method because the Pfaffl method takes into account primer efficiency rather than assuming that each round of PCR will yield a perfect

doubling of amplicon numbers. The resulting ratio, which is equal to the normalized fold-change in transcription of the gene of interest, was then run through a  $\log_2$  transformation to transform the results into a base 2 form for statistical analysis. The following formulas describe how to perform this Pfaffl-adjusted  $\Delta\Delta Ct$  for calculations of standard deviations, which are then to be used for statistical analysis:

$$ratio = \frac{(E_{target})^{\Delta Ct1}}{(E_{ref})^{\Delta Ct2}} = \frac{2^{\log_2(E_{target})^{\Delta Ct1}}}{2^{\log_2(E_{ref})^{\Delta Ct2}}} = 2^{\log_2(E_{target})^{\Delta Ct1} - \log_2(E_{ref})^{\Delta Ct2}}$$

$$\log_2(ratio) = \log_2 2^{\log_2(E_{target})^{\Delta Ct1} - \log_2(E_{ref})^{\Delta Ct2}} = \log_2(E_{target})^{\Delta Ct1} - \log_2(E_{ref})^{\Delta Ct2} = \Delta\Delta Ct_{\text{Pfaffl method, adjusted}}$$

where  $\Delta Ct1 = Ct_{\text{control, target gene}} - Ct_{\text{treatment, target}}$  and

$\Delta Ct2 = Ct_{\text{control, reference gene}} - Ct_{\text{treatment, reference gene}}$ .

#### 4.2.5. Reporter assay for cell culture

Media were collected 48 hours after transfection and centrifuged at  $1,000 \times G$  for 10 minutes to remove cell debris. Supernatants were stored at  $-80^\circ\text{C}$  until quantification. Sensitive and quantifiable results were obtained with  $\beta 2m$  ELISA kits (GenWay Biotech, Inc., San Diego, CA),  $\beta hCG$  ELISA kit (Phoenix Pharmaceuticals, Inc., Burlingame, CA) PSA ELISA kit (Abnova, Taipei, Taiwan), and SEAP reporter gene assays (Roche Diagnostics, Indianapolis, IN). In addition, for  $\beta hCG$  detection, the Consult<sup>TM</sup> diagnostics hCG urine cassette (PSS World Medical Inc., Jacksonville, FL, USA) was used as a convenient and rapid test, plus as proof-of-concept that a urine-based test for home diagnostic use is possible. A similar test for PSA detection, the SERATEC<sup>®</sup> PSA Semiquant kit (SERATEC<sup>®</sup>GmbH, Goettingen, Germany), was used

for rapid immunochromatography to further demonstrate the potential for the described system to be used in a home setting.

#### 4.2.6. *Murine orthotopic tumor model*

All experiments were performed with the approval of the Tulane University Institutional Animal Care and Use Committee. Female, 3- to 5- week old C57BL/6J mice were purchased from Jackson Laboratories (Bar Harbor, ME, USA) and allowed to stay for approximately one week to acclimate before starting any study. Mice were anesthetized via isoflurane and urine was drained from each bladder via transurethral catheterization. 100ul of MB49 cells with a concentration of  $10^6$  cells/ml were delivered via transurethral catheterizations into the bladders without being operated with electrocautery, and incubated for 1.5 hours. Catheters remained in place during the incubations to keep the cell suspensions in the bladders. At 90 minutes, catheters were removed and bladders were allowed to drain naturally.

#### 4.2.7. *In vivo transfections*

Mice were anesthetized via isoflurane and urine in the bladders were voided via catheterization. Gene delivery complexes were made as described under section 4.2.2 *In vitro transfection*, using 3.6  $\mu$ g of plasmid (pUC19, *<sup>p</sup>cmv-seap*, *<sup>p</sup>cox2-seap*, *<sup>p</sup>opn-seap*, *<sup>p</sup>cmv-psa*, *<sup>p</sup>cox2-psa*, or *<sup>p</sup>opn-psa*) complexed with PEI at an N:P ratio of 7.5:1 and a total volume was 100ul per dose. Complexes were delivered into bladders of either healthy mice or tumor-bearing mice on Day 8. (The day that cancer cells were introduced into

the bladders was defined as Day 0). Transfections proceeded for 2 hours, after which catheters were removed and the bladders allowed to drain naturally.

#### 4.2.8. *Urine-based reporter assays*

At 72-hours post-transfection, each mouse was assigned in an individual cage and stayed there for up to 3 hours. Urine samples were collected during the period using a pipet. Samples were centrifuged at  $1,000 \times G$  for 10 minutes to remove debris and stored at  $-80^{\circ}\text{C}$  until quantification. The weights of a urine sample and water with an equal volume were measured respectively and specific gravity of urine samples was the ratio of the weights of urine and water. SEAP expression was detected using SEAP reporter gene assays (Roche Diagnostics, Indianapolis, IN). PSA expression was detected using Total Prostate Specific Antigen Human SimpleStep ELISA<sup>TM</sup> kit (Abcam, Cambridge, MA).

#### 4.2.9. *Statistics*

Levels of reporter protein secretion were log-transformed to put them in the form of a normal distribution. Student's t-test was used to compare differences between group pairs. The ANOVA test followed by a post-hoc test was used to compare differences between groups when there were more than two group pairs (sham, pUC19, *P*<sub>cmv</sub>-driven plasmid, *P*<sub>cox2</sub>-driven plasmid, and *P*<sub>opn</sub>-driven plasmid). Significance was defined statistically as  $P < 0.05$ .

### 4.3. Results

#### 4.3.1. *First detection of reporters*

As a starting point, it was necessary to determine whether the  $\beta$ 2M,  $\beta$ hCG, and PSA proteins could even be detected under the most favorable conditions. Three murine cell lines – MF (normal fibroblasts), CT26 (colon cancer), and MB49 (bladder cancer) – were transfected with reporter plasmids driven by the strong *cmv* promoter (fig. 4.1). The  $\beta$ hCG and PSA reporters were easily detectable in the two cancer cell lines. The  $\beta$ 2M reporter was expressed well in only one of the cancer cell lines: MB49. Statistical analysis revealed that the poor  $\beta$ 2M expression was significantly lower than the other two reporters in the MF and CT26 cell lines.

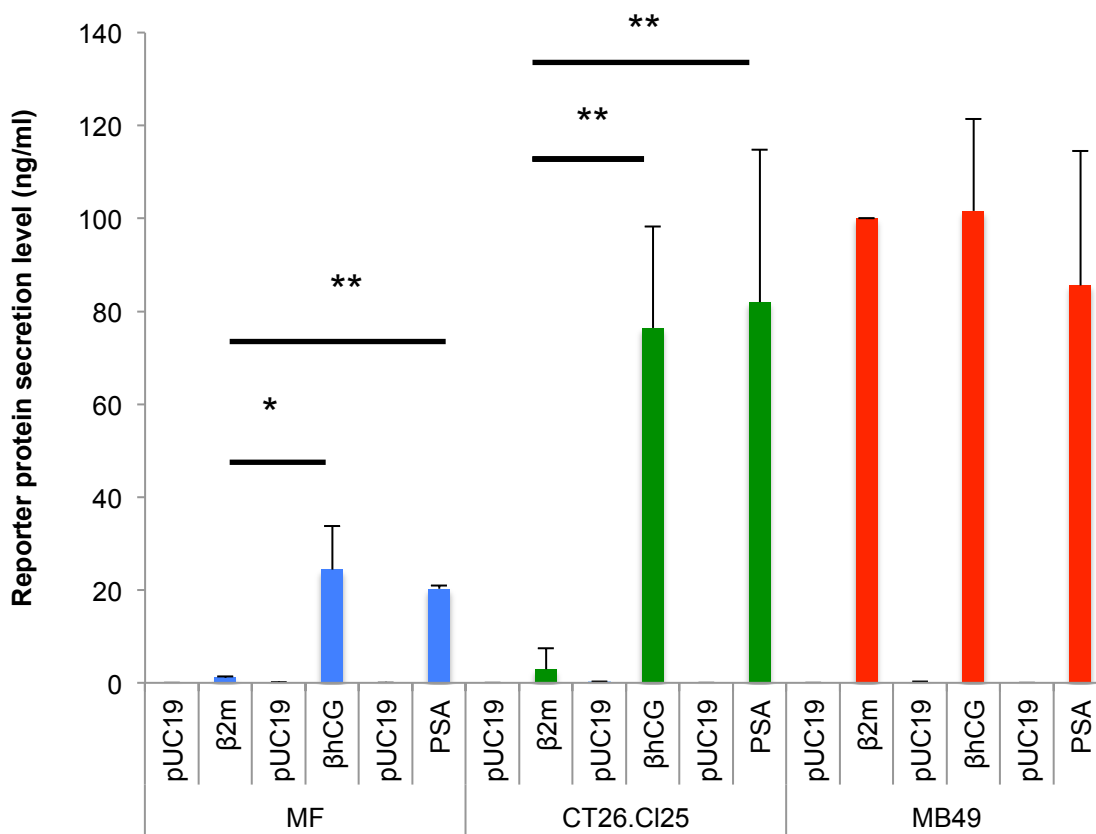


**Figure 4.1.** Secretion levels of three reporter proteins were compared in different cell lines that were transfected with the strong  $P_{cmv}$ . “\*” and “\*\*\*” indicate significant differences between  $\beta 2m$  the other two reporters in the indicated cell lines (t-test,  $n \geq 3$ , at least three independent experiments were performed and samples were run in duplicate). “\*” indicates  $p < 0.05$ , “\*\*\*” indicates  $p < 0.01$ ).

Further analysis of reporter expression was performed at the transcriptional level through PCR experiments. Again,  $P_{cmv}$  was used to drive the transcription of the three reporters. Although detection of transcription showed relatively higher levels than were seen in the reporter-detection experiments, similar patterns were seen: MB49 cells showed consistently high transcription of all three reporters, and  $\beta 2M$  expression was significantly lower than the other two reporters in the MF cell line. In the CT26 cell line, *psa* transcription was significantly higher than the other two reporters (*fig. 4.2*).

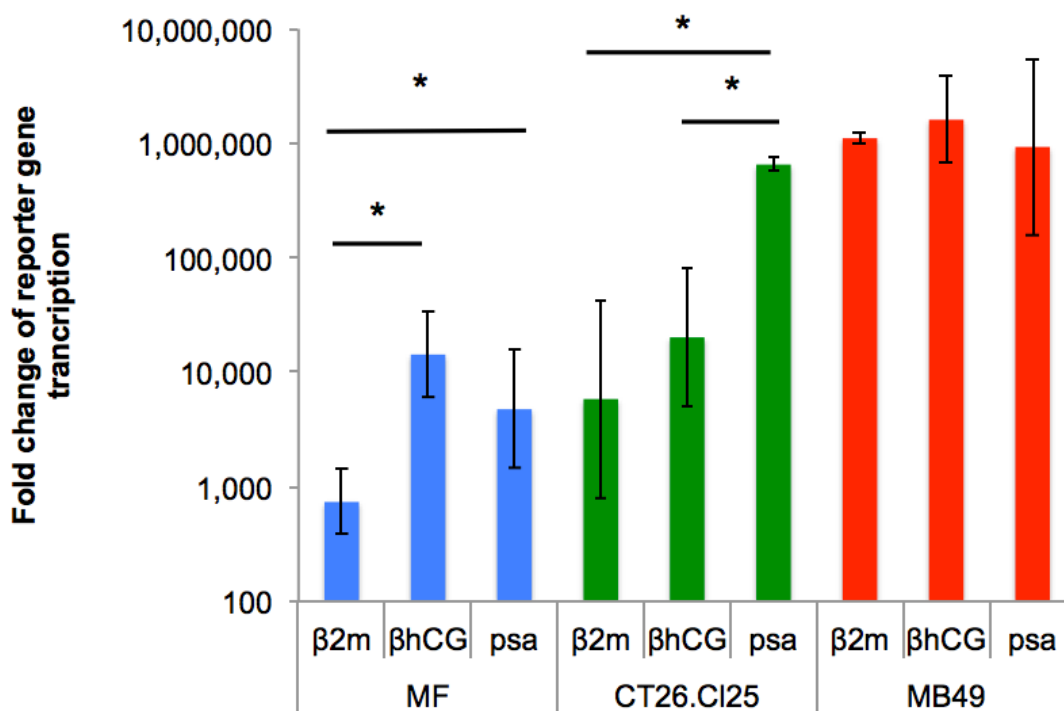


**Figure 4.2.** Fold change in the transcription of three reporter genes, in three cell lines. Cells were transfected with plasmids under the control of the strong  $P_{CMV}$ . Three independent experiments were performed and cDNA samples were run in triplicate. “\*” indicates a significant difference in detected transcription levels between the pairs indicated (t-test,  $n=3$ ,  $p<0.05$ ).

#### 4.3.2. Transcription of reporter genes when expression-targeting was employed

$\beta 2m$  transcription levels following transfection with  $P_{cox2}$ - or  $P_{opn}$ -driven plasmids was assessed via real-time PCR. Although fold change of  $\beta 2m$  transcription levels was significantly higher in two cancer cell lines transfected with expression-targeted groups than that in identically treated normal cell line (fig. 4.3a), normalized  $\beta 2m$  transcription was roughly the same in murine fibroblasts as it was in the two cancer cell lines for each of the two cancer-targeting promoters (fig. 4.3b). Normalization to transcription levels of

$P_{cmv}$ -driven trials is to eliminate the difference of transfection ability among different cells.

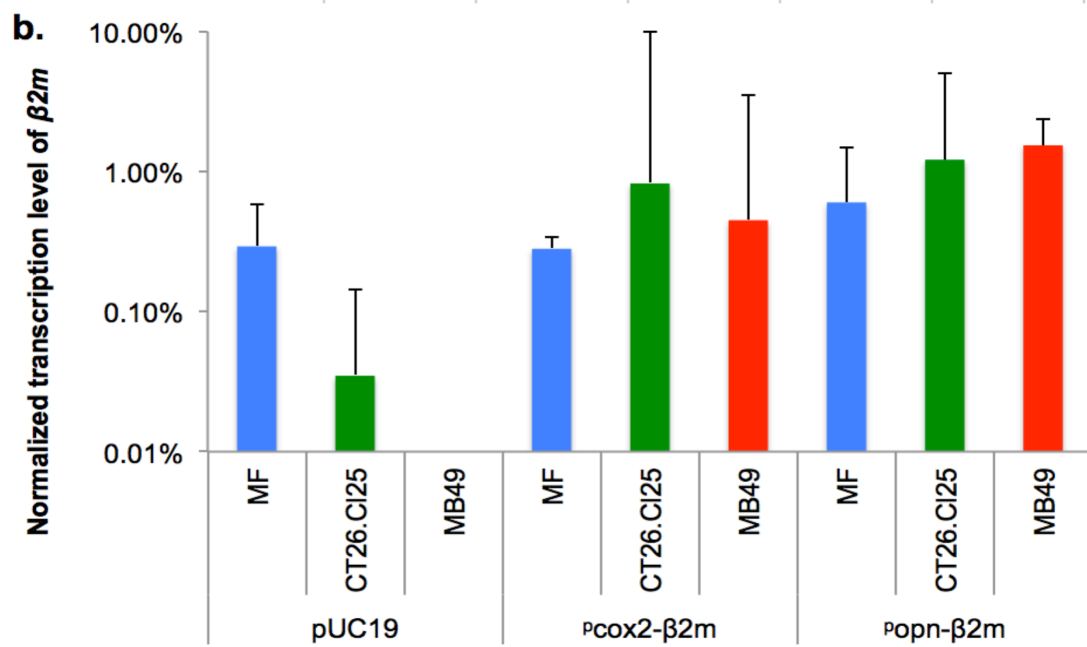
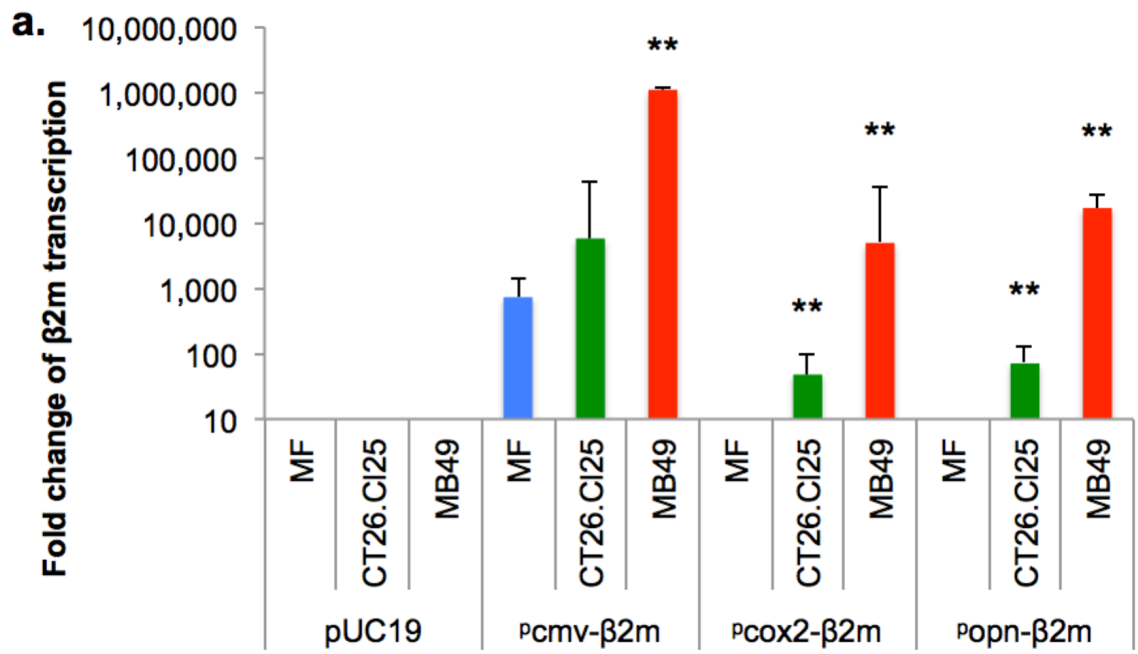


**Figure 4.3.** PCR results reflecting changes in  $\beta 2m$  transcription levels (a), and changes normalized to  $P_{cmv}$ -driven controls (b), in murine cell lines of normal fibroblasts (MF), and the cancer cell lines CT26.CI25 (colon) and MB49 (bladder). Three independent experiments were performed and cDNA samples were run in triplicate. “\*\*\*” indicates a significant difference in detected transcription levels between the cancer cell line and the normal cell line (t-test, n=3, p<0.01). Normalization to  $P_{cmv}$ -driven controls was performed in order to compensate the difference of transfection ability among different cell lines.

Next, transcription levels of  $\beta hCG$  were assessed in the same cell types using the same targeting promoters. Fold change of  $\beta hCG$  transcription levels was significantly higher in two cancer cell lines transfected with expression-targeted groups than that in identically treated normal cells (*fig. 4.4a*). In the two cancer cell lines, normalized levels of reporter mRNA were approximately 10-fold higher than what was observed for  $\beta 2m$  following transfection (*fig. 4.4b*). Negative controls utilizing the pUC19 null vector revealed no appreciable background in any of the cell lines. The targeting aspect was also very encouraging, with expression in the cancer cells showing some significance as compared to transfections of the normal fibroblasts.  $P_{opn}$ -driven  $\beta hCG$  transfections showed significantly higher  $\beta hCG$  transcription in both of the cancer cell lines versus the normal cell line, and  $P_{cox2}$ -driven transfections of  $\beta hCG$  showed significantly higher  $\beta hCG$  transcription in MB49 cells versus murine fibroblasts (*fig. 4.4b*). Similar results were seen for transfections of expression-targeted genes encoding the PSA reporter, with both targeting promoters yielding significantly more reporter transcription in both cancer cell types versus normal fibroblasts (*fig. 4.5*).

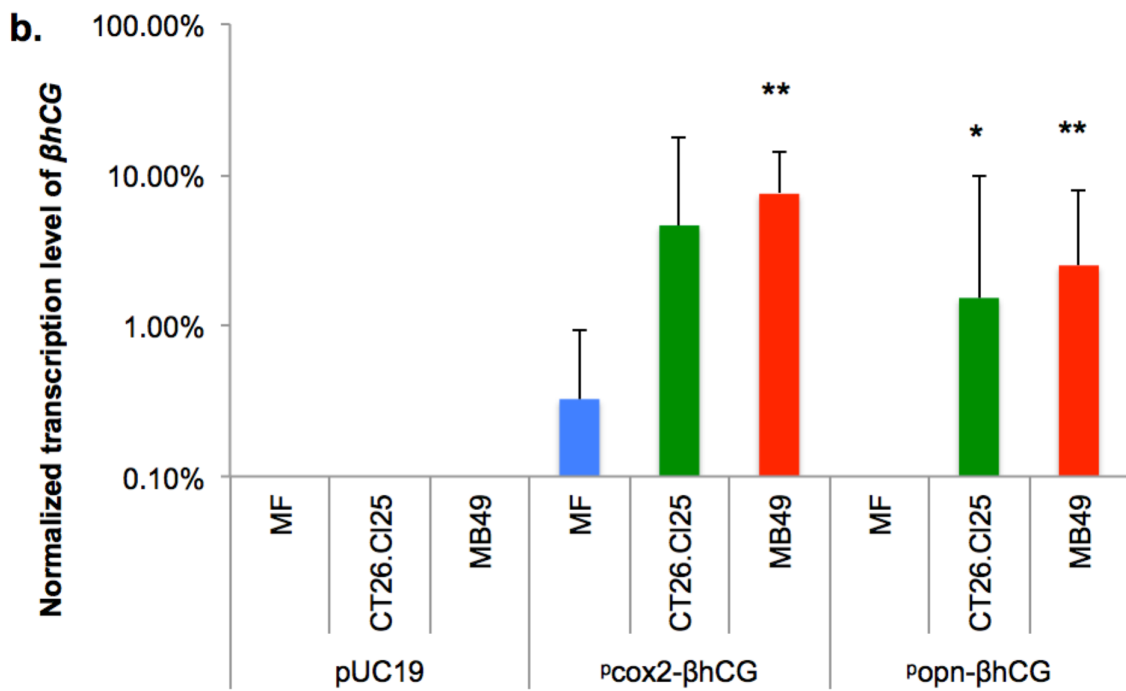
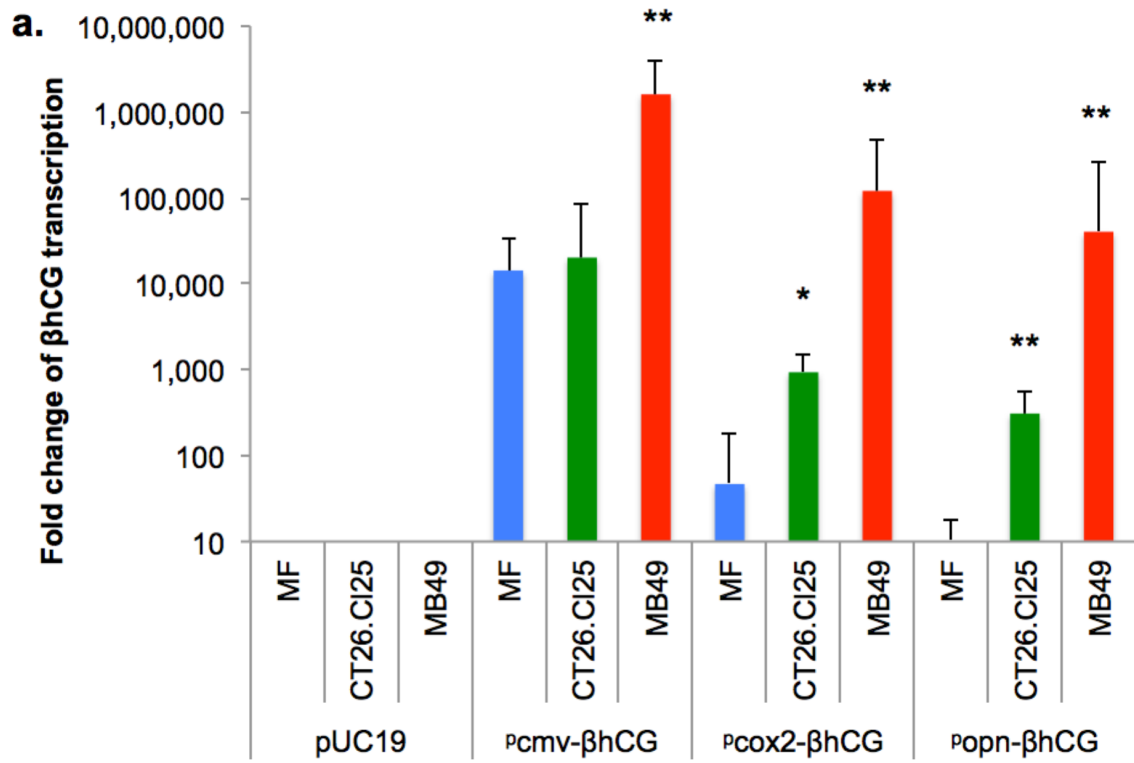


**Figure 4.4.** PCR results reflecting changes in  $\beta hCG$  transcription levels (a), and changes normalized to  $P_{cmv}$ -driven controls, in murine cell lines of normal fibroblasts (MF), and the cancer cell lines CT26.Cl25 (colon) and MB49 (bladder). Three independent experiments were performed and cDNA samples were run in triplicate. “\*” and “\*\*\*” indicate significant differences between the indicated cell line and the normal (MF) cell line ( $p < 0.05$  and  $0.01$ , respectively) (t-test,  $n=3$ ). Normalization to  $P_{cmv}$ -driven controls was performed in order to compensate the difference of transfection ability among different cell lines.

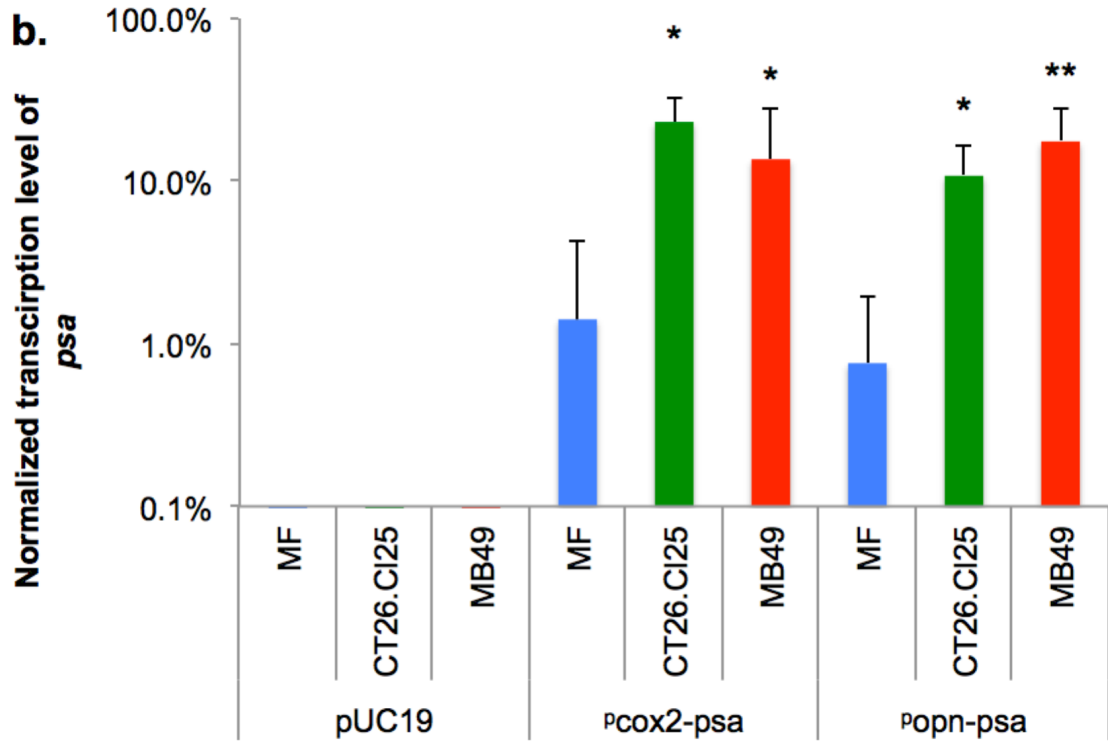
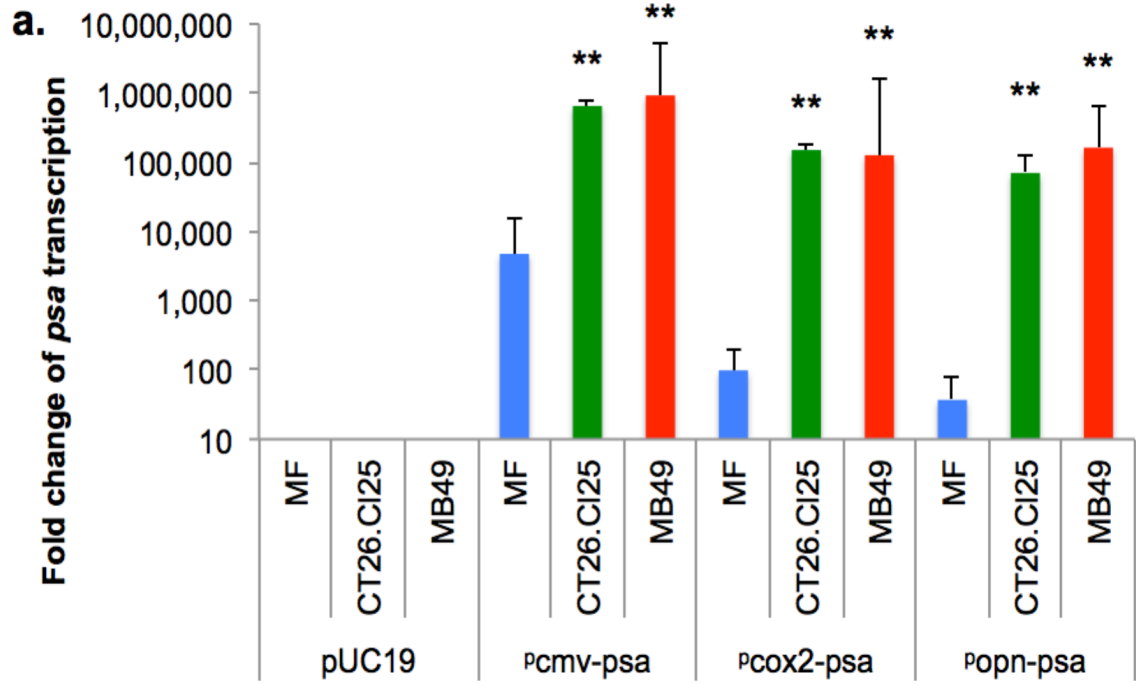
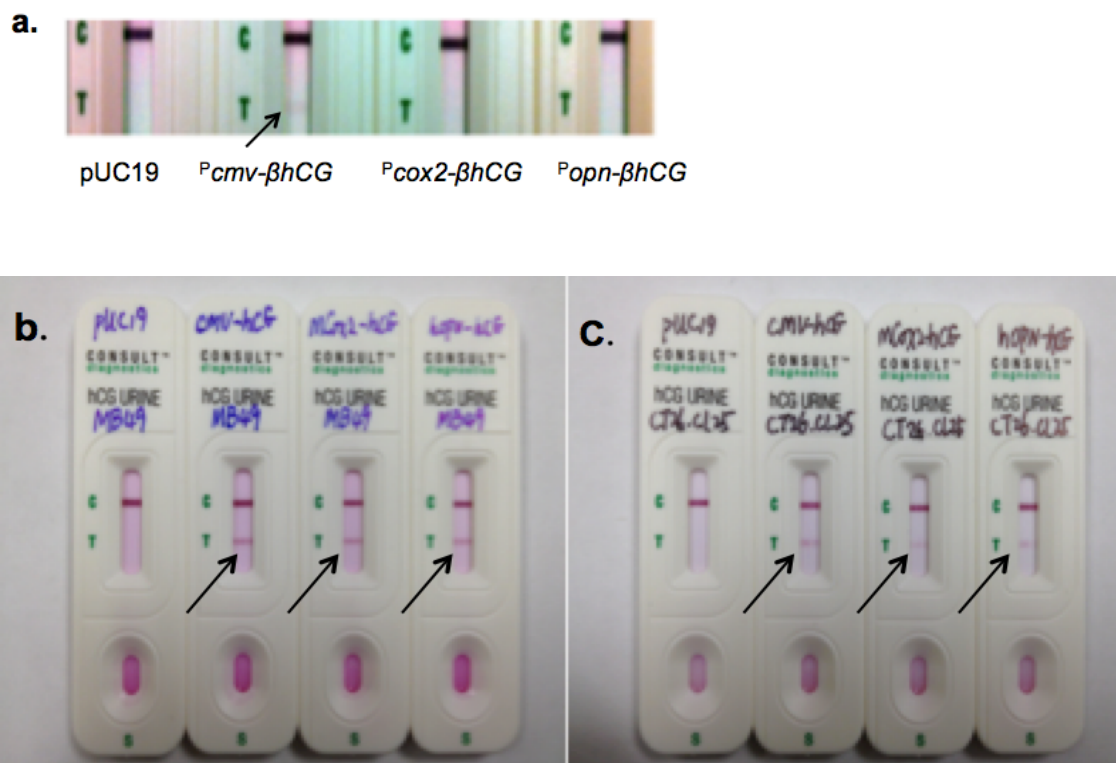


**Figure 4.5.** Fold change of *psa* transcription levels (a), and changes normalized to  $P_{cmv}$ -driven controls (b), in individual cell line, normal murine fibroblast (MF), colon cancer (CT26.CI25), and bladder cancer (MB49) cells. At least three independent experiments were performed and cDNA samples were run in triplicate. “\*” and “\*\*” indicates significant differences between normal cells (MF) and cancer cells (CT26.CI25 or MB49) that were treated with the same plasmid/PEI complexes [t-test,  $n \geq 3$ ,  $p < 0.05$  (\*) or  $p < 0.01$  (\*\*)]. Normalization to  $P_{cmv}$ -driven controls was performed in order to compensate the difference of transfection ability among different cell lines.

#### 4.3.3. *Lateral flow immunoassay results for cell culture*

An important potential application of these investigations is the development of urine-based lateral flow assays for urine based cancer detection in a home setting. For proof-of-concept, home pregnancy ( $\beta hCG$ ) kits and PSA kits were used to detect two of the expression-targeted reporters.

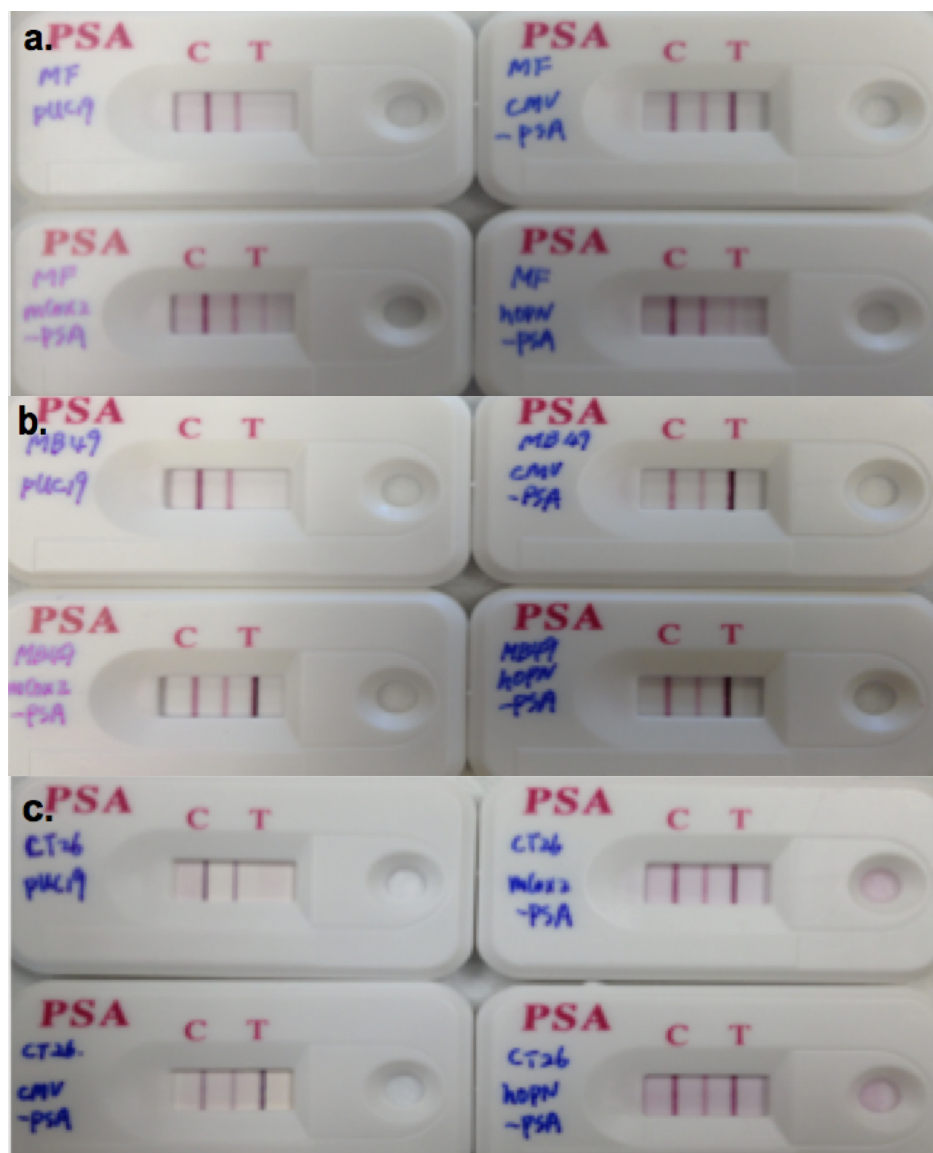
At 48 hours post-transfection, cell supernatants were tested by hCG urine cassette, which has a lower detection limit of 20mIU/ml. In MF groups (normal cells), only  $P_{cmv}$ - $\beta hCG$  -transfected samples showed positive results by 20 minutes of lateral flow while other groups all showed negative results even after 5 hours of incubation (*fig.4.6a*). In both the MB49 and CT26 cancer cell lines, positive readings were observed by 20 minutes after the addition of cell supernatant for samples transfected with  $P_{cmv}$ - $\beta hCG$ ,  $P_{cox2}$ - $\beta hCG$  and  $P_{opn}$ - $\beta hCG$  (*fig. 4.6b,c*).



**Figure 4.6.** Lateral flow assays indicating the presence or absence of  $\beta$ hCG in cell supernatants 48-hours after transfection with the indicated plasmids. Transfections took place in **a)** normal murine fibroblasts, **b)** MB49 cells, and **c)** CT26.Cl25 cells. In b) and c), arrows indicate the presence of test bands, which reflect the presence of targeted reporter expression in excess of 20mIU/ml.

PSA test kits also reflected similarly exciting results. The sensitivity of the PSA rapid tests was well known as 2ng/ml. The test kits, shown in Figure 7, contained a second line between the test (T) line and the control (C) line that served as a standard to indicate 4ng/ml of PSA. In MF groups, positive readings (Lines by the “T” on the kits) were observed for samples transfected with  $P_{cmv-psa}$  immediately after supernatant flowed through the test region. Transfections using the cancer-specific promoters  $P_{cox2}$  and  $P_{opt}$  displayed faint but positive readings after 10 minutes of incubation. Both of

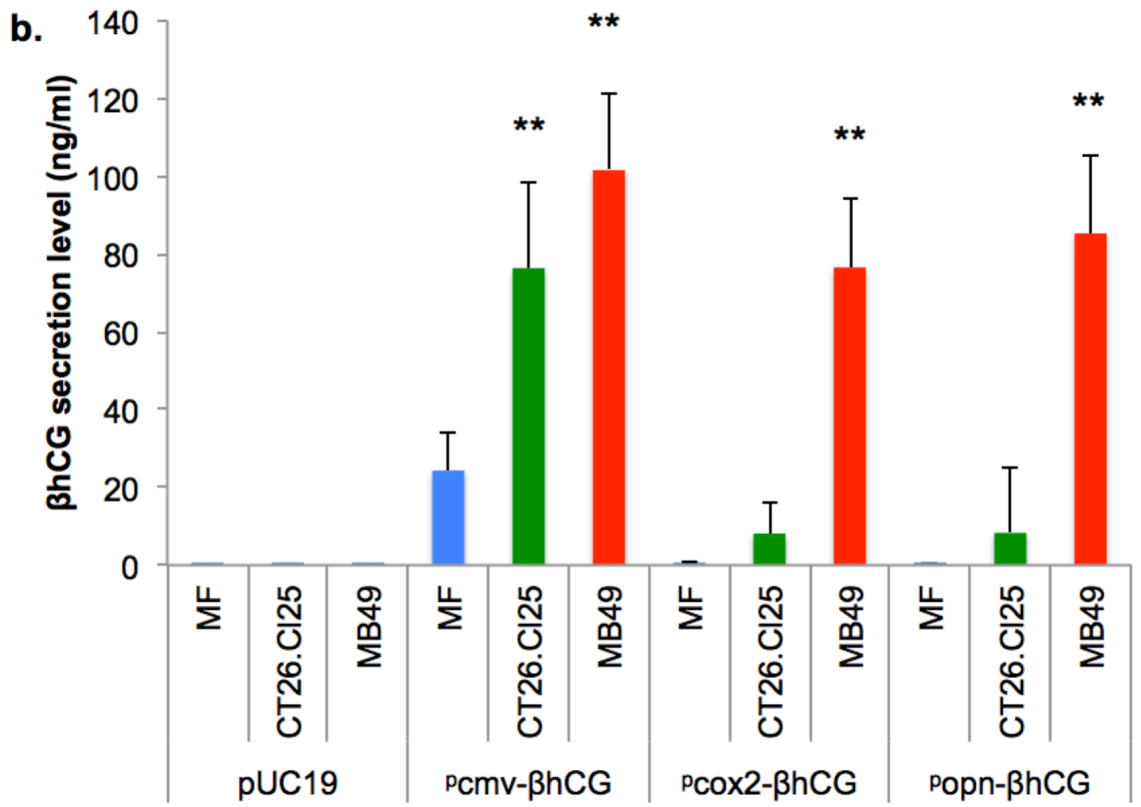
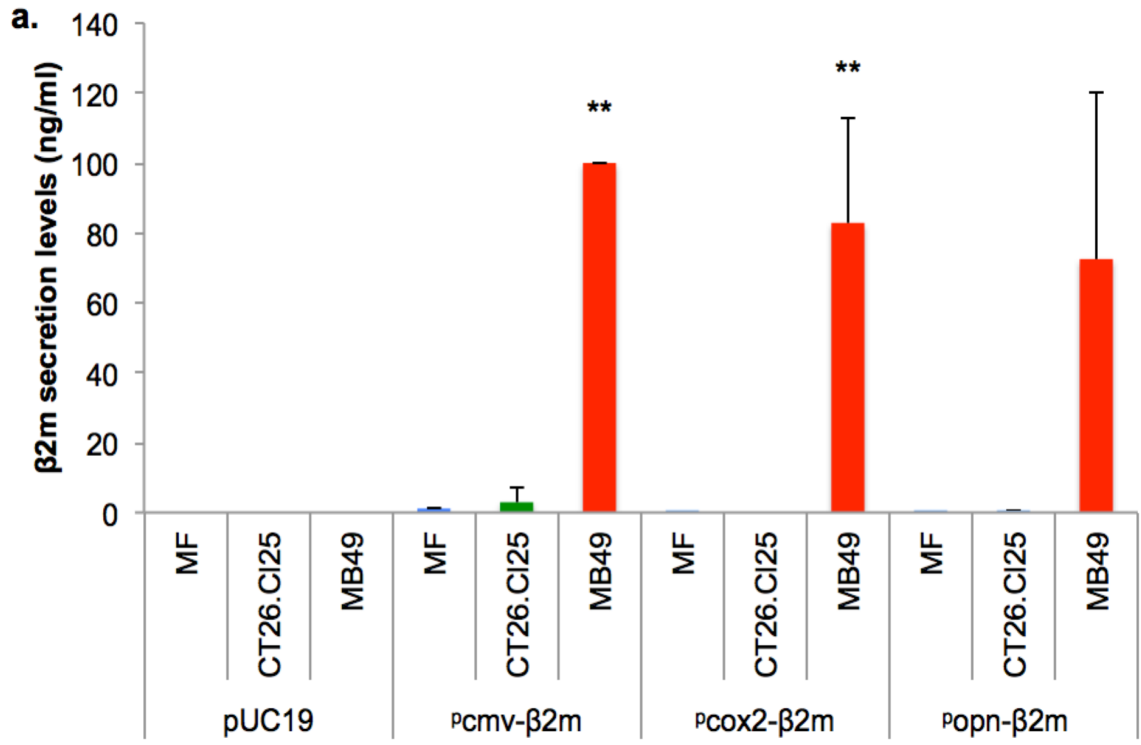
these bands were much weaker than the middle 4 ng/ml indicator line (*fig.4.7a*). In supernatants from transfected MB49 cells (*fig. 4.7b*), strong lines were present in samples transfected with  $P_{cmv-psa}$ ,  $P_{cox2-psa}$  and  $P_{opn-psa}$  immediately after samples of supernatants were loaded. All of these lines were stronger than the 4 ng/ml standards. The same results were obtained in the supernatants of transfected CT26 cells (*fig.4.7c*).



**Figure 4.7.** Lateral flow assays indicating the presence or absence of PSA in cell supernatants 48-hours after transfection with the indicated plasmids. Transfections took place in **a)** normal murine fibroblasts, **b)** MB49 cells, and **c)** CT26.C125 cells. C = Control band, T = Test band (sample being tested). The band between C and T corresponds to a 4 ng/ml standard.

#### 4.3.4. *Reporter expression, in vitro, as determined by immunoassays*

While mRNA levels are important for understanding what is going on inside the cell with respect to transcribing the delivered reporter plasmids, the ultimate success of the detection regimen depends upon the detection of the reporter proteins themselves. Figure 4.8 showed results reflecting detection of the reporter proteins in cell supernatants. Results were very encouraging in MB49 cells, for which expression-targeting yielded strong specificity versus normal fibroblasts, and strong reporter expression versus positive controls in all four cases. Results in the colon cancer cells were not as dramatic, with significance versus normal fibroblasts occurring only for transfections of <sup>P</sup>*cox2-psa* and <sup>P</sup>*opn-psa*.



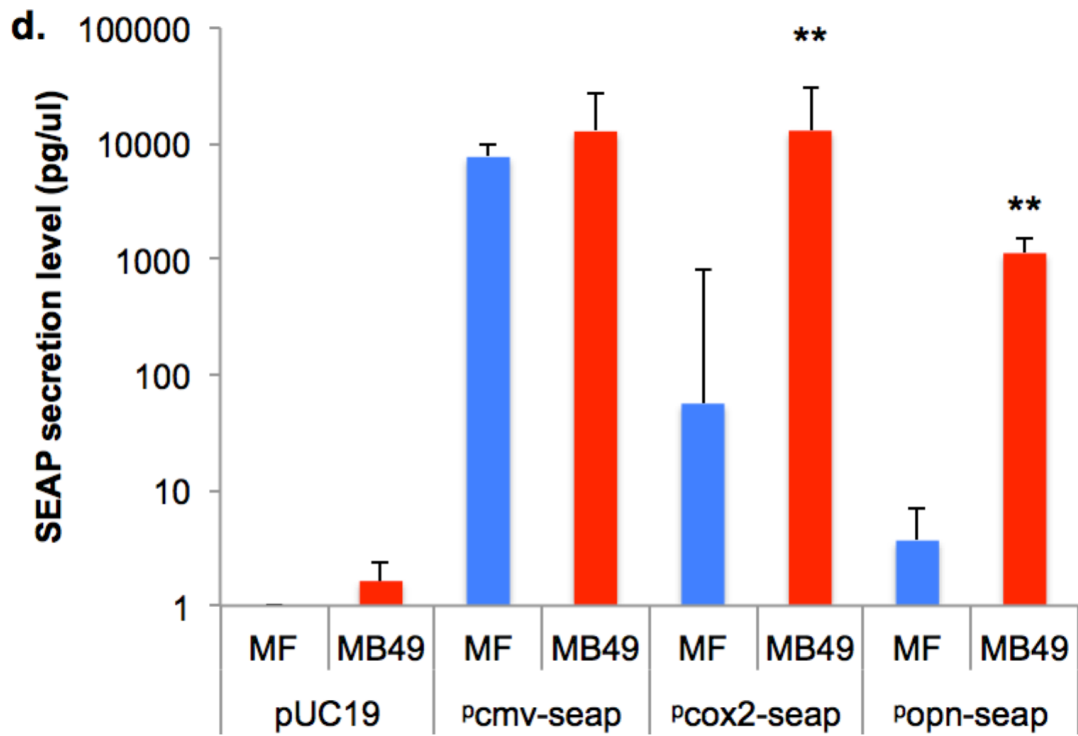
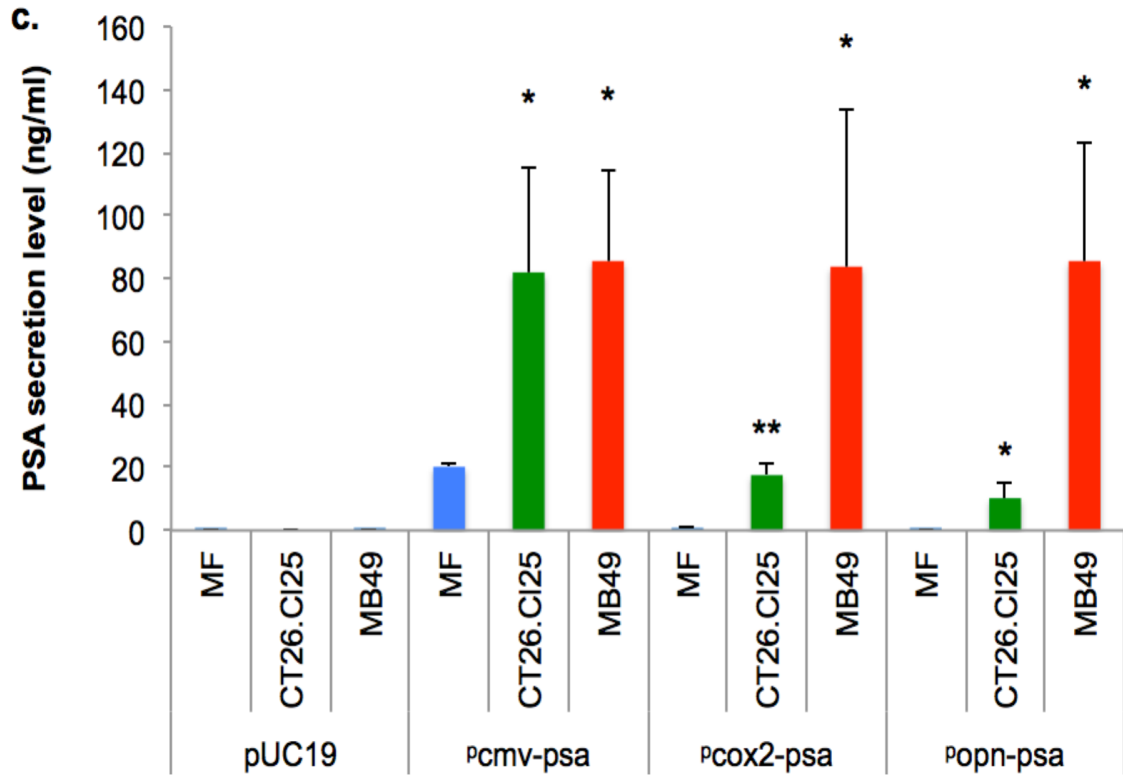


**Figure 4.8.** Reporter concentrations in the supernatants of normal murine fibroblasts (MF), murine colon cancer cells (CT26.Cl25) and murine bladder tumor cells (MB49) transfected with the indicated expression-targeted plasmids. Cell supernatants were run in duplicates. “\*” and “\*\*\*” indicate significant differences between the indicated cell line and the normal (MF) cell line ( $p < 0.05$  and  $0.01$ , respectively) (t-test,  $n \geq 3$ , more than three independent experiments were performed) **a)**  $\beta 2M$  **b)**  $\beta hCG$  **c)** PSA **d)** SEAP.

#### 4.3.5. Reporter expression, *in vivo*, as determined by immunoassays

Since the time-course experiment *in vivo* showed high reporter expression at 72 hours post-transfection in <sup>P</sup>*cox2-G.luc* groups (*fig 3.5*), here reporter secretion levels were analyzed in urine samples collected at 72 hours post-transfection from both normal mice and tumor-bearing mice. In tumor-bearing mice, <sup>P</sup>*cox2-psa*-treated mice produced significantly higher PSA concentrations versus tumor-bearing mice transfected with the pUC19 null vector (*fig 4.9a*). Of more direct significance as it relates to the cancer-detection system being investigated, both of the expression-targeting promoters, <sup>P</sup>*cox2* and <sup>P</sup>*opn*, yielded significantly higher PSA secretion into the urine of tumor-bearing versus normal mice when used to drive expression of the *psa* exon. If PSA concentrations in urine samples were adjusted by specific gravity, the same conclusion can still be made (*fig 4.9b*). The same expression/detection patterns were observed when the expression-targeting promoters were used to drive SEAP reporter exons (*fig. 4.10*). In tumor-bearing mice, both <sup>P</sup>*cmv-seap* and <sup>P</sup>*cox2-seap* trials produced significantly higher SEAP concentrations versus tumor-bearing mice transfected with the pUC19 null vector (*fig 4.10a*). However, only <sup>P</sup>*cox2-seap*-treated tumor-bearing mice yielded significantly higher SEAP secretion into the urine versus normal mice that were treated identically. There is little difference between original SEAP secretion levels and specific gravity-adjusted SEAP secretion levels (*fig 4.10b*).

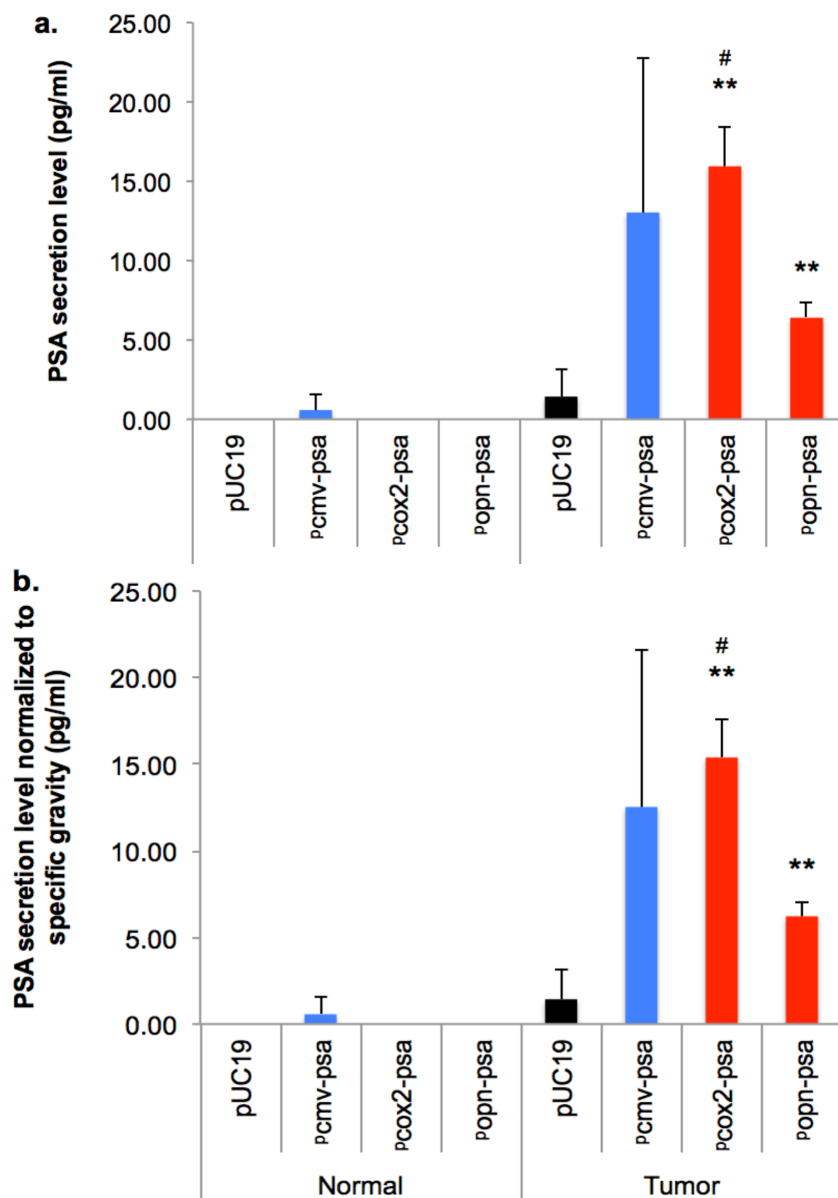


**Figure 4.9.** PSA concentrations (a) and PSA concentrations normalized to specific gravity (b) following transfection with the indicated plasmids. Urine samples were collected 72-hours post-transfection. “#” indicates a significant difference between the mean PSA level detected following transfections with *psa*-containing plasmids versus pUC19-treated negative controls (ANOVA, followed by

post hoc test,  $n=3$ , each group has three mice,  $p<0.05$ ). Limited by urine volume, urine samples were run in singlet. Standards were diluted using dilution buffer in the ELISA kit and standards were run in duplicate with an intra-assay coefficient variation of 8.4%. “\*\*\*” indicates significance differences between the means obtained for tumor-bearing versus normal mice receiving the same treatment (t-test,  $n=3$ , each group has three mice,  $p<0.01$ ).

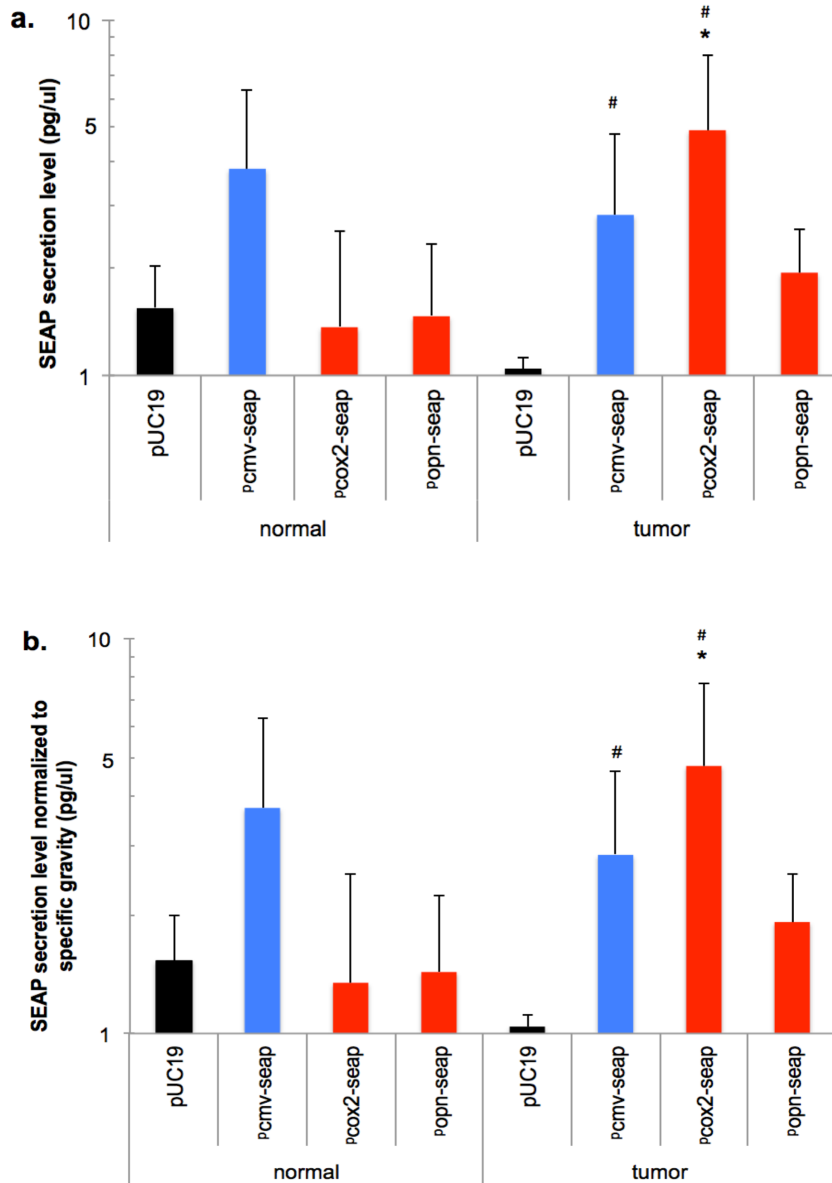


**Figure 4.10.** SEAP concentrations (a) and SEAP concentrations normalized to specific gravity (b) following transfection with the indicated plasmids. Urine samples were collected 72-hours post-transfection. “#” indicates a significant difference between the mean SEAP level detected following transfections with *seap*-containing plasmids versus pUC19-treated negative controls (ANOVA, followed by post hoc test,  $n \geq 3$ , each

group has at least three mice,  $p < 0.05$ ). “\*\*” indicates significance differences between the means obtained for tumor-bearing versus normal mice receiving the same treatment (t-test,  $n \geq 3$ , each group has at least three mice,  $p < 0.05$ ). Limited by urine volume, urine samples were run in singlet. Standards were diluted using dilution buffer in the chemiluminescent kit and standards were run in duplicate with an intra-assay coefficient variation of 5.3%.

#### 4.4. Discussion

These investigations were aimed at determining whether the technique of expression-targeted gene delivery could be used to elicit cancer cells to express standard biomarkers as an indication of the presence of tumor masses. Clinically, urine samples are easier to access than blood samples, and could provide a means by which patients could perform the reporter detection at home, following a transfection event administered by a physician. The system under investigation employed reporters that are secretable by cells and excretable in the urine. In the described experiments, the detection of biomarkers first took place by the analysis of cell supernatants *in vitro*, then via analysis of urine in a murine orthotopic model of bladder carcinoma.

In previous work by our laboratory, the secretable Gaussia luciferase was used to successfully detect the presence of cancer cells via urinalysis following expression-targeted gene delivery. In the work described here, plasmids encoding more common human proteins were engineered considering the reduction of possible immunogenic effects while expanding the number of probes that could be utilized simultaneously. The non-viral gene delivery vehicles are recommended for delivery of the plasmids to allow for repeated administrations of the plasmids in a given patient over the course of years.

High transcription levels are a vital factor in obtaining high secretion levels of reporter proteins. From real-time PCR data, it was found that  $\beta 2m$  expression-targeted trials in cancer cells did not produce transcription levels of  $\beta 2m$  that were distinguishable in tumor versus normal cells. However, transcription levels of both  $\beta hCG$  and  $psa$  genes,

directed by cancer-specific promoters, were significantly higher in cancer cells versus normal cells.  $\beta 2m$  therefore was not an ideal reporter. In normal fibroblast cells, the average fold change of  $\beta 2m$  transcription was lower than that of  $\beta hCG$  or  $psa$  regardless of the promoter tested (data not shown). This could indicate a universal mechanism that works to inhibit  $\beta 2m$  mRNA levels post-transcriptionally, or it could act on the protein itself in the cells tested. The murine  $\beta 2m$  mRNA sequence shares 71.67% identity with the human  $\beta 2m$  that was used for these experiments. A series of miRNAs such as mmu-miR-1905 and mmu-miR-677, which can bind to murine  $\beta 2m$  mRNA, may also bind to and help to degrade the human analog of  $\beta 2m$  mRNA if these miRNAs targeted sequences common to the two species. miRNAs that bind to coding regions of mRNAs are more inclined to inhibit translation than destabilize mRNAs.

Up-regulated transcription levels do not guarantee high secretion levels of proteins. For instance, CT26 cells, but not MB49 cells, that were transfected with  $P_{cox2-\beta hCG}$ ,  $P_{opn-\beta hCG}$ ,  $P_{cox2-psa}$ , or  $P_{opn-psa}$  showed significant elevation in  $\beta hCG$  or  $psa$  transcription levels versus those of similarly treated fibroblast cells. However, from ELISA results, CT26 cells that were transfected with these plasmids failed to show significantly large amount of  $\beta hCG$  or PSA when compared to similarly treated MF cells. Schwanhausser *et al.* discovered that mRNA levels accounted for about 40% of the variability in protein levels and the level of mRNA translation played an important role in determining the amount of protein amount inside cells (Schwanhausser *et al.*, 2013). Given that a gene was up-regulated to a high degree, the protein would become more likely to be secreted (Winter *et al.*, 2004). This implies that the more mRNA copies that

have accumulated in cells, the higher secretion capability the cell would have (assuming the protein is secretable). Although the transcription levels of reporter genes were significantly higher in CT26 cells versus MF cells, the changes in exogenous gene expression might not have been increased enough to produce a significant difference in secretion levels of *βhCG* or *psa* between CT26 and MF cells. This could also explain the low-to-undetectable level of  $\beta 2m$  secretion in CT26 cells that had been treated with plasmids driven by cancer-specific promoters.

High levels of reporter protein secretion were observed in MB49 cells transfected with plasmids encoding any of the three reporter genes. Even MB49 cells treated with *β2m*-encoding plasmids were able to secrete concentrations of  $\beta 2m$  comparable to those of  $\beta hCG$  or PSA in analogous experiments. It is possible that some invasive and malignant cells need to secrete *β2m* as an autocrine/paracrine factor, to promote tumor growth (Nomura et al., 2014). This could explain why MB49 cells had a higher protein secretion/gene transcription ratio for the investigated promoters; perhaps they had better exocytotic capability.

PSA and  $\beta hCG$  are both secreted proteins that have been used to monitor internal tumor growth by detecting them in mice urine samples. PSA is constitutively secreted by human prostatic epithelial cells (Webber et al., 1995), hCG is also able to secrete constitutively though its regulated secretory pathway exists in GH cell line (Bielinska et al., 1994) and other stimulating factors such as gonadotrophin-releasing hormone may be helpful for hCG secretion (de Medeiros and Norman, 2009). Selection of a

constitutively secreted protein seems promising for getting more accumulated proteins outside cells compared to proteins using regulated secretion pathways. Both  $\beta$ hCG and PSA were more secretable than  $\beta$ 2m in MF cells and CT26 cells. In CT26 cells, the change in transcription levels in  $P_{cmv-\beta hCG}$ -treated cells was significantly lower than in  $P_{cmv-psa}$ -treated cells. However, there was no significant difference of secreted protein concentrations between these two  $P_{cmv}$ -driven reporter gene transfection groups. As mentioned above, once a critical value of produced mRNA copies has been achieved, translation and secretion become the rate-limiting steps. Also in colon cell line, fold change of exogenous gene transcription in  $P_{cox2-\beta hCG}$ -treated cells was significantly lower than that in  $P_{cox2-psa}$ -treated cells. It seemed that *psa* mRNA was more stable and less vulnerable to degradation than  *$\beta$ hCG* mRNA. If cancer detection via expression-targeted gene delivery were to be applied in cancer cell lines such as CT26, *PSA* would be a protein preferable to  *$\beta$ hCG*.

*In vivo* local transfections have to overcome many barriers compared to *in vitro* transfections. The negative-charged glycosaminoglycan (GAG) layer that separates the urothelial layer from the bladder lumen could interact with DNA/polycation complexes, preventing them from entering into cells. Urinary GAG excretion has been seen to be significantly elevated in the bladders of bladder carcinoma patients (Atahan et al., 1996). The *in vivo* studies performed showed both SEAP and PSA could be detected from tumor-bearing mice in  $P_{cox2}$  transfection groups 72 hours after transfection. This was consistent with our previous research involving delivery of genes encoding *Gaussia* luciferase to the bladder. While  $P_{cox2}$ - or  $P_{opn}$ -driven reporter genes displayed

expression peaks at 48 hours post-transfection *in vivo*, generally higher expression was shown at 72-hours post-transfection for  $P_{cox2}$ -*Gluc*-treated group.

Although urine samples are easy to collect and process, their variations in volume, protein concentration, pH, and density are large even within a single individual (Thomas et al., 2010). Hence, the concentrations of endogenous components in urine are generally normalized to osmolality, specific gravity, or creatinine concentration. Specific gravity and creatinine normalization procedures have yielded a good correlation ( $R^2=0.94$ ) for normalizing urinary drug concentrations (Cone et al., 2009). However, another study suggested that uncorrected biomarker concentrations be used for biomarker studies in urine samples containing hematuria, which is very common in patients [or animals] with bladder carcinoma (Reid et al., 2012). We attempted to use specific gravity normalized reporter concentrations as well as unadjusted reporter concentrations in urine samples, with both methods yielding the same conclusions.

This study proved the concept of urine-based cancer diagnosis via expression-targeted gene delivery. It provides a fresh potential diagnosis option that is different from traditional cancer biomarker screening. “Secretable” is one of the most important criteria that biomarkers for this system should meet. It is not necessary for an endogenous protein being expressed by a cancer cell to be secretable; the expression-targeted system would link expression of that particular protein with the expression of a delivered transgene, thereby allowing detection of the endogenous biomarker by proxy.

## 4.5. Conclusion

A urinary-based cancer detection system was developed based upon expression-targeted delivery of plasmids encoding secretable reporters.  $\beta$ 2m,  $\beta$ hCG, PSA, and SEAP reporters were used, with results indicating that PSA and SEAP were good reporters in an orthotopic model of bladder cancer. (A non-bioactive fragment of  $\beta$ hCG would potentially also be very useful, based on the data obtained *in vitro* for  $\beta$ hCG.) On the targeting side, both  $P_{cox2}$  and  $P_{opn}$  were able to yield relatively high levels of downstream gene expression in bladder carcinoma cells, although the colon cancer cell line tested was less responsive *in vitro*. *In vivo* results demonstrated the utility of the detection system for bladder tumors, and existing urine-based lateral assays showed proof-of-concept for a potential home-based cancer detection system.

## Conclusions

This project is aimed to detect cancers via expression-targeted gene delivery. The cyclooxygenase-2 promoter ( $P_{cox2}$ ) and osteopontin promoter ( $P_{opn}$ ) were selected to drive the expression of *G.luc* both *in vitro* and *in vivo*.  $P_{cox2}$  and  $P_{opn}$  showed specificity in tumor-bearing mice versus normal mice but  $P_{opn}$  was not as good as  $P_{cox2}$ . A positive correlation was established between maximal luciferase levels in urine samples from  $P_{cox2}$ -*G.luc*-treated tumor-bearing mice and tumor burden. This system could detect bladder tumors larger than 19.1 mg. The sensitivity of this assay was not high enough and may not be appropriate for early detection of bladder cancer.

Further development of the detection system involved branching out from *G.luc* in the search for additional secretable reporters that could be detected in the urine. *In vitro* results indicated that *βhCG*, *psa* and *seap* were good reporter genes while *β2m* was not good for the detection system. *In vivo*, the PSA and SEAP reporters were elevated in tumor-bearing mice having undergone treatments with  $P_{cox2}$ -driven transgenes encoding these proteins. However, the elevation of PSA levels in urine cannot be detected by a commercial lateral flow assay.

For future works, we should optimize our system to amplify reporter levels via the following attempts: 1) construct multiple copies of promoters or introduce a two-step

transcription amplification system to increase promoter strength; 2) optimize reporter genes to obtain better secretion ability; 3) try other non-viral transfection reagents such as cyclic PEI. This project also relies on a sensitive diagnostic assay to detect reporters. The current commercial  $\beta$ hCG and PSA lateral flow assays were not made for the purpose of cancer detection. We need more sensitive lateral flow assays that are customized for this purpose in the future.

## **Appendix A An Evaluation of Gene Delivery using Cyclic Poly(ethylene imine) and Exact Linear Analogs**

### **A1. Introduction**

Fundamentally, gene therapy involves the expression of exogenous DNA, which relies upon the successful transport of intact DNA into the nuclei of the target cells. Gene therapy offers promise to manage or possibly cure many genetic disorders in which a malfunctioning gene is attenuated by a “healthy” exogenous gene (Zhang et al., 2010, Putnam, 2006). Gene therapy also has been probed for use in disease prevention, such as vaccinations, as well as anti-cancer therapies (Putnam, 2006, Zhang and Godbey, 2011b, Zhang et al., 2009, Zhang et al., 2008, Pack et al., 2005, Vile et al., 2000, Kerr, 2003, McNeish et al., 2004). Because of the poor stability of DNA *in vivo*, appropriate vectors are required to protect the genetic payload during transport, as well as affect its delivery across the cell membrane and into the nucleus. While viral capsids represent attractive vectors due to their high efficiency, concerns exist about their immunogenicity (Marshall, 2000, Machitani et al., 2011) and their cost (Pack et al., 2005). Cationic polymer vectors have emerged as a promising alternative because of their scalable production, as well as

synthetic ease of tuning their size, structure, and functionality. While a number of amine-containing, cationic polymers have been explored, including PEI (Boussif et al., 1995), poly-L-lysine (PLL), poly(2-(dimethylamino)ethylmethacrylate) (PDMAEMA), and polyamidoamine (PAMAM) dendrimers, non-viral gene delivery still suffers from lower transfection efficiencies when compared to viral capsids and high cytotoxicity attributed to their polycationic character (Pack et al., 2005, Putnam, 2006, Prevette et al., 2010, Tang et al., 1996).

Of these polymeric carriers, PEI-based polymers remain one of the most successful classes of synthetic vectors for gene transfection (Boussif et al., 1995). At physiological pH, the cationic backbone of the polymer efficiently complexes with the anionic phosphates of DNA; however, such polycations also exhibit cytotoxicity (Putnam, 2006, Parhamifar et al., 2010). As a result, amine-rich polymers have been the subject of numerous studies aimed at understanding the relationship between structural parameters, such as molecular weight, degree of branching, amine spacing, and amine number on DNA/polymer complexation potential, transfection efficiency, and cytotoxicity (Godbey et al., 1999, Prevette et al., 2010, Tang et al., 1996, Grayson and Godbey, 2008, Fischer et al., 1999, Abdallah et al., 1996, Ogris et al., 1998, Morimoto et al., 2003, Thomas and Klibanov, 2002).

Though much research with PEI has shown that the molecular weight is a critical parameter for optimizing gene delivery (Godbey et al., 1999, Abdallah et al., 1996, Fischer et al., 1999, Ogris et al., 1998, Morimoto et al., 2003, Thomas and Klibanov,

2002), truly systematic studies of PEI architectural effects on transfection efficiency and cytotoxicity remain wanting. This neglect is largely a consequence of the synthetic challenge in preparing PEI libraries in which the architecture is varied systematically yet the amine composition (e.g. primary vs. secondary or tertiary) and molecular weight remain the same. Without access to such architectural analogs, it is difficult to draw meaningful conclusions as to the specific relationship between macromolecular structure and biological activity. For example, there is still some debate as to whether branched PEI shows higher transfection efficiency than linear PEI; this comparison is complicated because of the multiple parameters which are changed, including the substitution of the amines, the absolute molecular weight, the molecular weight dispersity of the sample, the charge density/compactness and the structural flexibility, as well as the degree of branching.

In one of the more systematic studies addressing the effect of polymer architecture on gene transfection, Tang et al (Tang et al., 1996) studied whole PAMAM dendrimers relative to degraded PAMAM dendrimers for use as gene delivery agents. The partially degraded PAMAM dendrimers exhibited better transfection efficiency than the parent non-degraded dendrimers or highly degraded dendrimers. While additional reports exist for the gene delivery capabilities of well-defined non-linear polymers such as dendrimers (Merkel et al., 2009) and star polymers (Xu et al., 2009, Nakayama, 2012, Cai et al., 2012, Georgiou, 2014), truly systematic comparisons remain rare. Herein, we explore the properties of two PEI polymers that contain the same number and type of amines, but

differ only in their architecture. This has been carried out by preparing for the first time well-defined cyclic PEI as well as their exact linear analogs.

Cyclic polymers exhibit unique physical properties owing to their unusual topology, but detailed studies have been limited due to technical difficulties in preparation and purification (Laurent and Grayson, 2009, Zhu et al., 2003, Lescanec et al., 1995, Hadjichristidis et al., 2001). Cyclic macromolecular topologies also impart unique and potentially useful biological properties. For example, Szoka and coworkers demonstrated that cyclic polymer scaffolds exhibit increased blood circulation times in vivo (Nasongkla et al., 2009) and also yield greater tumor accumulation than their linear polymer counterparts (Chen et al., 2009). Recently, a versatile cyclization method utilizing the highly efficient copper-catalyzed azide-alkyne cycloaddition (CuAAC) reaction has been developed to yield a wide variety of high purity cyclic polymers, including polystyrene (Laurent and Grayson, 2006), polyesters (Hoskins and Grayson, 2009), and block copolymers (Eugene and Grayson, 2008). This route offers synthetic access to a wide variety of cyclic macromolecules to enable their evaluation for a range of applications. Recent studies of cyclic PDMAEMA has suggested that cyclic polymers have advantages for nucleic acid delivery (Wei et al., 2013).

In order to investigate the utility of cyclic PEI for gene delivery, linear poly(2-ethyl-2-oxazoline) (PEOx) precursors (Aoi and Okada, 1996, Kobayashi et al., 1982, Lambermont-Thijs et al., 2010) were prepared via the ring-opening polymerization of 2-ethyl-2-oxazoline such that azide and alkyne functionalities were located at opposite ends

of the polymer chain. Utilization of the CuAAC cyclization technique provided cyclic PEOx samples with the identical molecular weight as their linear precursors. The acid-catalyzed hydrolysis of these cyclic and linear PEOx sets therefore provided access to a library of cyclic and linear PEI samples that were subsequently investigated as vehicles for the delivery of plasmids encoding red fluorescent protein (RFP).

## **A2. Methods and Materials**

### *A2.1. DNA protection and complex stability assay*

#### *Buffers and solutions:*

*1× alkaline buffer:* defined by 1 L containing 5mL of 10N of NaOH, 2mL of 0.5M of EDTA (pH 8.0); *1× digestion buffer:* 0.1M of sodium acetate, 5 mM of MgSO<sub>4</sub>, titrated to pH 8.0; *dilution buffer:* 25 mM of tris-HCl, 50% glycerol (v/v), pH 7.6 (at 4°C); *8× stop solution:* equal volumes of 0.5M of EDTA (pH 8.0), 2N NaOH, and 0.5M NaCl solutions.

#### *DNase digestion:*

The reaction mixture for DNase digestion contained 2.5  $\mu$ L of 4× digestion buffer, 5.0  $\mu$ L of either DNA or PEI/DNA complexes, and 2.5  $\mu$ L of DNase 1 dissolved in dilution buffer. The digestions were allowed to proceed for 3 min at room temperature, and were halted by the addition of 6  $\mu$ L of 8× stop solution.

After the addition of the 8× stop solution, samples were loaded into an alkaline gel containing 0.5% agarose for electrophoresis for one hour at 100 V. The gel was made by

melting agarose in three parts water, to which one part hot 4× alkaline buffer was added to yield a 0.5% gel.

#### A2.2. *Cells and Media*

Human foreskin fibroblasts (HFF-1) (ATCC, Manassas, VA) were cultured in Dulbecco's Modified Eagle Medium supplemented with 15% fetal bovine serum and 100 U/ml each of penicillin and streptomycin. Cells were maintained at 37°C, 5% CO<sub>2</sub>, and saturated humidity.

#### A2.3. *Transfection experiments*

Cells were plated in 24-well tissue culture dishes at a concentration of 21,000 cells/well and allowed to incubate for 16 hours prior to transfection. PEI/DNA complexes were prepared at different N:P ratios directly before every transfection. Cell media were removed from each well and replaced with 417.8 μl serum-free transfection medium. 20.89 μl of PEI/DNA complex solution were added to the cells and transfections were allowed to proceed for 2 hours, after which the transfection media were replaced with 417.8 μl of the growth medium specific to those cells. Cells were then incubated for a total of 24 hours after transfection.

#### A2.4. *Luciferase Assay*

HFF-1 cells were transfected as described for 24-well plates with plasmids encoding Gaussia luciferase, a secretable reporter that was detected in cell culture supernatants. Gaussia luciferase expression was measured using 20 ul supernatant samples with

Gaussia Luciferase assay kits (New England BioLabs), used according to manufacturer's instructions. Luminescence was detected using a Victor X3 2030 Multilable Plate Reader (PerkinElmer, Waltham, MA).

#### *A2.5. Viability assay*

Cells were transfected with null vectors pUC19 (New England Biolabs, Ipswich, MA, USA) in the 24-well plates, with the addition of a SHAM control where 21  $\mu$ l of 0.9% saline were added to a well instead of PEI/DNA complexes. Transfections proceeded for two hours for linear PEI analogs. At 24 hours following transfection, growth media were removed from each well and cells were washed twice with 210  $\mu$ l of PBS buffer to remove non-adherent cells. 62.7  $\mu$ l trypsin were then added to each well followed by incubation for several minutes until all remaining cells detached. 146.2  $\mu$ l of complete medium was then added to each well systematically to collect a maximum number of cells. Flow cytometry was utilized for cell counting. Percent viability was defined as (the number of live cells for the sample well) / (the number of live cells for the Sham well).

#### *A2.6. Dynamic Light Scattering Measurements*

PEI/DNA complexes were made at 40:1 (cyclic and linear PEIs, samples 4c, 3c, 3d), 7.5:1 (branched), and 0:1 (DNA-only control). The DNA used consisted of linear fragments originating from herring sperm, (Sigma, Cat. # D3159). A total of 1.5 ml was made for each sample (equal to 15 transfection doses, a volume needed for the particular apparatus being used, a NICOMP 380, Partical Sizing Systems, Port Richey, FL.) Samples were analyzed using a 20  $\mu$ sec channel width for 2-minute analysis cycles.

Three such cycles were used for each sample.

#### *A2.7. Zeta Potential Measurements*

The same samples used for dynamic light scattering were used for zeta potential analysis. DNA controls consisted of 1.8  $\mu\text{g}$  of DNA in 50  $\mu\text{l}$  normal saline, diluted with 10 ml of 1mM KCl. For each sample of PEI/DNA complexes, 1 ml of the sample used for DLS analysis was diluted with 0.5 ml of 1 mM KCl. A total of 1.5 ml of each diluted sample was used for analysis via a NanoBrook 90 Plus PALS zeta potential analyzer (Brookhaven Instruments, Holtsville, NY).

### **A3. Results**

#### *A3.1. DNA protection and complex stability assay*

PEI/DNA complexes were made with the three architectures of PEI, and exposed to DNase I for 3 minutes. The concentrations of DNase I were varied as indicated in Figure 3. The method of displaying the amount of DNase I is based upon 5 Units of the enzyme being diluted 1:2 for this series of experiments. From the figure, it can be seen from the position of the smear in the free-DNA lanes that the unbound DNA is digested more as DNase I concentration is increased (the smear runs faster, indicating smaller fragments), until it is completely digested by exposure to 5/2 U of DNase I for 3 minutes. It can also be seen that DNA protected by B-PEI remains very well-protected, as shown by the lack of a smear even at 5/2 U of DNase I. Cyclic and Linear PEIs offer some protection, but not as much as branched PEI. The intensity and distance travelled in the gel indicate that

cyclic PEI offers more protection to the DNA it carries than does linear PEI of the same size.

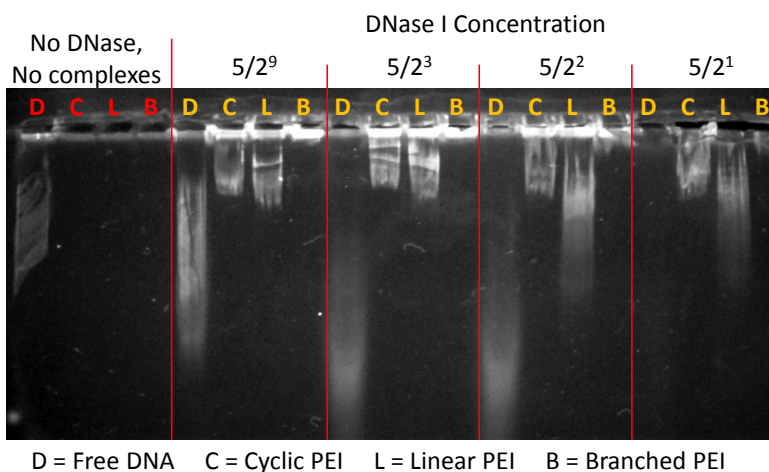


**Figure A1:** DNA protection and complex stability assay. PEI/DNA complexes were made with cyclic **4d**, linear **3d**, and branched PEI at N:P ratios of 20:1, 20:1, and 7.5:1, respectively, with free DNA serving as a control. Complexes were exposed to DNase I at the indicated concentrations for 3 minutes, after which the reaction was stopped and the samples were immediately loaded into an alkaline gel to separate the DNA from its carrier.

### A3.2. Gene delivery

Transfection studies were performed with the full library of linear PEI, cyclic PEI and linear triazole control PEI samples upon human foreskin fibroblast (HFF-1) cells (ATCC, Manassas, VA) using 25kD branched PEI as a positive control (Fig. A2a). The polymers were used to complex and deliver plasmids encoding a red fluorescent protein (pCMV-DsRed- Express, Clontech, Mountain View, CA). It was found that polymers with fewer

(21-42) repeat units, such as **3a-b** and **4a-b**, generally did not yield positively transfected cells. On the other hand, polymers of more repeat units (70-84) such as **3c-d** and **4c-d** yielded significant RFP expression.

Additional transfection studies with Gaussia luciferase were performed with freshly synthesized batches of **4c**, **3c**, and **3d**, along with a different preparation of branched PEI, to assess the difference in the total amount of gene expressed for the three architectures (Fig. A3). Samples of **3d** were included to further investigate the potential of these different PEI architectures for gene delivery. It was again found that the cyclic architecture tended to outperform the linear counterpart in terms of transfection efficiency.

In general, cyclic polymers showed significantly higher transfection efficiencies of RFP than their linear counterparts and, at optimal N:P ratios (ratio of nitrogen in PEI to phosphorus in DNA), yielded transfection efficiencies comparable to those of the 25kDa (~ 600 repeat units) branched PEI positive control (Abdallah et al., 1996, Thomas and Klibanov, 2002). The linear PEI triazole control polymer with 80 repeat units (**7g**) generally yielded transfection efficiencies that were similar to those observed for the linear PEIs having 70 (**3c**) and 84 (**3d**) repeat units, suggesting that the substantial increase in transfection observed for the cyclic polymers is a result of PEI architecture rather than a modification of the end group functionalities.

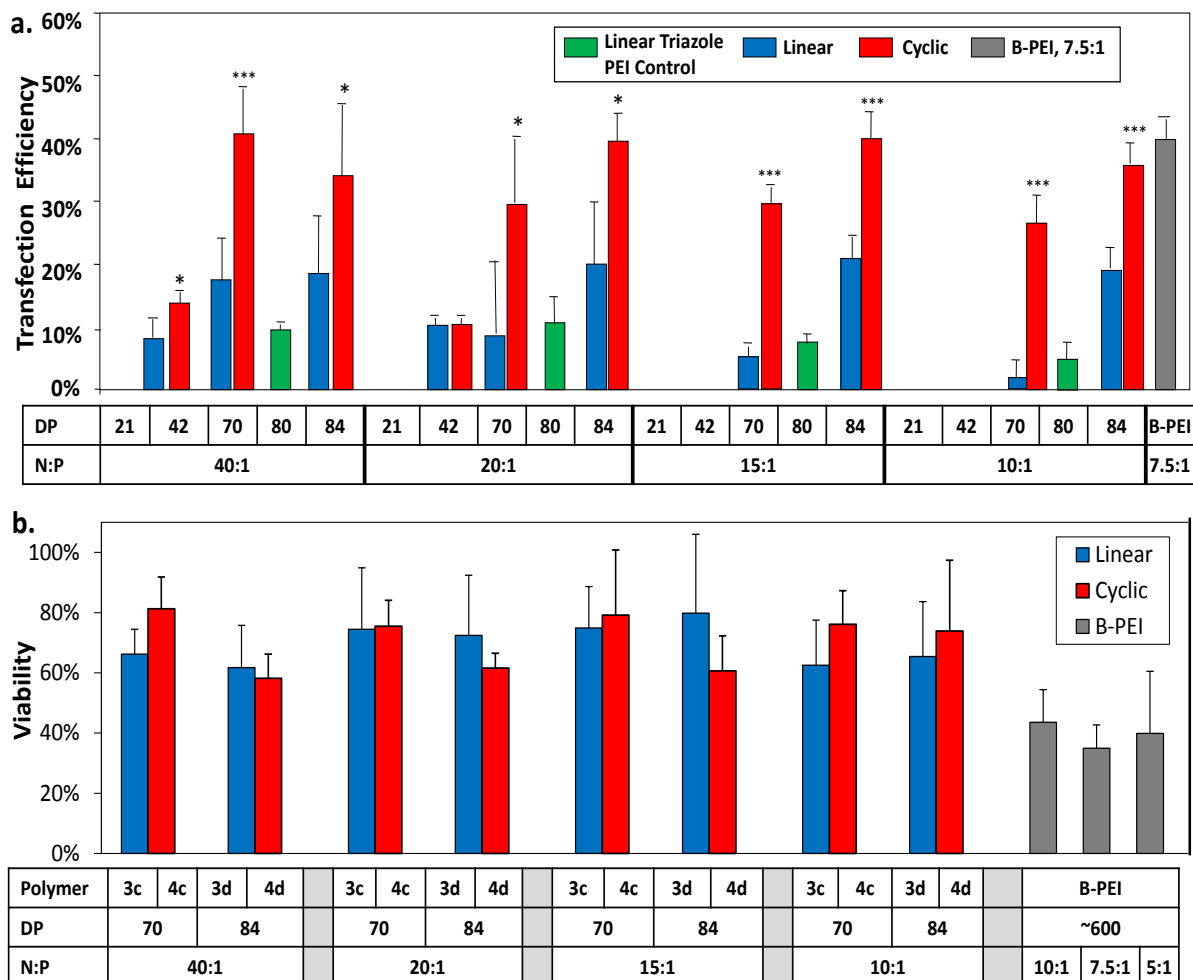


**Figure A2.** a) Transfection efficiencies with HFF-1 cells for linear and cyclic PEI at different N:P ratios. (\* = Significantly different from the linear version of the same polymer at the same N:P,  $P < 0.05$ ; \*\*\* = Significantly different from the linear version of the same polymer at the same N:P,  $P < 0.005$ ) b) Viability of cyclic polymers 4c and 4d normalized to SHAM and branched PEI (B-PEI) at different N:P ratios for HFF-1 cells. There was no difference in means between the normalized numbers of viable cells obtained with polymer 4c and 4d, at all N:P tested, and Sham-treated groups. (ANOVA,  $n \geq 3$  for each group,  $P = 0.125$ ).

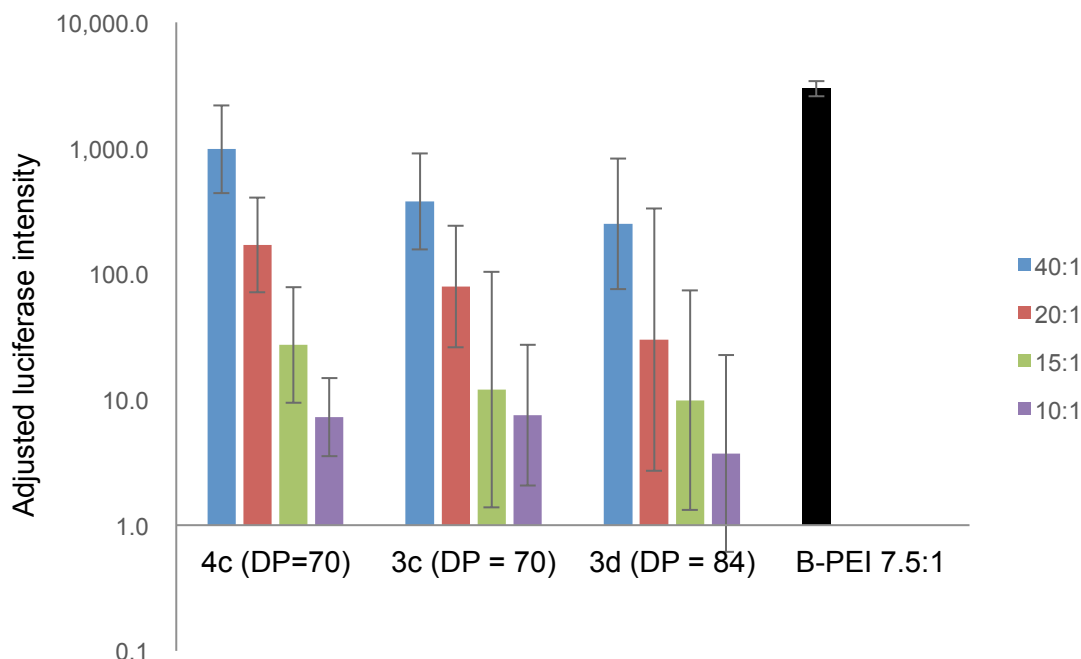


**Figure A3.** Results of transfections with Gaussia luciferase reporter plasmids, as delivered by cyclic (4c), linear (3c and 3d), and branched (B-PEI) at four different N:P ratios. Two-hour transfections took place in HFF-1 cells.

### A3.3. Cell viability

Viability studies were performed on HFF-1 cells using the two best-performing cyclic PEI samples **4c** and **4d** (70 and 84 repeat units) as well as their linear analogs, **3c** and **3d**, and compared with branched PEI of 600 repeat units (*fig. A2b*). The cyclic polymers used at the 20:1, 15:1, or 10:1 (or 40:1 for the 84-repeat version) N:P ratios were seen to be significantly less cytotoxic than branched PEI used at a 7.5:1 N:P (ANOVA,  $n \geq 3$ ,  $P=0.0002$ ).

#### *A3.4. Further characterization*

PEI/DNA complexes were made with cyclic, linear, and branched PEIs for comparisons of size (Fig. A4a) and surface charge concentration (zeta potential) (Fig. A4b). Transfection complexes made with cyclic (**4c**) and linear (**3c**, **3d**) PEIs were made at the 40:1 N:P ratio, and those using branched PEI were made at 7.5:1. It was noted from dynamic light scattering data that DNA was condensed in the presence of PEI, with the PEIs that yielded better transfection efficiency (**4c** and B-PEI) also yielding more DNA condensation. The zeta potentials of the tested PEI/DNA formulations reflected the excess of PEI ( $N:P > 1$ ). With the branched architecture having a slightly higher average zeta potential, despite having the relatively lower N:P ratio (7.5:1 versus 40:1).

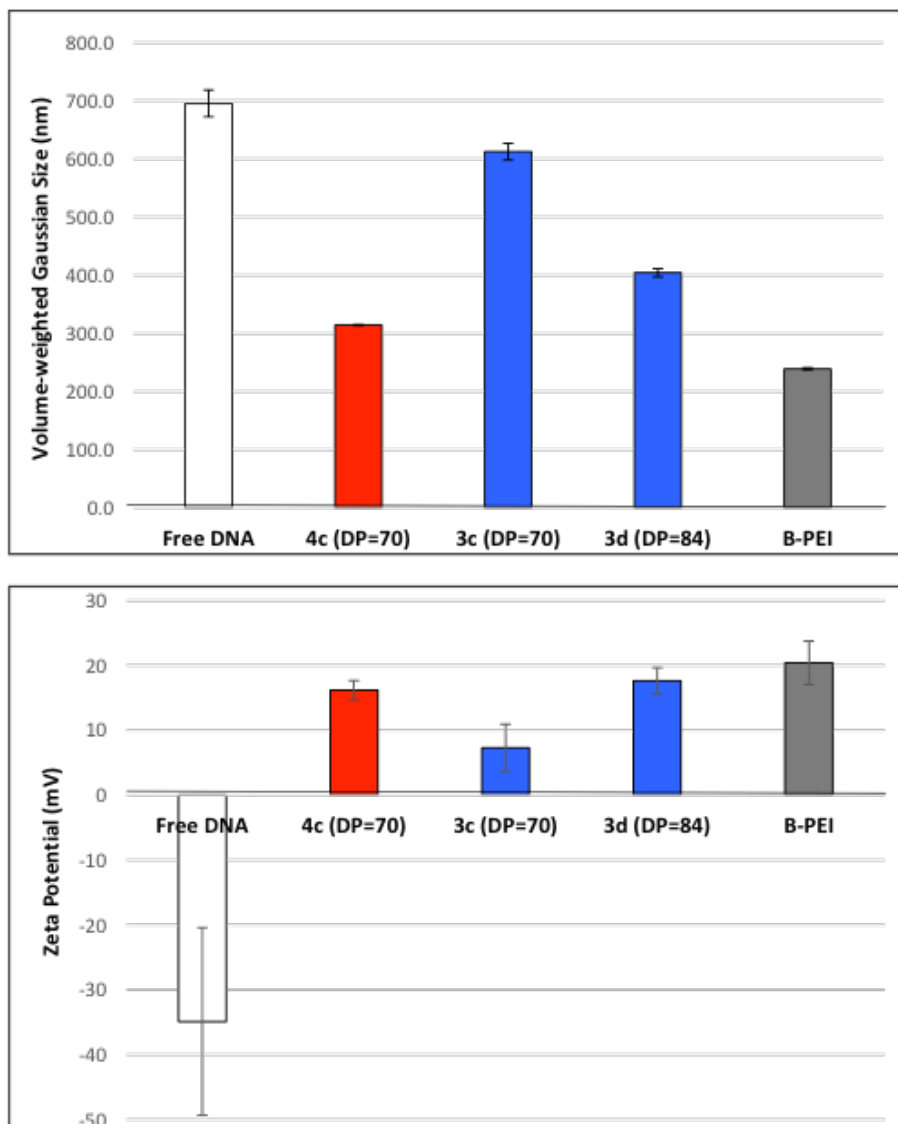


**Figure A4.** a) Sizes of transfection complexes, as determined via dynamic light scattering. b) Zeta potentials of transfection complexes. For both panels, complexes made with cyclic (4c) and linear (3c, 3d) PEIs were made at the 40:1 N:P ratio, those using branched PEI were made at 7.5:1.

## A4. Discussion

The transfection efficiency of the two largest and most promising cyclic polymers (70 and 84 repeat units, depicted in red, *fig. A2a*) were compared against their linear analogs at each of four different N:P ratios (40:1; 20:1; 15:1; and 10:1, depicted in blue) in HFF cells. The transfection efficiency was consistently higher for each cyclic PEI than its linear analog, regardless of N:P ratio and molecular weight, confirming that the cyclic PEI architecture affords a unique advantage in affecting gene delivery. Furthermore, DNA protection (*fig. A1*) and condensation studies (*fig. A4*) show that the cyclic PEI offers more protection and condenses DNA to a smaller size than the linear PEI. The linear PEI triazole control (depicted in green *fig. A2a*) sample with 80 repeat units (**7g**) exhibited transfection efficiencies in line with the azido/alkyne functionalized linear PEIs (**3c, d**) with 70 and 84 repeat units, suggesting that the improved transfection observed for the cyclic polymers is not a result of the triazole functionality or any trace contaminants that may remain from the CuAAC reaction. Branched PEI is typically used as a benchmark for transfection (Wang et al., 2013, Fu et al., 2012), so these cyclic and linear PEI data were also compared to a “gold standard” 25 kDa MW branched PEI (Abdallah et al., 1996, Thomas and Klivanov, 2002) (~600 repeat units) at an optimized 7.5:1 N:P ratio. While the transfection efficiency for branched PEI generally improves with increasing molecular weight (Godbey et al., 1999, Fischer et al., 1999), the cyclic PEIs with only 70 and 84 repeat units exhibited significantly improved transfection for the HAE cells relative to the optimized, branched PEI (not shown), and performed equally as well as the much larger branched PEI in the case of HFF cells (*Fig. A2a*). These observations together suggest that the cyclic topology may offer a unique

advantage with respect to the more traditional linear and branched PEIs for gene delivery applications.

While the exact origin of the cyclic polymers' increased transfection efficiency is still under investigation, there are two significant physical differences between the linear and cyclic analogs that likely play a role. First, the cyclic polymers exhibit a more compact conformation which, when protonated, results in a higher charge density than their linear counterparts. This hypothesis concurs with previously reported studies comparing star and linear PEIs that attributes the improved transfection efficiency of stars to their increased charge density (Nakayama, 2012, Cai et al., 2012). A related physical consequence of the cyclic topology is a reduced flexibility relative to linear analogs, which may have entropic as well as enthalpic consequences for binding DNA. It is proposed, then, that an enhanced interaction with DNA is a major factor in the observed improvement in RFP expression for the cyclic PEI samples. The dynamic light scattering data (Fig. A4a) does show the cyclic polymer (**4c**) condensing DNA to a smaller size than its linear analog (**3c**), which correlates to a PEI sample that yielded higher transfection efficiency. DNA protection analysis also showed greater protection afforded by the cyclic PEIs versus their linear analogs. Interestingly, the cyclic polymers also show minimal changes in transfection efficiencies as N:P ratios are varied, while the analogous linear polymers studied (and the branched PEI polymer, reported elsewhere (Boussif et al., 1995)) show an apparent decreasing transfection efficiency as the N:P ratio is decreased toward 1:1.

Often, factors that improve transfection efficiency, such as increasing molecular weight, also significantly increase toxicity (Godbey et al., 1999), requiring a practical

compromise between these two critical parameters. In general, the cyclic polymers were less toxic than the 25kDa branched PEI (~600 repeat units), despite the fact that the cyclic polymers were used at much higher N:P ratios. However, more significantly, this study demonstrated that the cyclic PEI exhibits significantly greater transfection efficiency relative to linear analogs (Fig. A2a). Compared with the transfection efficiencies of branched PEI controls, the cyclic architecture yielded comparable (or greater, depending on cell type) transfection efficiency *while* exhibiting reduced cytotoxicity, which represents an alternative and exciting approach for simultaneously optimizing these two critical parameters for gene delivery. The reduced toxicity relative to the branched controls is likely a consequence of significantly reduced molecular weight of the cyclic samples. However, the full effect of PEI architecture and the triazole functional group on cell viability will require further investigation.

## **A5. Conclusion**

The delivery of genes encoding a red fluorescent protein was explored with 4 different molecular weights of linear and cyclic PEIs, at 4 different N:P ratios. The delivery of genes encoding Gaussia luciferase was also evaluated with 3 freshly synthesized batches of 4c, 3c, and 3d at 4 different N:P ratios. Cyclic PEIs were found to significantly outperform their linear analogs at every molecular weight and N:P ratio. Likewise, the cyclic PEIs also performed as well as, or better than, the current gold standard: 25K branched PEI, but with significantly reduced toxicity. In agreement with previous reported studies, it is believed that the improved transfection efficiencies are, in part, the result of increased charge density resulting from the more compact structure of

the cyclic polymers. These studies confirm that the cyclic architecture provides unique advantages for gene delivery and also highlight the value of systematic architectural studies for optimizing polymer-based vectors for gene delivery.

## Appendix B Plasmid Maps

Maps are provided in this section for all the plasmids involved in this work.

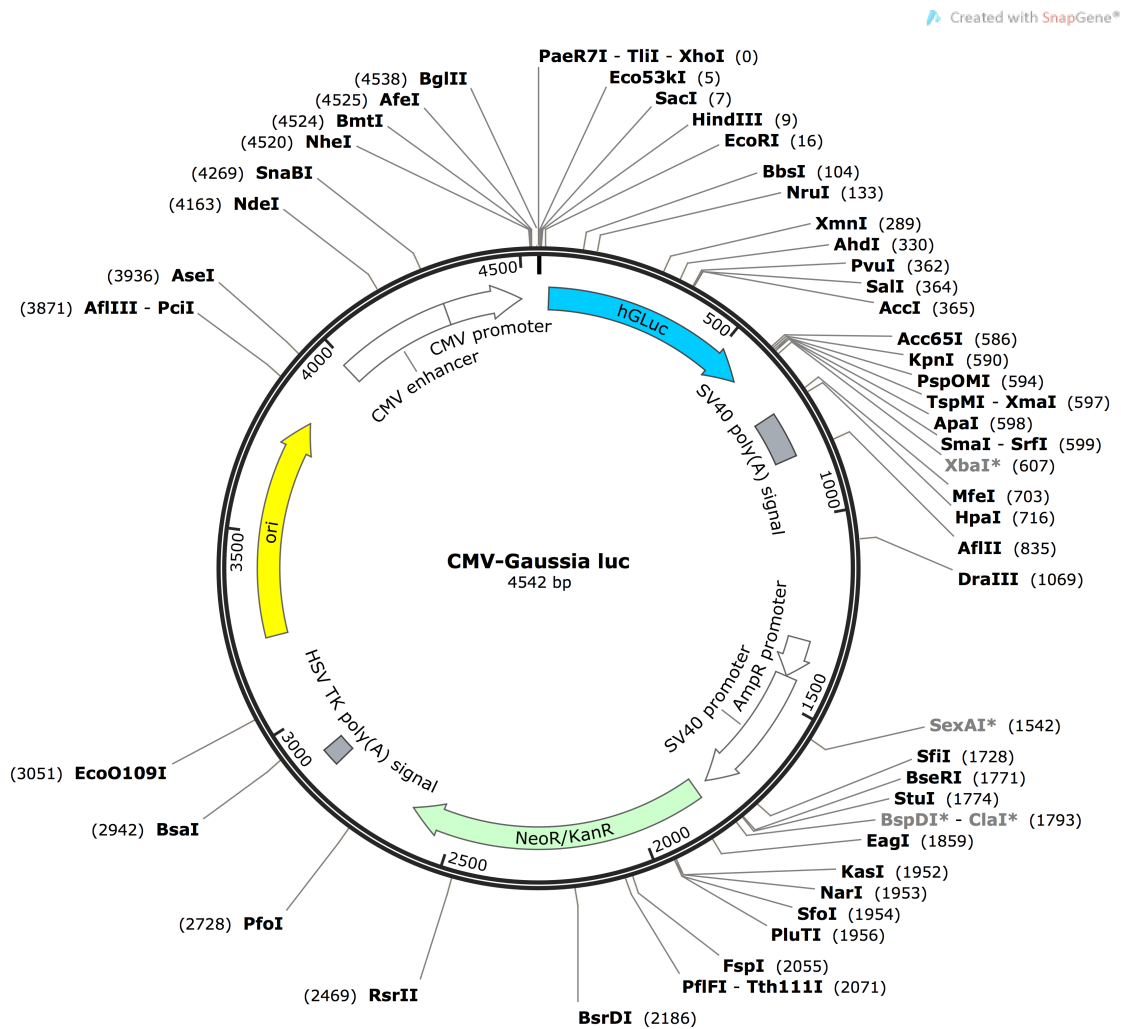


Figure B1. <sup>P</sup>CMV-Gaussia luc map.

Created with SnapGene®

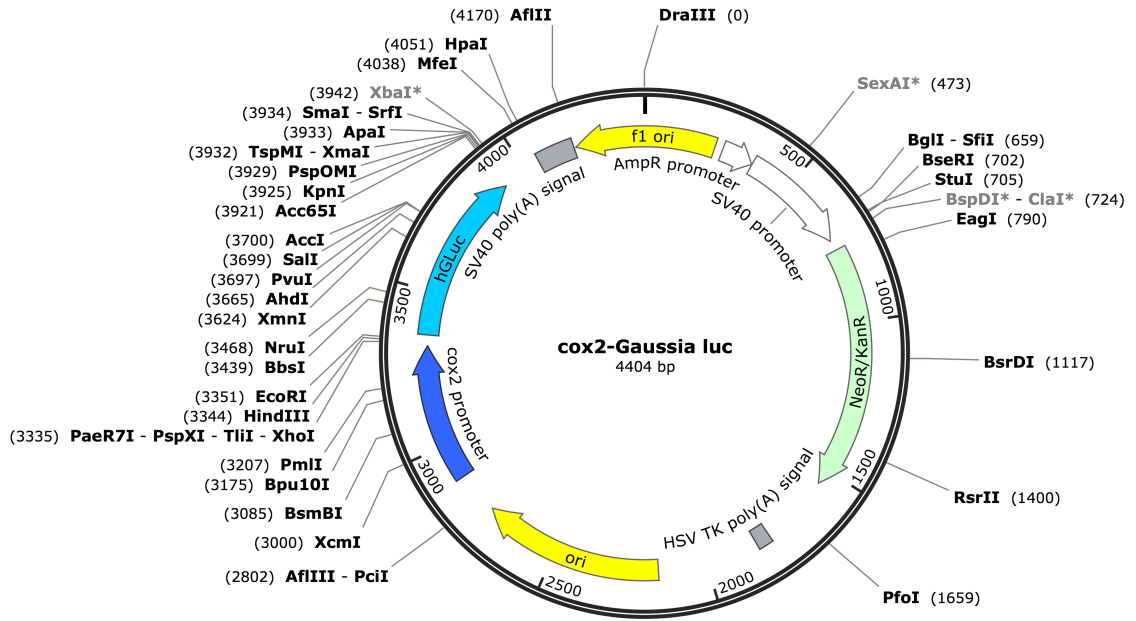


Figure B2. *P<sub>cox2</sub>-Gaussia luc* map.

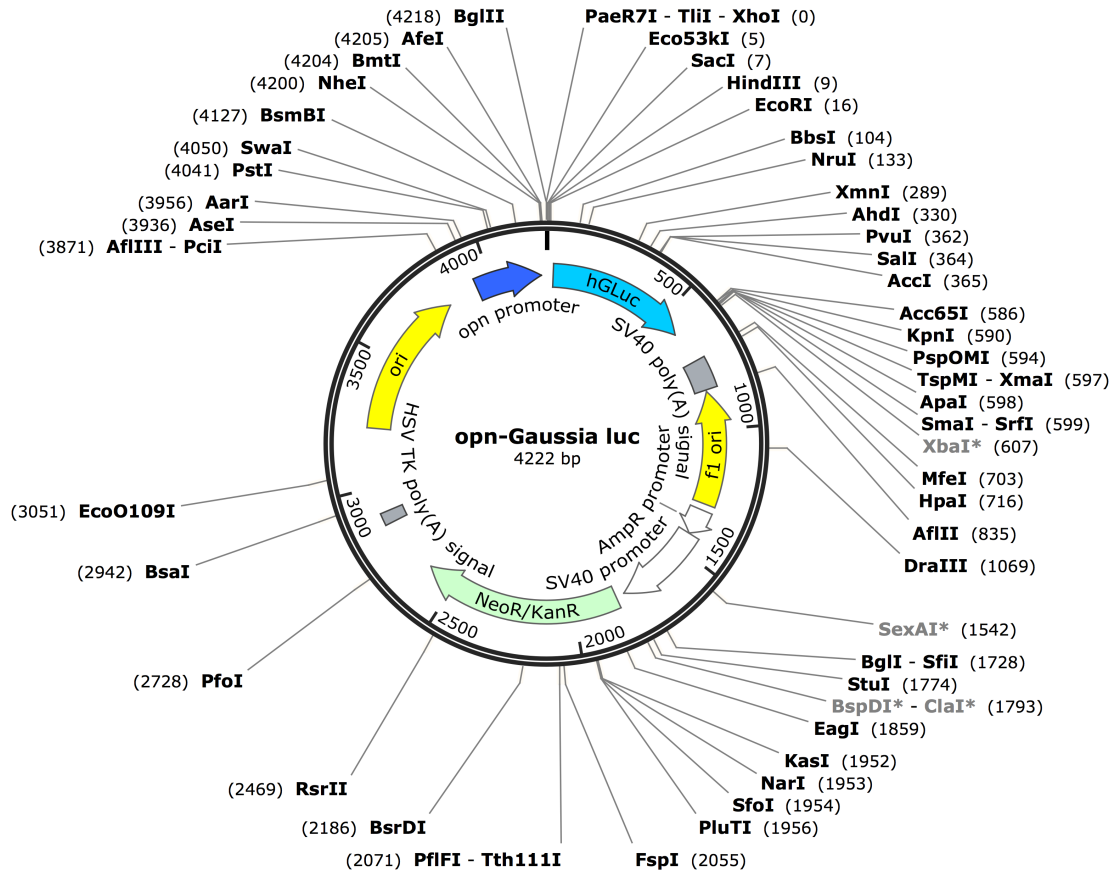


Figure B3. *p-opn-Gaussia luc* map.

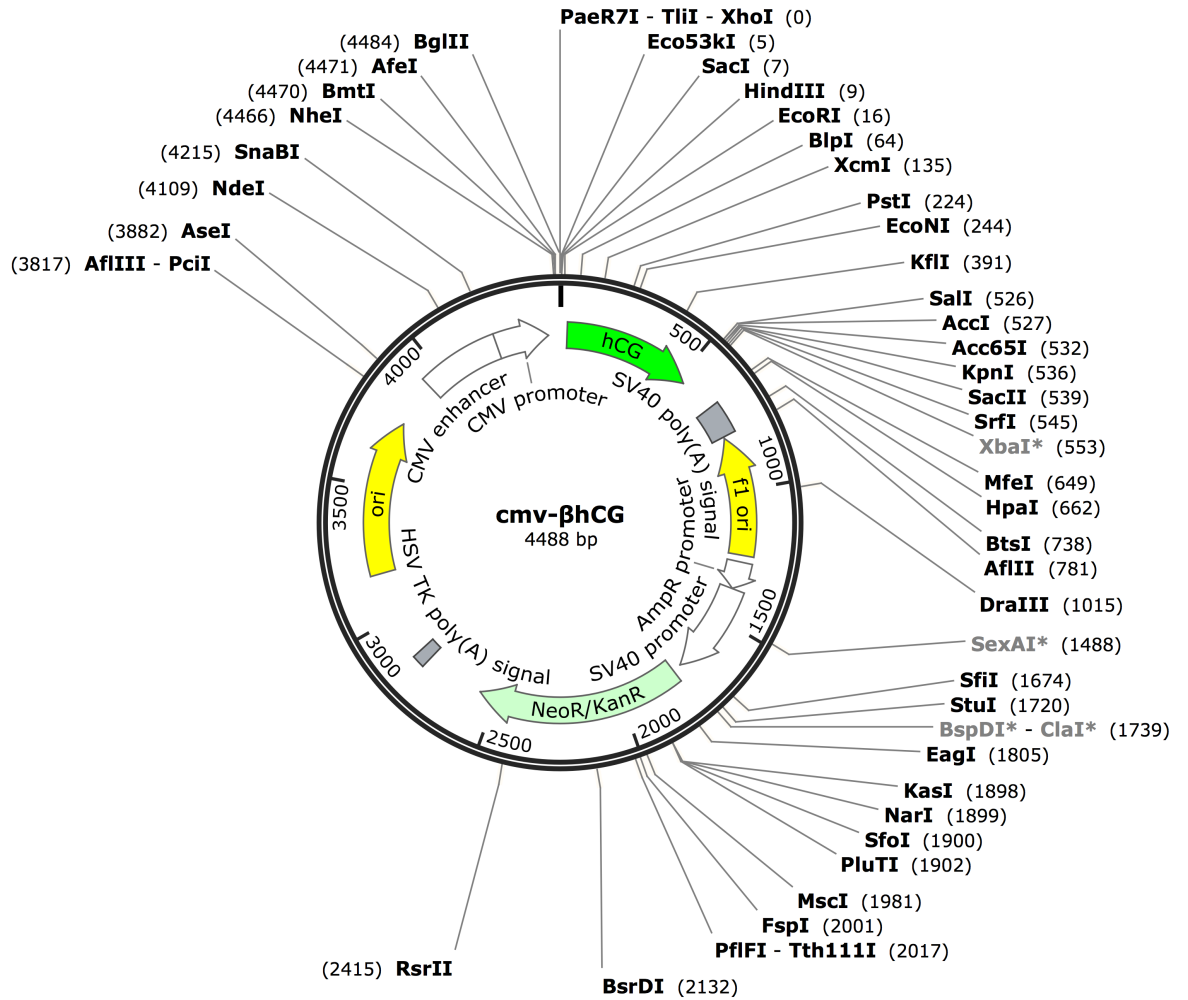


Figure B4. <sup>P</sup>CMV-βhCG map.

Created with SnapGene®

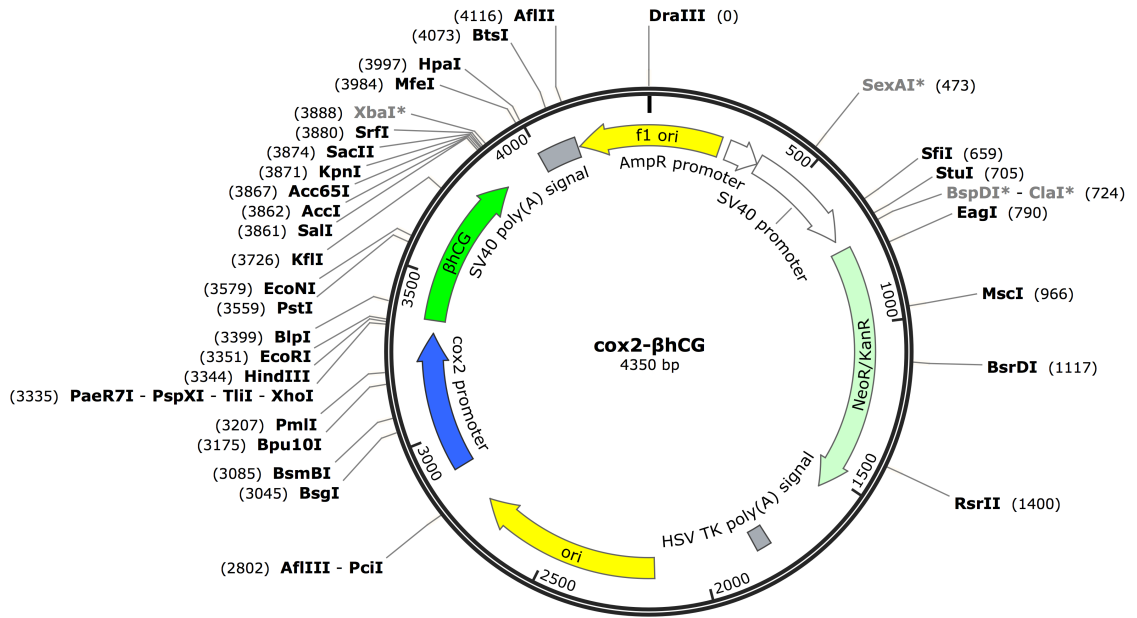


Figure B5. *p\_cox2-βhCG* map.

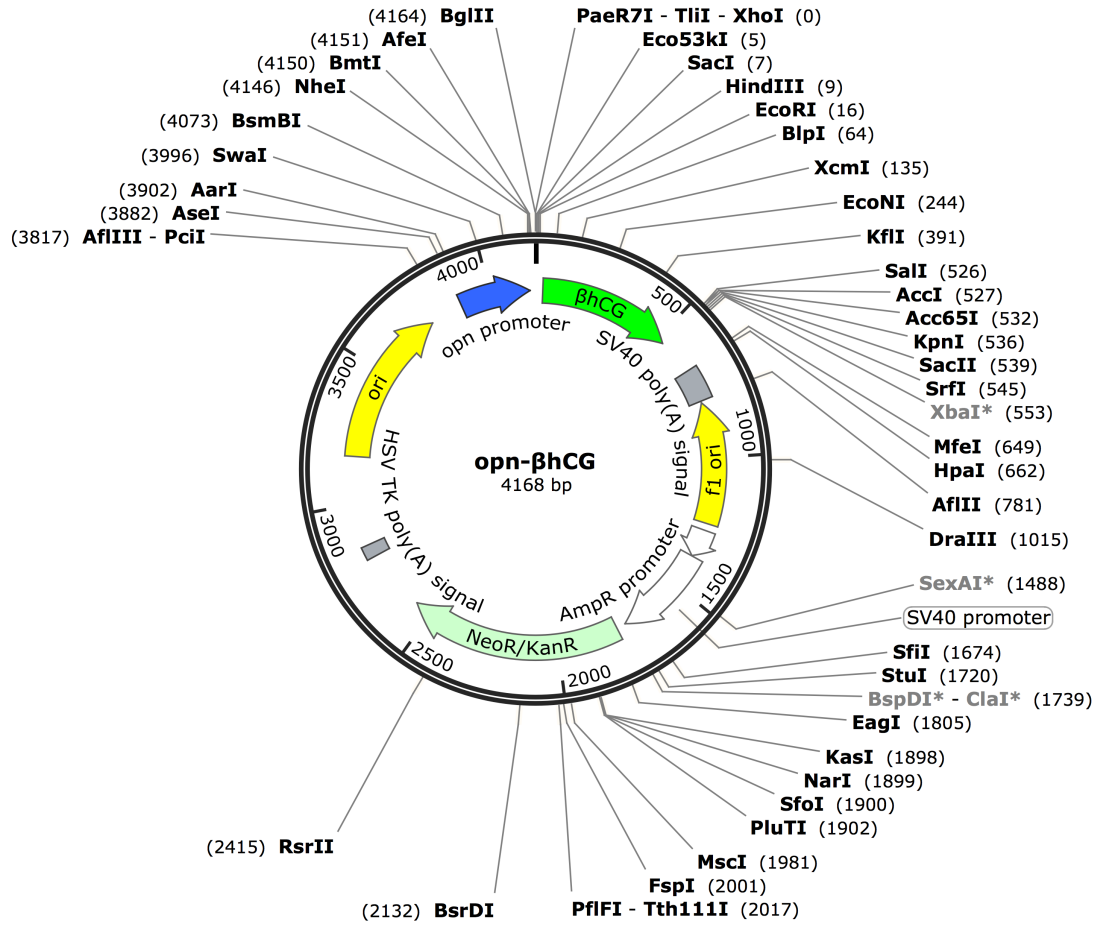


Figure B6. *P-opn-βhCG* map.

Created with SnapGene®

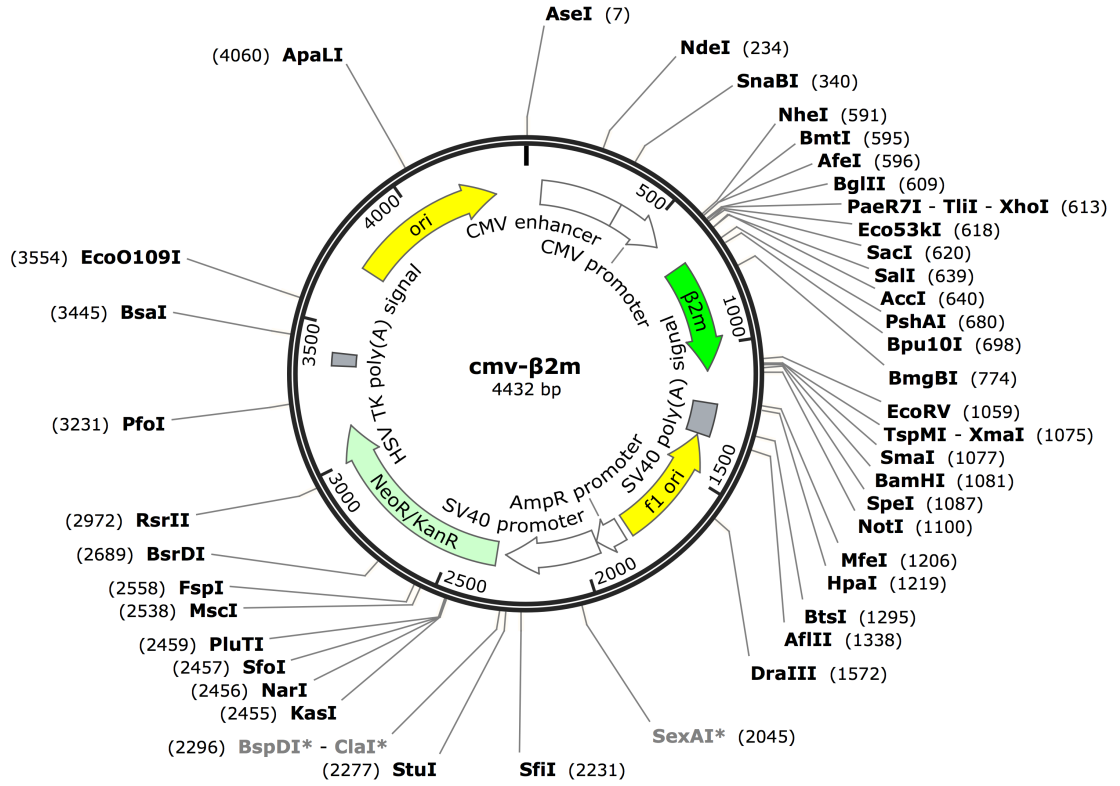


Figure B7. <sup>P</sup>CMV-β2m map.



Created with SnapGene®

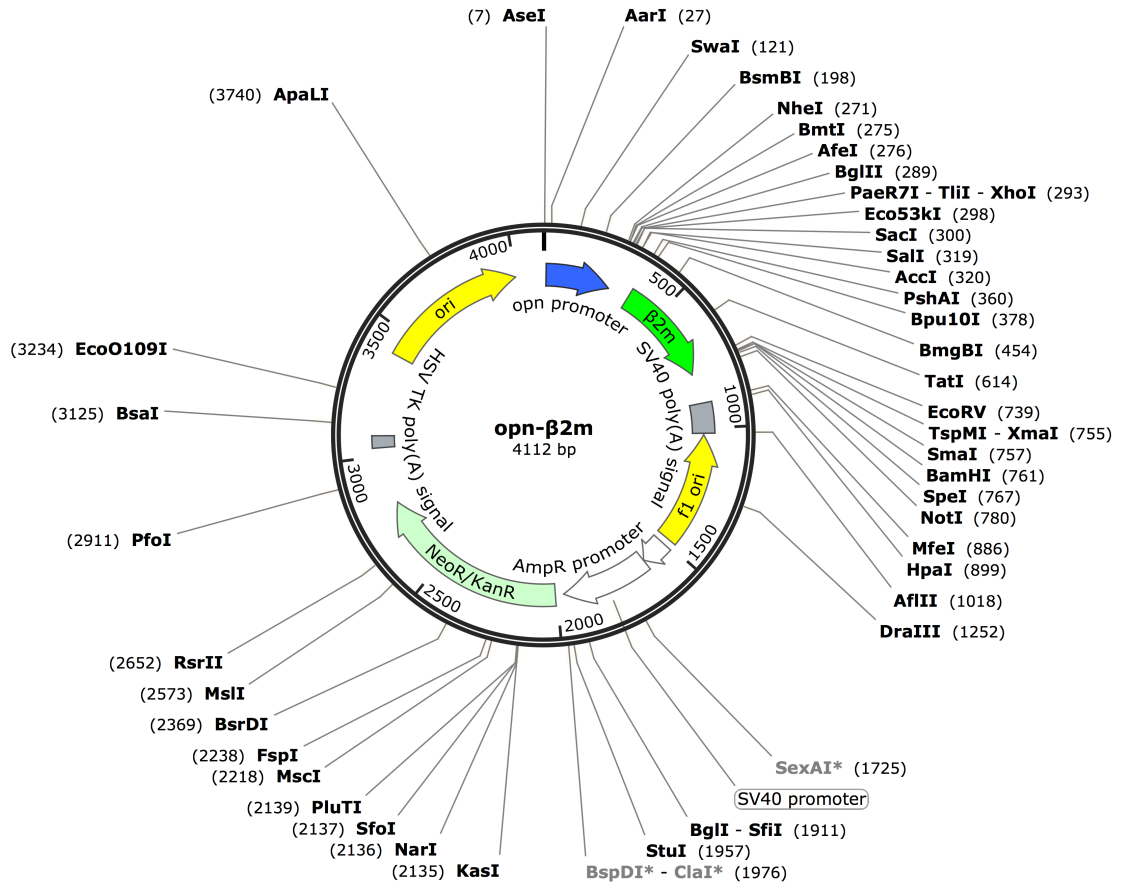


Figure B9. <sup>P</sup>*opn-β2m* map.

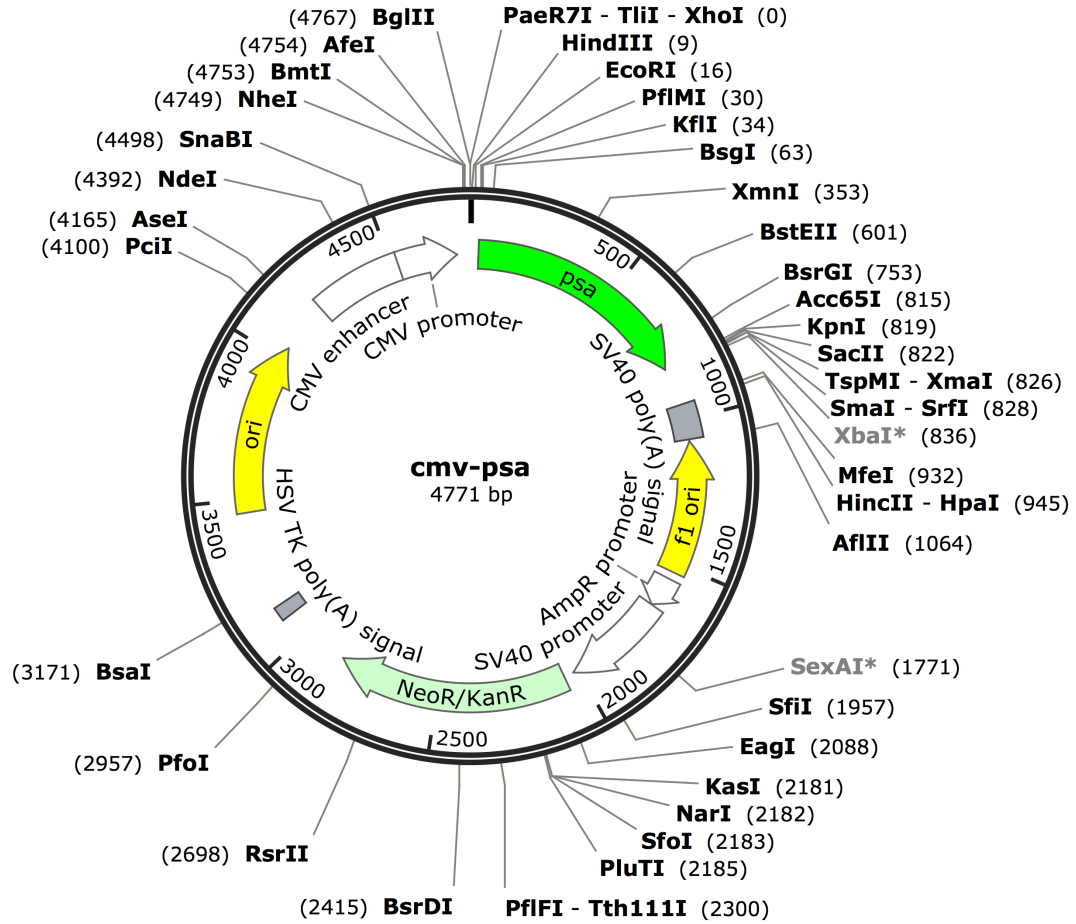


Figure B10. <sup>P</sup>CMV-psa map.

Created with SnapGene®

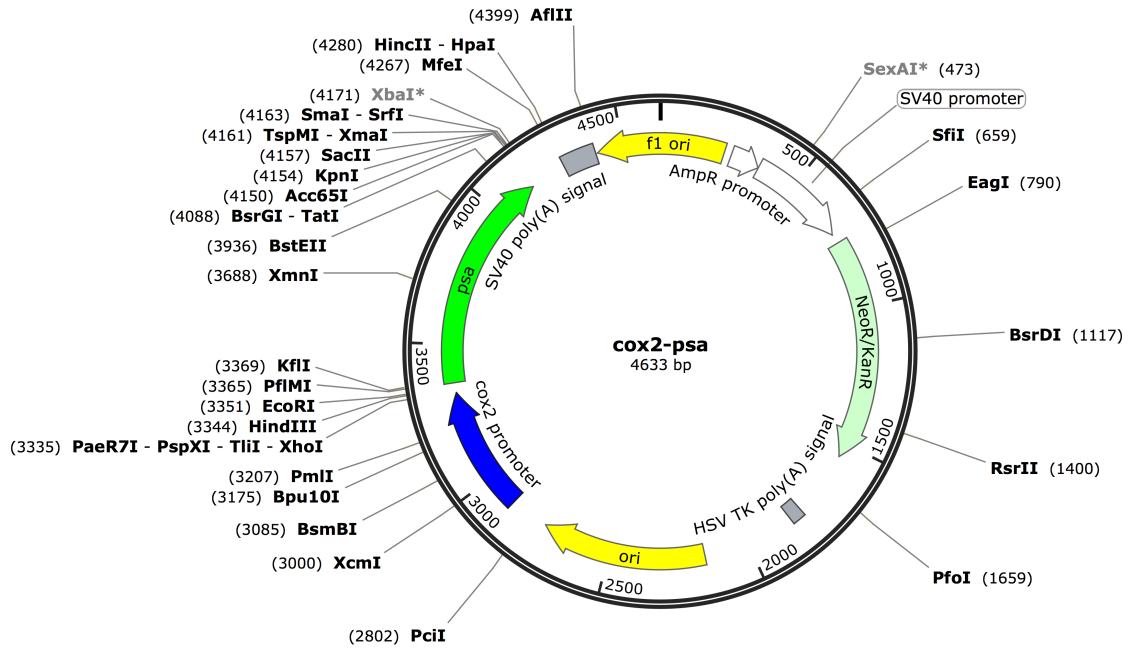


Figure B11. <sup>P</sup>*cox2-psa* map.

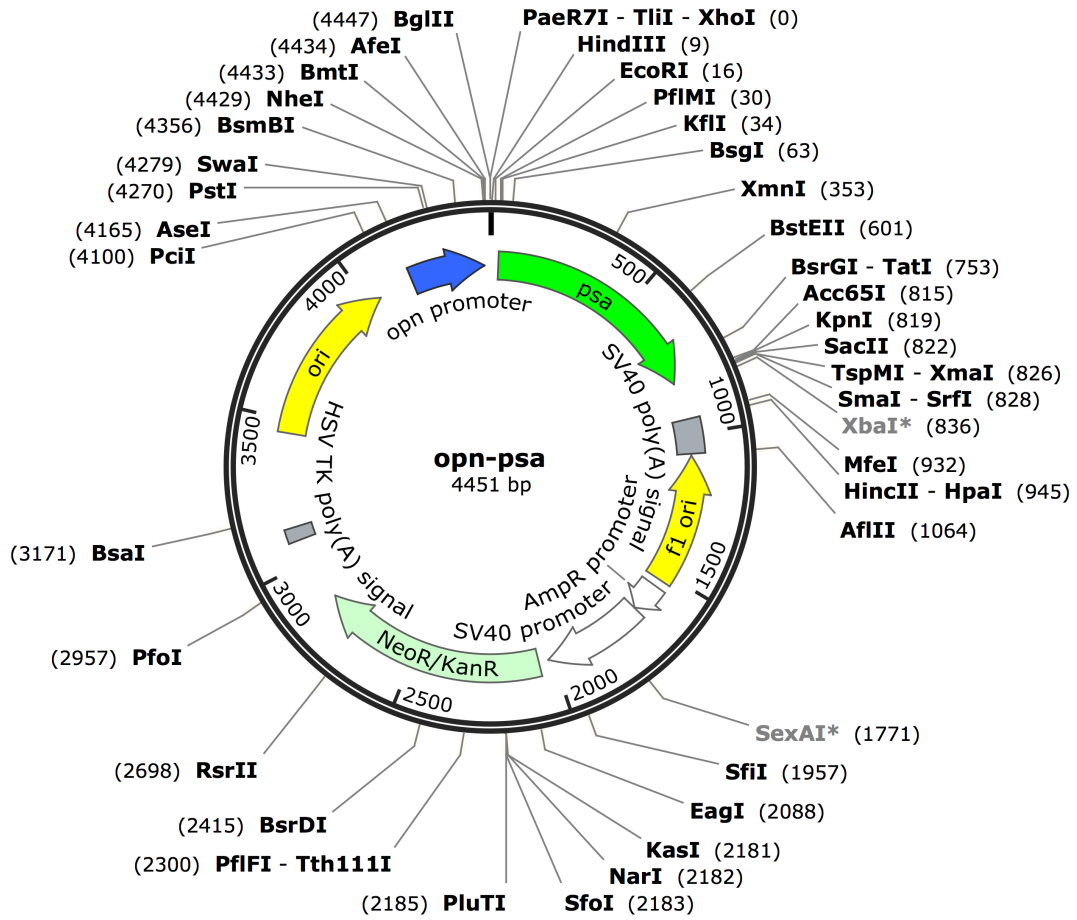


Figure B12. *pOpn-psa* map.

Created with SnapGene®

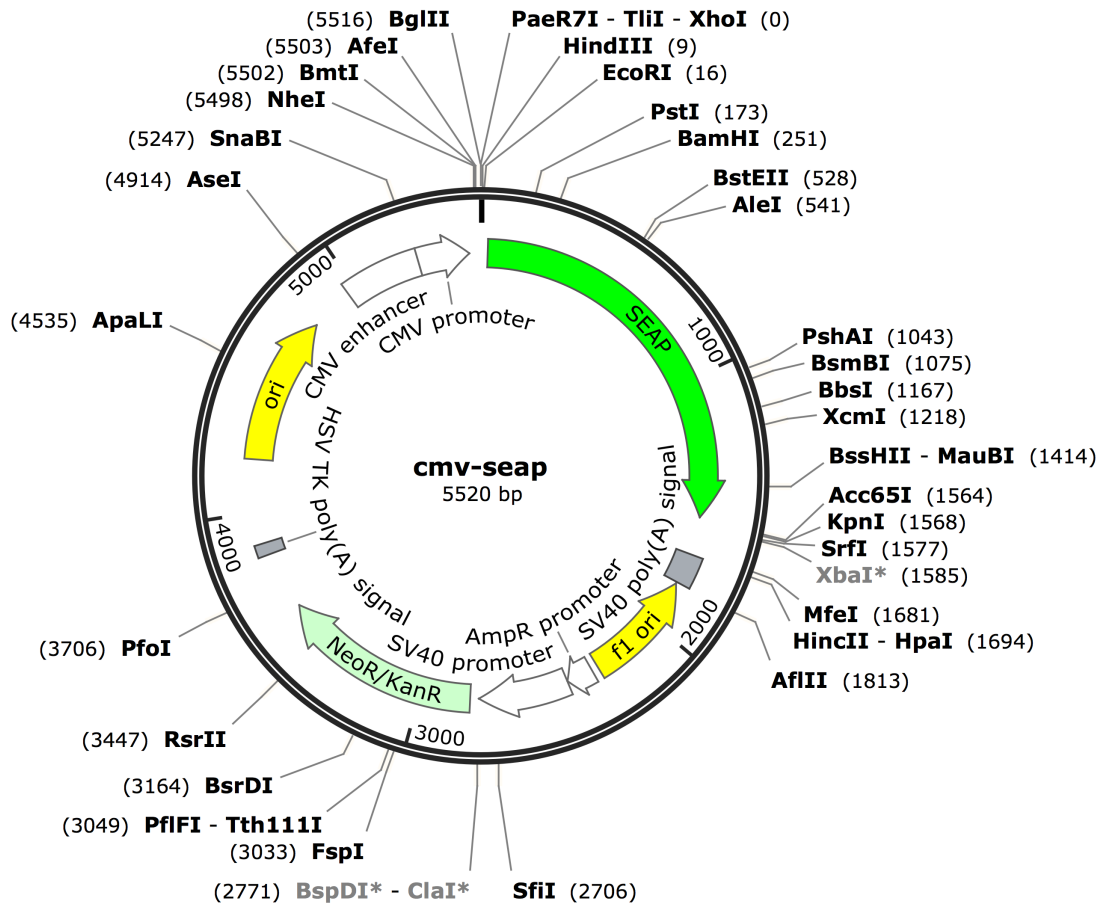


Figure B13. <sup>P</sup>CMV-seap map.

Created with SnapGene®

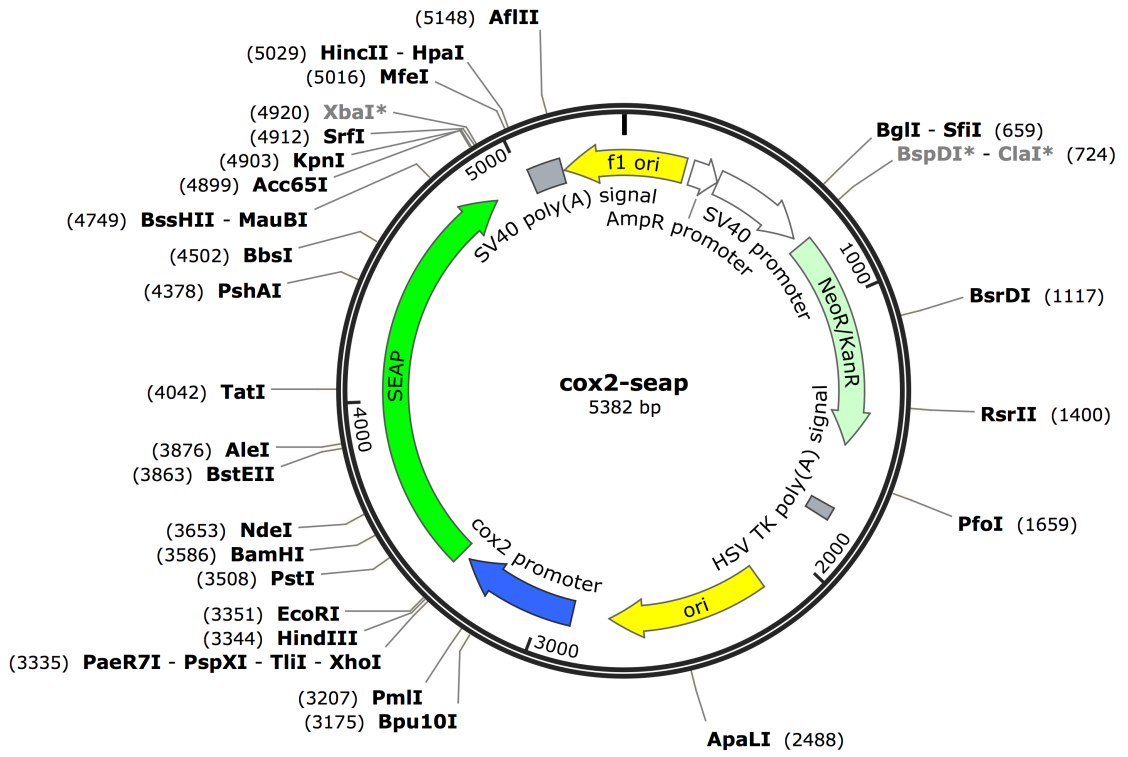


Figure B14. <sup>P</sup>*cox2-seap* map.

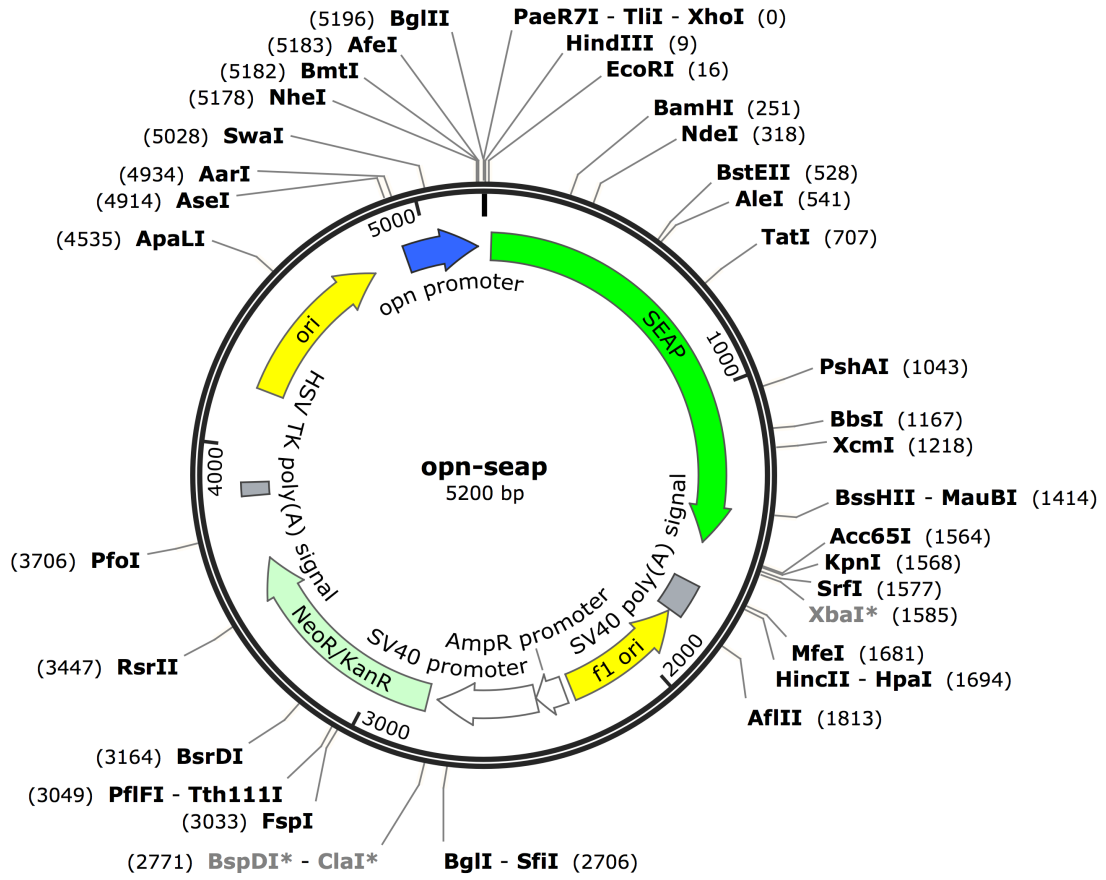


Figure B15. *p<sub>opn-seap</sub>* map.

## List of References

ABDALLAH, B., HASSAN, A., BENOIST, C., GOULA, D., BEHR, J. P. & DEMENEIX, B. A. 1996. A powerful nonviral vector for in vivo gene transfer into the adult mammalian brain: polyethylenimine. *Hum Gene Ther*, 7, 1947-54.

AGRAWAL, D., CHEN, T. G., IRBY, R., QUACKENBUSH, J., CHAMBERS, A. F., SZABO, M., CANTOR, A., COPPOLA, D. & YEATMAN, T. J. 2002. Osteopontin identified as lead marker of colon cancer progression, using pooled sample expression profiling. *Journal of the National Cancer Institute*, 94, 513-521.

ALAM, J. & COOK, J. L. 1990. Reporter Genes - Application to the Study of Mammalian Gene-Transcription. *Analytical Biochemistry*, 188, 245-254.

AMERICAN CANCER SOCIETY. *Biopsy types* [Online]. Available: <http://www.cancer.org/treatment/understandingyourdiagnosis/examsandtestdescriptions/orwomenfacingabreastbiopsy/breast-biopsy-biopsy-types> [Accessed March 28th 2015].

AMERICAN CANCER SOCIETY. *Bladder cancer key statistics* [Online]. Available: <http://www.cancer.org/cancer/bladdercancer/detailedguide/bladder-cancer-key-statistics> [Accessed February 4th 2015].

AMERICAN CANCER SOCIETY. *Bladder cancer survival rates* [Online]. Available: <http://www.cancer.org/cancer/bladdercancer/detailedguide/bladder-cancer-survival-rates> [Accessed March 28th 2015].

AMERICAN CANCER SOCIETY. *Cancer facts statistics* [Online]. Available: <http://www.cancer.org/research/cancerfactsstatistics/index> [Accessed Feb. 27th 2015].

AMERICAN CANCER SOCIETY. *Endoscopy* [Online]. Available: <http://www.cancer.org/treatment/understandingyourdiagnosis/examsandtestdescriptions/endoscopy/index> [Accessed March 28th 2015].

AMERICAN CANCER SOCIETY. *Imaging tests* [Online]. Available: <http://www.cancer.org/treatment/understandingyourdiagnosis/examsandtestdescriptions/imagingradiologytests/imaging-radiology-tests-ultrasound> [Accessed March 28th 2015].

- ANDERSEN, J. B., STERNBERG, C., POULSEN, L. K., BJORN, S. P., GIVSKOV, M. & MOLIN, S. 1998. New unstable variants of green fluorescent protein for studies of transient gene expression in bacteria. *Applied and Environmental Microbiology*, 64, 2240-2246.
- AOI, K. & OKADA, M. 1996. Polymerization of oxazolines. *Progress in Polymer Science*, 21, 151-208.
- ATAHAN, O., KAYIGIL, O., HIZEL, N., YAVUZ, O. & METIN, A. 1996. Urinary glycosaminoglycan excretion in bladder carcinoma. *Scandinavian Journal of Urology and Nephrology*, 30, 173-177.
- ATKIN, W. S., SAUNDERS, B. P., BRITISH SOCIETY FOR, G., ASSOCIATION OF COLOPROCTOLOGY FOR GREAT, B. & IRELAND 2002. Surveillance guidelines after removal of colorectal adenomatous polyps. *Gut*, 51 Suppl 5, V6-9.
- BALSALOBRE, A., DAMIOLA, F. & SCHIBLER, U. 1998. A serum shock induces circadian gene expression in mammalian tissue culture cells. *Cell*, 93, 929-37.
- BAO, R., SELVAKUMARAN, M. & HAMILTON, T. C. 2000. Use of a surrogate marker (human secreted alkaline phosphatase) to monitor in vivo tumor growth and anticancer drug efficacy in ovarian cancer xenografts? *Gynecologic Oncology*, 78, 373-379.
- BAO, R. D., CONNOLLY, D. C., MURPHY, M., GREEN, J., WEINSTEIN, J. K., PISARCIK, D. A. & HAMILTON, T. C. 2002. Activation of cancer-specific gene expression by the survivin promoter. *Journal of the National Cancer Institute*, 94, 522-528.
- BARADA, K., MOURAD, F. H., NOUTSI, B. & SAADE, N. E. 2015. Electrocautery-induced localized colonic injury elicits increased levels of pro-inflammatory cytokines in small bowel and decreases jejunal alanine absorption. *Cytokine*, 71, 109-18.
- BERGER, J., HAUBER, J., HAUBER, R., GEIGER, R. & CULLEN, B. R. 1988. Secreted Placental Alkaline-Phosphatase - a Powerful New Quantitative Indicator of Gene-Expression in Eukaryotic Cells. *Gene*, 66, 1-10.
- BIELINSKA, M., RZYMKIEWICZ, D. & BOIME, I. 1994. Human Luteinizing-Hormone and Chorionic-Gonadotropin Are Targeted to a Regulated Secretory Pathway in Gh(3) Cells. *Molecular Endocrinology*, 8, 919-928.
- BOHLE, A., JURCZOK, A., ARDELT, P., WULF, T., ULMER, A. J., JOCHAM, D. & BRANDAU, S. 2002. Inhibition of bladder carcinoma cell adhesion by oligopeptide combinations in vitro and in vivo. *Journal of Urology*, 167, 357-363.
- BOUSSIF, O., LEZOUALCH, F., ZANTA, M. A., MERGNY, M. D., SCHERMAN, D., DEMENEIX, B. & BEHR, J. P. 1995. A versatile vector for gene and oligonucleotide

transfer into cells in culture and in vivo: polyethylenimine. *Proc Natl Acad Sci U S A*, 92, 7297-301.

BROCKS, C. P., BUTTNER, H. & BOHLE, A. 2005. Inhibition of tumor implantation by intravesical gemcitabine in a murine model of superficial bladder cancer. *Journal of Urology*, 174, 1115-1118.

BROOKS, J. D. 2012. Translational genomics: The challenge of developing cancer biomarkers. *Genome Research*, 22, 183-187.

BROWN, L. F., BERSE, B., VANDEWATER, L., PAPADOPOULOSSENGI, A., PERRUZZI, C. A., MANSEAU, E. J., DVORAK, H. F. & SENGER, D. R. 1992. Expression and Distribution of Osteopontin in Human Tissues - Widespread Association with Luminal Epithelial Surfaces. *Molecular Biology of the Cell*, 3, 1169-1180.

BURNIER, J. V. & BURNIER, M. N. 2013. Experimental and clinical metastasis : a comprehensive review, New York, Springer.

CAI, X., DONG, C., DONG, H., WANG, G., PAULETTI, G. M., PAN, X., WEN, H., MEHL, I., LI, Y. & SHI, D. 2012. Effective gene delivery using stimulus-responsive cationic polymer designed with redox-sensitive disulfide and acid-labile imine linkers. *Biomacromolecules*, 13, 1024-34.

CAMPER, S. A., YAO, Y. A. S. & ROTTMAN, F. M. 1985. Hormonal-Regulation of the Bovine Prolactin Promoter in Rat Pituitary-Tumor Cells. *Journal of Biological Chemistry*, 260, 2246-2251.

CAUBERG EVELYNE, C. C., DE LA ROSETTE, J. J. & DE REIJK, T. M. 2011. Emerging optical techniques in advanced cystoscopy for bladder cancer diagnosis: A review of the current literature. *Indian J Urol*, 27, 245-51.

CHADE, D. C., ANDRADE, P. M., BORRA, R. C., LEITE, K. R., ANDRADE, E., VILLANOVA, F. E. & SROUGI, M. 2008. Histopathological characterization of a syngeneic orthotopic murine bladder cancer model. *Int Braz J Urol*, 34, 220-6; discussion 226-9.

CHAN, E., PATEL, A., HESTON, W. & LARCHIAN, W. 2009a. Mouse orthotopic models for bladder cancer research. *Bju International*, 104, 1286-1291.

CHAN, E. S. Y., PATEL, A. R., SMITH, A. K., KLEIN, J. B., THOMAS, A. A., HESTON, W. D. & LARCHIAN, W. A. 2009b. Optimizing Orthotopic Bladder Tumor Implantation in a Syngeneic Mouse Model. *Journal of Urology*, 182, 2926-2931.

CHAN, P. C. R., KULASINGAM, V. & LEM-RAGOSNIG, B. 2012. Validating urinary measurement of beta-2-microglobulin with a Roche reagent kit designed for serum measurements. *Clinical Biochemistry*, 45, 1533-1535.

- CHANG, C. H., SCOTT, G. K., BALDWIN, M. A. & BENZ, C. C. 1999. Exon 4-encoded acidic domain in the epithelium-restricted Ets factor, ESX, confers potent transactivating capacity and binds to TATA-binding protein (TBP). *Oncogene*, 18, 3682-95.
- CHARD, T. 1992. Pregnancy Tests - a Review. *Human Reproduction*, 7, 701-710.
- CHEN, B., JERGER, K., FRECHET, J. M. & SZOKA, F. C., JR. 2009. The influence of polymer topology on pharmacokinetics: differences between cyclic and linear PEGylated poly(acrylic acid) comb polymers. *J Control Release*, 140, 203-9.
- CHEN, J. S., LIU, J. C., SHEN, L., RAU, K. M., KUO, H. P., LI, Y. M., SHI, D., LEE, Y. C., CHANG, K. J. & HUNG, M. C. 2004. Cancer-specific activation of the survivin promoter and its potential use in gene therapy. *Cancer Gene Therapy*, 11, 740-747.
- CHEN, X. G. & GODBEY, W. T. 2015. The potential of the human osteopontin promoter and single-nucleotide polymorphisms for targeted cancer gene therapy. *Curr Gene Ther*, 15, 82-92.
- CHEUNG, G., SAHAI, A., BILLIA, M., DASGUPTA, P. & KHAN, M. S. 2013a. Recent advances in the diagnosis and treatment of bladder cancer. *BMC Med*, 11, 13.
- CHEUNG, G., SAHAI, A., BILLIA, M., DASGUPTA, P. & KHAN, M. S. 2013b. Recent advances in the diagnosis and treatment of bladder cancer. *Bmc Medicine*, 11.
- CHIN, J. L., KADHIM, S. A., BATISLAM, E., KARLIK, S. J., GARCIA, B. M., NICKEL, J. C. & MORALES, A. 1996. Mycobacterium cell wall: an alternative to intravesical bacillus Calmette Guerin (BCG) therapy in orthotopic murine bladder cancer. *J Urol*, 156, 1189-93.
- CHOUDHARY, S., KUMAR, A., KALE, R. K., RAISZ, L. G. & PILBEAM, C. C. 2004. Extracellular calcium induces COX-2 in osteoblasts via a PKA pathway. *Biochemical and Biophysical Research Communications*, 322, 395-402.
- CHUAH, M. K., PETRUS, I., DE BLESER, P., LE GUINER, C., GERNOUX, G., ADJALI, O., NAIR, N., WILLEMS, J., EVENS, H., RINCON, M. Y., MATRAI, J., DI MATTEO, M., SAMARA-KUKO, E., YAN, B., ACOSTA-SANCHEZ, A., MELIANI, A., CHEREL, G., BLOUIN, V., CHRISTOPHE, O., MOULLIER, P., MINGOZZI, F. & VANDENDRIESSCHE, T. 2014. Liver-Specific Transcriptional Modules Identified by Genome-Wide In Silico Analysis Enable Efficient Gene Therapy in Mice and Non-Human Primates. *Molecular Therapy*, 22, 1605-1613.
- CHUNG, E., YAMASHITA, H., AU, P., TANNOUS, B. A., FUKUMURA, D. & JAIN, R. K. 2009. Secreted Gaussia luciferase as a biomarker for monitoring tumor progression and treatment response of systemic metastases. *PLoS One*, 4, e8316.

- CHUNG, I. & DEISSEROTH, A. B. 2004. Recombinant adenoviral vector containing tumor-specific L-plastin promoter fused to cytosine deaminase gene as a transcription unit: generation and functional test. *Arch Pharm Res*, 27, 633-9.
- CONE, E. J., CAPLAN, Y. H., MOSER, F., ROBERT, T., SHELBY, M. K. & BLACK, D. L. 2009. Normalization of Urinary Drug Concentrations with Specific Gravity and Creatinine. *Journal of Analytical Toxicology*, 33, 1-7.
- CULLEN, B. R. & MALIM, M. H. 1992. Secreted Placental Alkaline-Phosphatase as a Eukaryotic Reporter Gene. *Methods in Enzymology*, 216, 362-368.
- DANDA, R., KRISHNAN, G., GANAPATHY, K., KRISHNAN, U. M., VIKAS, K., ELCHURI, S., CHATTERJEE, N. & KRISHNAKUMAR, S. 2013. Targeted expression of suicide gene by tissue-specific promoter and microRNA regulation for cancer gene therapy. *PLoS One*, 8, e83398.
- DE MEDEIROS, S. F. & NORMAN, R. J. 2009. Human choriogonadotrophin protein core and sugar branches heterogeneity: basic and clinical insights. *Human Reproduction Update*, 15, 69-95.
- DENHARDT, D. T., MISTRETTA, D., CHAMBERS, A. F., KRISHNA, S., PORTER, J. F., RAGHURAM, S. & RITTLING, S. R. 2003. Transcriptional regulation of osteopontin and the metastatic phenotype: Evidence for a Ras-activated enhancer in the human OPN promoter. *Clinical & Experimental Metastasis*, 20, 77-84.
- DENKERT, C., KOCH, I., FURSTENBERG, A., KOBEL, M. & HAUPTMANN, S. 2002. Regulation and function of Cyclooxygenase-2 (COX-2) in ovarian carcinoma cells. *European Journal of Cancer*, 38, S86-S86.
- DOBEK, G. L. & GODBEY, W. T. 2011. An Orthotopic Model of Murine Bladder Cancer. *Jove-Journal of Visualized Experiments*.
- DOBEK, G. L., ZHANG, X. J., BALAZS, D. A. & GODBEY, W. T. 2011. Analysis of promoters and expression-targeted gene therapy optimization based on doubling time and transfectability. *Faseb Journal*, 25, 3219-3228.
- EUGENE, D. M. & GRAYSON, S. M. 2008. Efficient preparation of cyclic poly(methyl acrylate)-block-poly(styrene) by combination of atom transfer radical polymerization and click cyclization. *Macromolecules*, 41, 5082-5084.
- FAN, F. & WOOD, K. V. 2007. Bioluminescent assays for high-throughput screening. *Assay and Drug Development Technologies*, 5, 127-136.
- FASS, L. 2008. Imaging and cancer: a review. *Mol Oncol*, 2, 115-52.
- FICHERA, A., MICHELASSI, F. & ARENAS, R. B. 1998. Selective expression of carcinoembryonic antigen promoter in cancer cell lines: targeting strategy for gene therapy in colorectal cancer. *Dis Colon Rectum*, 41, 747-54.

- FISCHER, D., BIEBER, T., LI, Y., ELSASSER, H. P. & KISSEL, T. 1999. A novel non-viral vector for DNA delivery based on low molecular weight, branched polyethylenimine: effect of molecular weight on transfection efficiency and cytotoxicity. *Pharm Res*, 16, 1273-9.
- FLETCHER, B. S., KUJUBU, D. A., PERRIN, D. M. & HERSCHMAN, H. R. 1992. Structure of the Mitogen-Inducible Tis10 Gene and Demonstration That the Tis10-Encoded Protein Is a Functional Prostaglandin G/H Synthase. *Journal of Biological Chemistry*, 267, 4338-4344.
- FU, C., LIN, L., SHI, H., ZHENG, D., WANG, W., GAO, S., ZHAO, Y., TIAN, H., ZHU, X. & CHEN, X. 2012. Hydrophobic poly (amino acid) modified PEI mediated delivery of rev-casp-3 for cancer therapy. *Biomaterials*, 33, 4589-96.
- FUKAZAWA, T., MAEDA, Y., SLADEK, F. M. & OWEN-SCHAUB, L. B. 2004. Development of a cancer-targeted tissue-specific promoter system. *Cancer Research*, 64, 363-369.
- FUKUDA, S. & PELUS, L. M. 2006. Survivin, a cancer target with an emerging role in normal adult tissues. *Molecular Cancer Therapeutics*, 5, 1087-1098.
- FUZERY, A. K., LEVIN, J., CHAN, M. M. & CHAN, D. W. 2013. Translation of proteomic biomarkers into FDA approved cancer diagnostics: issues and challenges. *Clin Proteomics*, 10, 13.
- GEORGIOU, T. K. 2014. Star polymers for gene delivery. *Polymer International*, 63, 1130-1133.
- GLICK, N. R. 1991. Principles and Practice of Endocrinology and Metabolism - Becker, K.I. *Mental Retardation*, 29, 111-111.
- GODBEY, W. T. & ATALA, A. 2003. Directed apoptosis in Cox-2-overexpressing cancer cells through expression-targeted gene delivery. *Gene Therapy*, 10, 1519-1527.
- GODBEY, W. T., WU, K. K. & MIKOS, A. G. 1999. Size matters: molecular weight affects the efficiency of poly(ethylenimine) as a gene delivery vehicle. *J Biomed Mater Res*, 45, 268-75.
- GRAYSON, S. M. & GODBEY, W. T. 2008. The role of macromolecular architecture in passively targeted polymeric carriers for drug and gene delivery. *J Drug Target*, 16, 329-56.
- GU, J., KAGAWA, S., TAKAKURA, M., KYO, S., INOUE, M., ROTH, J. A. & FANG, B. 2000a. Tumor-specific transgene expression from the human telomerase reverse transcriptase promoter enables targeting of the therapeutic effects of the Bax gene to cancers. *Cancer Res*, 60, 5359-64.

GU, J., KAGAWA, S., TAKAKURA, M., KYO, S., INOUE, M., ROTH, J. A. & FANG, B. L. 2000b. Tumor-specific transgene expression from the human telomerase reverse transcriptase promoter enables targeting of the therapeutic effects of the Bax gene to cancers. *Cancer Research*, 60, 5359-5364.

GUNTHER, J. H., JURCZOK, A., WULF, T., BRANDAU, S., DEINERT, I., JOCHAM, D. & BOHLE, A. 1999. Optimizing syngeneic orthotopic murine bladder cancer (MB49). *Cancer Research*, 59, 2834-2837.

HADJICHRISTIDIS, N., PITSIKALIS, M., PISPAS, S. & IATROU, H. 2001. Polymers with complex architecture by living anionic polymerization. *Chemical Reviews*, 101, 3747-3792.

HEIM, R., CUBITT, A. B. & TSIEN, R. Y. 1995. Improved Green Fluorescence. *Nature*, 373, 663-664.

HIGASHIYAMA, M., ITO, T., TANAKA, E. & SHIMADA, Y. 2007. Prognostic significance of osteopontin expression in human gastric carcinoma. *Annals of Surgical Oncology*, 14, 3419-3427.

HIRAMATSU, N., KASAI, A., HAYAKAWA, K., YAO, J. & KITAMURA, M. 2006. Real-time detection and continuous monitoring of ER stress in vitro and in vivo by ES-TRAP: evidence for systemic, transient ER stress during endotoxemia. *Nucleic Acids Res*, 34, e93.

HIRAMATSU, N., KASAI, A., MENG, Y. M., HAYAKAWA, K., YAO, J. & KITAMURA, M. 2005. Alkaline phosphatase vs luciferase as secreted reporter molecules in vivo. *Analytical Biochemistry*, 339, 249-256.

HOSKINS, J. N. & GRAYSON, S. M. 2009. Synthesis and Degradation Behavior of Cyclic Poly(epsilon-caprolactone). *Macromolecules*, 42, 6406-6413.

HU, Z., LIN, D. M., YUAN, J. S., XIAO, T., ZHANG, H. S., SUN, W. Y., HAN, N. J., MA, Y., DI, X. B., GAO, M. X., MA, J. F., ZHANG, J. H., CHENG, S. J. & GAO, Y. N. 2005. Overexpression of osteopontin is associated with more aggressive phenotypes in human non-small cell lung cancer. *Clinical Cancer Research*, 11, 4646-4652.

HUYN, S. T., BURTON, J. B., SATO, M., CAREY, M., GAMBHIR, S. S. & WU, L. 2009. A potent, imaging adenoviral vector driven by the cancer-selective mucin-1 promoter that targets breast cancer metastasis. *Clin Cancer Res*, 15, 3126-34.

IYER, M., WU, L., CAREY, M., WANG, Y., SMALLWOOD, A. & GAMBHIR, S. S. 2001. Two-step transcriptional amplification as a method for imaging reporter gene expression using weak promoters. *Proceedings of the National Academy of Sciences of the United States of America*, 98, 14595-14600.

- JAIN, V. K. & MAGRATH, I. T. 1991. A Chemiluminescent Assay for Quantitation of Beta-Galactosidase in the Femtogram Range - Application to Quantitation of Beta-Galactosidase in lacZ-Transfected Cells. *Analytical Biochemistry*, 199, 119-124.
- JAMES, R. M., NEIL, C., WEBSTER, J., ROOS, S., CLARK, A. J. & WHITELOW, C. B. A. 2000. Multiple copies of beta-lactoglobulin promoter do not function as LCR. *Biochemical and Biophysical Research Communications*, 272, 284-289.
- JIANG, T. T., XING, B. G. & RAO, J. H. 2008. Recent Developments of Biological Reporter Technology for Detecting Gene Expression. *Biotechnology and Genetic Engineering Reviews*, Vol 25, 25, 41-75.
- JOCHAM, D., STEPP, H. & WAIDELICH, R. 2008. Photodynamic diagnosis in urology: state-of-the-art. *Eur Urol*, 53, 1138-48.
- JUNKER, K., BOERNER, D., SCHULZE, W., UTTING, M., SCHUBERT, J. & WERNER, W. 2003. Analysis of genetic alterations in normal bladder urothelium. *Urology*, 62, 1134-8.
- JURCZOK, A., FORNARA, P. & SOLING, A. 2008. Bioluminescence imaging to monitor bladder cancer cell adhesion in vivo: a new approach to optimize a syngeneic, orthotopic, murine bladder cancer model. *Bju International*, 101, 120-124.
- KAIN, S. R., ADAMS, M., KONDEPUDI, A., YANG, T. T., WARD, W. W. & KITTS, P. 1995. Green Fluorescent Protein as a Reporter of Gene-Expression and Protein Localization. *Biotechniques*, 19, 650-655.
- KAIN, S. R. & GANGULY, S. 2001. Overview of genetic reporter systems. *Curr Protoc Mol Biol*, Chapter 9, Unit9 6.
- KAMAT, A. M., HEGARTY, P. K., GEE, J. R., CLARK, P. E., SVATEK, R. S., HEGARTY, N., SHARIAT, S. F., XYLINAS, E., SCHMITZ-DRAGER, B. J., LOTAN, Y., JENKINS, L. C., DROLLER, M., VAN RHIJN, B. W. & KARAKIEWICZ, P. I. 2013. ICUD-EAU International Consultation on Bladder Cancer 2012: Screening, Diagnosis, and Molecular Markers. *European Urology*, 63, 4-15.
- KASMAN, L. & VOELKEL-JOHNSON, C. 2013. An orthotopic bladder cancer model for gene delivery studies. *J Vis Exp*, 50181.
- KERR, D. 2003. Clinical development of gene therapy for colorectal cancer. *Nat Rev Cancer*, 3, 615-22.
- KIM, J. H., SKATES, S. J., UEDE, T., WONG, K. K., SCHORGE, J. O., FELTMATE, C. M., BERKOWITZ, R. S., CRAMER, D. W. & MOK, S. C. 2002. Osteopontin as a potential diagnostic biomarker for ovarian cancer. *Jama-Journal of the American Medical Association*, 287, 1671-1679.

KIM, N. W., PIATYSZEK, M. A., PROWSE, K. R., HARLEY, C. B., WEST, M. D., HO, P. L., COVIELLO, G. M., WRIGHT, W. E., WEINRICH, S. L. & SHAY, J. W. 1994. Specific association of human telomerase activity with immortal cells and cancer. *Science*, 266, 2011-5.

KIM, Y. S. & FISCHER, S. M. 1998. Transcriptional regulation of cyclooxygenase-2 in mouse skin carcinoma cells - Regulatory role of CCAAT/enhancer-binding proteins in the differential expression of cyclooxygenase-2 in normal and neoplastic tissues. *Journal of Biological Chemistry*, 273, 27686-27694.

KNOWLES, M. A. & HURST, C. D. 2015. Molecular biology of bladder cancer: new insights into pathogenesis and clinical diversity. *Nature Reviews Cancer*, 15, 25-41.

KO, S. C., CHEON, J., KAO, C. H., GOTOH, A., SHIRAKAWA, T., SIKES, R. A., KARSENTY, G. & CHUNG, L. W. K. 1996. Osteocalcin promoter-based toxic gene therapy for the treatment of osteosarcoma in experimental models. *Cancer Research*, 56, 4614-4619.

KOBAYASHI, S., TOKUZAWA, T. & SAEGUSA, T. 1982. Cationic Ring-Opening Isomerization Polymerization of 2-[Para-(Substituted)Phenyl]-2-Oxazolines - Effects of the Substituent on the Reactivities. *Macromolecules*, 15, 707-710.

KOCH, P. E., GUO, Z. S., KAGAWA, S., GU, J., ROTH, J. A. & FANG, B. 2001. Augmenting transgene expression from carcinoembryonic antigen (CEA) promoter via a GAL4 gene regulatory system. *Molecular Therapy*, 3, 278-283.

KOGA, H., SAKISAKA, S., OHISHI, M., KAWAGUCHI, T., TANIGUCHI, E., SASATOMI, K., HARADA, M., KUSABA, T., TANAKA, M., KIMURA, R., NAKASHIMA, Y., NAKASHIMA, O., KOJIRO, M., KUROHIJI, T. & SATA, M. 1999. Expression of cyclooxygenase-2 in human hepatocellular carcinoma: Relevance to tumor dedifferentiation. *Hepatology*, 29, 688-696.

KOOPMANN, J., FEDARKO, N. S., JAIN, A., MAITRA, A., IACOBUZIO-DONAHUE, C., RAHMAN, A., HRUBAN, R. H., YEO, C. J. & GOGGINS, M. 2004. Evaluation of osteopontin as biomarker for pancreatic adenocarcinoma. *Cancer Epidemiology Biomarkers & Prevention*, 13, 487-491.

KUZNETSOV, K., LAMBERT, R. & REY, J. F. 2006. Narrow-band imaging: potential and limitations. *Endoscopy*, 38, 76-81.

LAMBERMONT-THIJS, H. M. L., VAN DER WOERDT, F. S., BAUMGAERTEL, A., BONAMI, L., DU PREZ, F. E., SCHUBERT, U. S. & HOOGENBOOM, R. 2010. Linear Poly(ethylene imine)s by Acidic Hydrolysis of Poly(2-oxazoline)s: Kinetic Screening, Thermal Properties, and Temperature-Induced Solubility Transitions. *Macromolecules*, 43, 927-933.

LANGAN, T. J. & CHOU, R. C. 2011. Synchronization of mammalian cell cultures by serum deprivation. *Methods Mol Biol*, 761, 75-83.

- LAURENT, B. A. & GRAYSON, S. M. 2006. An efficient route to well-defined macrocyclic polymers via "Click" cyclization. *Journal of the American Chemical Society*, 128, 4238-4239.
- LAURENT, B. A. & GRAYSON, S. M. 2009. Synthetic approaches for the preparation of cyclic polymers. *Chem Soc Rev*, 38, 2202-13.
- LEE, J. S., BAE, M. H., CHOI, S. H., LEE, S. H., CHO, Y. S., PARK, H. J., KWON, C. H. & JOO, K. J. 2012. Tumor establishment features of orthotopic murine bladder cancer models. *Korean J Urol*, 53, 396-400.
- LESCANEC, R. L., HAJDUK, D. A., KIM, G. Y., GAN, Y., YIN, R., GRUNER, S. M., HOGENESCH, T. E. & THOMAS, E. L. 1995. Comparison of the Lamellar Morphology of Microphase-Separated Cyclic Block-Copolymers and Their Linear Precursors. *Macromolecules*, 28, 3485-3489.
- LEVEAU, J. H. J. & LINDOW, S. E. 2001. Predictive and interpretive simulation of green fluorescent protein expression in reporter bacteria. *Journal of Bacteriology*, 183, 6752-6762.
- LI, D. & CHAN, D. W. 2014. Proteomic cancer biomarkers from discovery to approval: it's worth the effort. *Expert Rev Proteomics*, 11, 135-6.
- LI, M., WANG, J., GENG, Y., LI, Y., WANG, Q., LIANG, Q. & QI, Q. 2012. A strategy of gene overexpression based on tandem repetitive promoters in *Escherichia coli*. *Microb Cell Fact*, 11, 19.
- LI, X., ZHANG, J., GAO, H. L., VIETH, E., BAE, K. H., ZHANG, Y. P., LEE, S. J., RAIKWAR, S., GARDNER, T. A., HUTCHINS, G. D., VANDERPUTTEN, D., KAO, C. H. & JENG, M. H. 2005. Transcriptional targeting modalities in breast cancer gene therapy using adenovirus vectors controlled by alpha-lactalbumin promoter. *Molecular Cancer Therapeutics*, 4, 1850-1859.
- LIM, H. Y., JOO, H. J., CHOI, J. H., YI, J. W., YANG, M. S., CHO, D. Y., KIM, H. S., NAM, D. K., LEE, K. B. & KIM, H. C. 2000. Increased expression of cyclooxygenase-2 protein in human gastric carcinoma. *Clinical Cancer Research*, 6, 519-525.
- LIVAK, K. J. & SCHMITTGEN, T. D. 2001. Analysis of relative gene expression data using real-time quantitative PCR and the 2(-Delta Delta C(T)) Method. *Methods*, 25, 402-8.
- LODILLINSKY, C., RODRIGUEZ, V., VAUTHAY, L., SANDES, E., CASABE, A. & EIJAN, A. M. 2009. Novel invasive orthotopic bladder cancer model with high cathepsin B activity resembling human bladder cancer. *J Urol*, 182, 749-55.
- LOKESHWAR, V. B. & SOLOWAY, M. S. 2001. Current bladder tumor tests: Does their projected utility fulfill clinical necessity? *Journal of Urology*, 165, 1067-1077.

LUDWIG, J. A. & WEINSTEIN, J. N. 2005. Biomarkers in cancer staging, prognosis and treatment selection. *Nature Reviews Cancer*, 5, 845-856.

LUO, Y., CHEN, X. H. & O'DONNELL, M. A. 2004. Use of prostate specific antigen to measure bladder tumor growth in a mouse orthotopic model. *Journal of Urology*, 172, 2414-2420.

MACHITANI, M., YAMAGUCHI, T., SHIMIZU, K., SAKURAI, F., KATAYAMA, K., KAWABATA, K. & MIZUGUCHI, H. 2011. Adenovirus Vector-Derived VA-RNA-Mediated Innate Immune Responses. *Pharmaceutics*, 3, 338-53.

MAMMAS, I. N. & SPANDIDOS, D. A. 2012. George N. Papanicolaou (1883-1962): Fifty years after the death of a great doctor, scientist and humanitarian. *JBUON*, 17, 180-4.

MANNELLO, F., CONDEMI, L., CARDINALI, A., BIANCHI, G. & GAZZANELLI, G. 1998. High concentrations of prostate-specific antigen in urine of women receiving oral contraceptives. *Clinical Chemistry*, 44, 181-183.

MARGULIS, V., SHARIAT, S. F., ASHFAQ, R., THOMPSON, M., SAGALOWSKY, A. I., HSIEH, J. T. & LOTAN, Y. 2007. Expression of cyclooxygenase-2 in normal urothelium, and superficial and advanced transitional cell carcinoma of bladder. *Journal of Urology*, 177, 1163-1168.

MARSHALL, E. 2000. Gene therapy on trial. *Science*, 288, 951-7.

MAZZALI, M., KIPARI, T., OPHASCHAROENSUK, V., WESSON, J. A., JOHNSON, R. & HUGHES, J. 2002. Osteopontin - a molecule for all seasons. *Qjm-an International Journal of Medicine*, 95, 3-13.

MCNEISH, I. A., BELL, S. J. & LEMOINE, N. R. 2004. Gene therapy progress and prospects: cancer gene therapy using tumour suppressor genes. *Gene Ther*, 11, 497-503.

MERKEL, O. M., MINTZER, M. A., SITTERBERG, J., BAKOWSKY, U., SIMANEK, E. E. & KISSEL, T. 2009. Triazine dendrimers as nonviral gene delivery systems: effects of molecular structure on biological activity. *Bioconjug Chem*, 20, 1799-806.

MERTENS, L. S., NEUZILLET, Y., HORENBLAS, S. & VAN RHIJN, B. W. G. 2014. TIMELINE Landmarks in non-muscle-invasive bladder cancer. *Nature Reviews Urology*, 11, 476-480.

MIYAKE, M., GOODISON, S., GIACOIA, E. G., RIZWANI, W., ROSS, S. & ROSSER, C. J. 2012. Influencing factors on the NMP-22 urine assay: an experimental model. *Bmc Urology*, 12.

MOHAMMED, S. I., KNAPP, D. W., BOSTWICK, D. G., FOSTER, R. S., KHAN, K. N. M., MASFERRER, J. L., WOERNER, B. M., SNYDER, P. W. & KOKI, A. T. 1999.

Expression of cyclooxygenase-2 (COX-2) in human invasive transitional cell carcinoma (TCC) of the urinary bladder. *Cancer Research*, 59, 5647-5650.

MOORE, L. E., PFEIFFER, R. M., ZHANG, Z., LU, K. H., FUNG, E. T. & BAST, R. C., JR. 2012. Proteomic biomarkers in combination with CA 125 for detection of epithelial ovarian cancer using prediagnostic serum samples from the Prostate, Lung, Colorectal, and Ovarian (PLCO) Cancer Screening Trial. *Cancer*, 118, 91-100.

MORIMOTO, K., NISHIKAWA, M., KAWAKAMI, S., NAKANO, T., HATTORI, Y., FUMOTO, S., YAMASHITA, F. & HASHIDA, M. 2003. Molecular weight-dependent gene transfection activity of unmodified and galactosylated polyethyleneimine on hepatoma cells and mouse liver. *Mol Ther*, 7, 254-61.

NAGARAJ, N. & MANN, M. 2011. Quantitative Analysis of the Intra- and Inter-Individual Variability of the Normal Urinary Proteome. *Journal of Proteome Research*, 10, 637-645.

NAKAYAMA, Y. 2012. Hyperbranched polymeric "star vectors" for effective DNA or siRNA delivery. *Acc Chem Res*, 45, 994-1004.

NASONGKLA, N., CHEN, B., MACARAEG, N., FOX, M. E., FRECHET, J. M. J. & SZOKA, F. C. 2009. Dependence of Pharmacokinetics and Biodistribution on Polymer Architecture: Effect of Cyclic versus Linear Polymers. *Journal of the American Chemical Society*, 131, 3842-+.

NATIONAL CANCER INSTITUTE. *Diagnosis staging* [Online]. Available: <http://www.cancer.gov/cancertopics/diagnosis-staging/understanding-lab-tests-fact-sheet> [Accessed March 28th 2015].

NEGORO, H., KANEMATSU, A., DOI, M., SUADICANI, S. O., MATSUO, M., IMAMURA, M., OKINAMI, T., NISHIKAWA, N., OURA, T., MATSUI, S., SEO, K., TAINAKA, M., URABE, S., KIYOKAGE, E., TODO, T., OKAMURA, H., TABATA, Y. & OGAWA, O. 2012. Involvement of urinary bladder Connexin43 and the circadian clock in coordination of diurnal micturition rhythm. *Nature Communications*, 3.

NIELSEN, S., CHOU, C. L., MARPLES, D., CHRISTENSEN, E. I., KISHORE, B. K. & KNEPPER, M. A. 1995. Vasopressin increases water permeability of kidney collecting duct by inducing translocation of aquaporin-CD water channels to plasma membrane. *Proc Natl Acad Sci U S A*, 92, 1013-7.

NILSSON, E. E., WESTFALL, S. D., MCDONALD, C., LISON, T., SADLER-RIGGLEMAN, I. & SKINNER, M. K. 2002. An in vivo mouse reporter gene (human secreted alkaline phosphatase) model to monitor ovarian tumor growth and response to therapeutics. *Cancer Chemotherapy and Pharmacology*, 49, 93-100.

NOMURA, T., HUANG, W. C., ZHAU, H. Y. E., JOSSON, S., MIMATA, H. & CHUNG, L. W. K. 2014. beta(2)-Microglobulin-mediated Signaling as a Target for Cancer Therapy. *Anti-Cancer Agents in Medicinal Chemistry*, 14, 343-352.

- O'REGAN, A. & BERMAN, J. S. 2000. Osteopontin: a key cytokine in cell-mediated and granulomatous inflammation. *International Journal of Experimental Pathology*, 81, 373-390.
- OGRIS, M., STEINLEIN, P., KURSA, M., MECHTLER, K., KIRCHEIS, R. & WAGNER, E. 1998. The size of DNA/transferrin-PEI complexes is an important factor for gene expression in cultured cells. *Gene Ther*, 5, 1425-33.
- OLDBERG, A., FRANZEN, A. & HEINEGARD, D. 1986. Cloning and Sequence-Analysis of Rat Bone Sialoprotein (Osteopontin) Cdna Reveals an Arg-Gly-Asp Cell-Binding Sequence. *Proceedings of the National Academy of Sciences of the United States of America*, 83, 8819-8823.
- OSAKI, T., TANIO, Y., TACHIBANA, I., HOSOE, S., KUMAGAI, T., KAWASE, I., OIKAWA, S. & KISHIMOTO, T. 1994. Gene-Therapy for Carcinoembryonic Antigen-Producing Human Lung-Cancer Cells by Cell-Type-Specific Expression of Herpes-Simplex Virus Thymidine Kinase Gene. *Cancer Research*, 54, 5258-5261.
- PACK, D. W., HOFFMAN, A. S., PUN, S. & STAYTON, P. S. 2005. Design and development of polymers for gene delivery. *Nat Rev Drug Discov*, 4, 581-93.
- PARHAMIFAR, L., LARSEN, A. K., HUNTER, A. C., ANDRESEN, T. L. & MOGHIMI, S. M. 2010. Polycation cytotoxicity: a delicate matter for nucleic acid therapy-focus on polyethylenimine. *Soft Matter*, 6, 4001-4009.
- PENG, Y. F., SHI, Y. H., DING, Z. B., ZHOU, J., QIU, S. J., HUI, B., GU, C. Y., YANG, H., LIU, W. R. & FAN, J. 2013. alpha-Fetoprotein promoter-driven Cre/LoxP-switched RNA interference for hepatocellular carcinoma tissue-specific target therapy. *PLoS One*, 8, e53072.
- PFAFFL, M. W. 2001. A new mathematical model for relative quantification in real-time RT-PCR. *Nucleic Acids Research*, 29.
- PIERCE, D. A., SHIMIZU, Y., PRESTON, D. L., VAETH, M. & MABUCHI, K. 1996. Studies of the mortality of atomic bomb survivors. Report 12, Part I. Cancer: 1950-1990. *Radiat Res*, 146, 1-27.
- PREVETTE, L. E., LYNCH, M. L. & REINEKE, T. M. 2010. Amide spacing influences pDNA binding of poly(amidoamine)s. *Biomacromolecules*, 11, 326-32.
- PUTNAM, D. 2006. Polymers for gene delivery across length scales. *Nat Mater*, 5, 439-51.
- QIN, L. H., DING, Y. Z., PAHUD, D. R., CHANG, E., IMPERIALE, M. J. & BROMBERG, J. S. 1997. Promoter attenuation in gene therapy: Interferon-gamma and tumor necrosis factor-alpha inhibit transgene expression. *Human Gene Therapy*, 8, 2019-2029.

- RANGASWAMI, H., BULBULE, A. & KUNDU, G. C. 2006. Nuclear factor inducing kinase: A key regulator in osteopontin-induced MAPK/I kappa B kinase dependent NF-kappa B-mediated promatrix metalloproteinase-9 activation. *Glycoconjugate Journal*, 23, 221-232.
- REID, C. N., STEVENSON, M., ABOGUNRIN, F., RUDDOCK, M. W., EMMERT-STREIB, F., LAMONT, J. V. & WILLIAMSON, K. E. 2012. Standardization of Diagnostic Biomarker Concentrations in Urine: The Hematuria Caveat. *Plos One*, 7.
- RICCIONI, M. E., URGESI, R., CIANCI, R., BIZZOTTO, A., SPADA, C. & COSTAMAGNA, G. 2012. Colon capsule endoscopy: Advantages, limitations and expectations. Which novelties? *World J Gastrointest Endosc*, 4, 99-107.
- RICHARDS, C. A., AUSTIN, E. A. & HUBER, B. E. 1995. Transcriptional Regulatory Sequences of Carcinoembryonic Antigen - Identification and Use with Cytosine Deaminase for Tumor-Specific Gene-Therapy. *Human Gene Therapy*, 6, 881-893.
- RISTIMAKI, A., HONKANEN, N., JANKALA, H., SIPPONEN, P. & HARKONEN, M. 1997. Expression of cyclooxygenase-2 in human gastric carcinoma. *Cancer Research*, 57, 1276-1280.
- RODRIGUES, L. R., TEIXEIRA, J. A., SCHMITT, F. L., PAULSSON, M. & LINDMARK-MANSSON, H. 2007. The role of osteopontin in tumor progression and metastasis in breast cancer. *Cancer Epidemiology Biomarkers & Prevention*, 16, 1087-1097.
- ROSS, J. S. 2009. Breast cancer biomarkers and HER2 testing after 10 years of anti-HER2 therapy. *Drug News Perspect*, 22, 93-106.
- RUDLAND, P. S., PLATT-HIGGINS, A., EL-TANANI, M., RUDLAND, S. D. S., BARRACLOUGH, R., WINSTANLEY, J. H. R., HOWITT, R. & WEST, C. R. 2002. Prognostic significance of the metastasis-associated protein osteopontin in human breast cancer. *Cancer Research*, 62, 3417-3427.
- SCHULTZ GS, L. G., WYSOCKI A. August 2005. Extracellular matrix: Review of its roles in acute and chronic wounds. *World Wide Wounds*, 10-14.
- SCHWANHAUSSER, B., BUSSE, D., LI, N., DITTMAR, G., SCHUCHHARDT, J., WOLF, J., CHEN, W. & SELBACH, M. 2013. Corrigendum: Global quantification of mammalian gene expression control. *Nature*, 495, 126-7.
- SEOW, S. W., CAI, S. R., RAHMAT, J. N., BAY, B. H., LEE, Y. K., CHAN, Y. H. & MAHENDRAN, R. 2010. Lactobacillus rhamnosus GG induces tumor regression in mice bearing orthotopic bladder tumors. *Cancer Science*, 101, 751-758.
- SHARIAT, S. F., MATSUMOTO, K., KIM, J. H., AYALA, G. E., ZHOU, J. H., JIAN, W. G., BENEDICT, W. F. & LERNER, S. P. 2003. Correlation of cyclooxygenase-2

expression with molecular markers, pathological features and clinical outcome of transitional cell carcinoma of the bladder. *Journal of Urology*, 170, 985-989.

SIDERS, W. M., HALLORAN, P. J. & FENTON, R. G. 1998. Melanoma-specific cytotoxicity induced by a tyrosinase promoter-enhancer herpes simplex virus thymidine kinase adenovirus. *Cancer Gene Therapy*, 5, 281-291.

SMALE, S. T. 2010. Beta-galactosidase assay. *Cold Spring Harb Protoc*, 2010, pdb prot5423.

SONG, J. Y., LEE, J. K., LEE, N. W., YEOM, B. W., KIM, S. H. & LEE, K. W. 2009. Osteopontin expression correlates with invasiveness in cervical cancer. *Australian & New Zealand Journal of Obstetrics & Gynaecology*, 49, 434-438.

SOUBA, W. W. & WILMORE, D. W. 2001. *Surgical research*, San Diego, CA, Academic Press.

STEPHAN, C., RALLA, B. & JUNG, K. 2014. Prostate-specific antigen and other serum and urine markers in prostate cancer. *Biochimica Et Biophysica Acta-Reviews on Cancer*, 1846, 99-112.

SUMMERHAYES, I. C. & FRANKS, L. M. 1979. Effects of donor age on neoplastic transformation of adult mouse bladder epithelium in vitro. *J Natl Cancer Inst*, 62, 1017-23.

TAKAHASHI, M., SATO, T., SAGAWA, T., LU, Y., SATO, Y., IYAMA, S., YAMADA, Y., FUKAURA, J., TAKAHASHI, S., MIYANISHI, K., YAMASHITA, T., SASAKI, K., KOGAWA, K., HAMADA, H., KATO, J. & NIITSU, Y. 2002. E1B-55K-deleted adenovirus expressing E1A-13S by AFP-enhancer/promoter is capable of highly specific replication in AFP-producing hepatocellular carcinoma and eradication of established tumor. *Molecular Therapy*, 5, 627-634.

TANG, M. X., REDEMANN, C. T. & SZOKA, F. C., JR. 1996. In vitro gene delivery by degraded polyamidoamine dendrimers. *Bioconjug Chem*, 7, 703-14.

TANNOUS, B. A., KIM, D. E., FERNANDEZ, J. L., WEISSLEDER, R. & BREAKFIELD, X. O. 2005. Codon-optimized Gaussia luciferase cDNA for mammalian gene expression in culture and in vivo. *Molecular Therapy*, 11, 435-443.

THAM, S. M., NG, K. H., POOK, S. H., ESUVARANATHAN, K. & MAHENDRAN, R. 2011. Tumor and Microenvironment Modification during Progression of Murine Orthotopic Bladder Cancer. *Clinical & Developmental Immunology*.

THOMAS, C. E., SEXTON, W., BENSON, K., SUTPHEN, R. & KOOMEN, J. 2010. Urine Collection and Processing for Protein Biomarker Discovery and Quantification. *Cancer Epidemiology Biomarkers & Prevention*, 19, 953-959.

- THOMAS, M. & KLIBANOV, A. M. 2002. Enhancing polyethylenimine's delivery of plasmid DNA into mammalian cells. *Proc Natl Acad Sci U S A*, 99, 14640-5.
- THOMPSON, J. F., HAYES, L. S. & LLOYD, D. B. 1991. Modulation of Firefly Luciferase Stability and Impact on Studies of Gene-Regulation. *Gene*, 103, 171-177.
- THORNE, N., INGLESE, J. & AULDL, D. S. 2010. Illuminating Insights into Firefly Luciferase and Other Bioluminescent Reporters Used in Chemical Biology. *Chemistry & Biology*, 17, 646-657.
- THORNTON, C., JOHNSON, G. & AGRAWAL, S. 2012. Detection of Invasive Pulmonary Aspergillosis in Haematological Malignancy Patients by using Lateral-flow Technology. *Jove-Journal of Visualized Experiments*.
- TIERNAN, J. P., PERRY, S. L., VERGHESE, E. T., WEST, N. P., YELURI, S., JAYNE, D. G. & HUGHES, T. A. 2013. Carcinoembryonic antigen is the preferred biomarker for in vivo colorectal cancer targeting. *Br J Cancer*, 108, 662-7.
- TINIAKOS, D. G., YU, H. & LIAPIS, H. 1998. Osteopontin expression in ovarian carcinomas and tumors of low malignant potential (LMP). *Human Pathology*, 29, 1250-1254.
- TRUDEL, E. & BOURQUE, C. W. 2010. Central clock excites vasopressin neurons by waking osmosensory afferents during late sleep. *Nat Neurosci*, 13, 467-74.
- TSIEN, R. Y. 1998. The green fluorescent protein. *Annu Rev Biochem*, 67, 509-44.
- TURINI, M. E. & DUBOIS, R. N. 2002. Cyclooxygenase-2: A therapeutic target. *Annual Review of Medicine*, 53, 35-57.
- VERBEECK, R. K. & MUSUAMBA, F. T. 2009. Pharmacokinetics and dosage adjustment in patients with renal dysfunction. *European Journal of Clinical Pharmacology*, 65, 757-773.
- VILE, R. G., RUSSELL, S. J. & LEMOINE, N. R. 2000. Cancer gene therapy: hard lessons and new courses. *Gene Ther*, 7, 2-8.
- WANG, J., LEI, Y., XIE, C., LU, W., YAN, Z., GAO, J., XIE, Z., ZHANG, X. & LIU, M. 2013. Targeted gene delivery to glioblastoma using a C-end rule RGERPPR peptide-functionalised polyethylenimine complex. *Int J Pharm*, 458, 48-56.
- WANG, J. H., YAO, M. Z., ZHANG, Z. L., GU, J. F., ZHANG, Y. H., LI, B. H., SUN, L. Y. & LIU, X. Y. 2003. Enhanced suicide gene therapy by chimeric tumor-specific promoter based on HSF1 transcriptional regulation. *Febs Letters*, 546, 315-320.
- WARDLAW, S. A., ZHANG, N. & BELINSKY, S. A. 2002. Transcriptional regulation of basal cyclooxygenase-2 expression in murine lung tumor-derived cell lines by

CCAAT/enhancer-binding protein and activating transcription factor/cAMP response element-binding protein. *Molecular Pharmacology*, 62, 326-333.

WEBBER, M. M., WAGHRAY, A. & BELLO, D. 1995. Prostate-specific antigen, a serine protease, facilitates human prostate cancer cell invasion. *Clinical Cancer Research*, 1, 1089-1094.

WEI, H., CHU, D. S. H., ZHAO, J. L., PAHANG, J. A. & PUN, S. H. 2013. Synthesis and Evaluation of Cyclic Cationic Polymers for Nucleic Acid Delivery. *Acs Macro Letters*, 2, 1047-1050.

WILD, D. 2013. The immunoassay handbook : theory and applications of ligand binding, ELISA, and related techniques, Oxford ; Waltham, MA, Elsevier.

WINTER, E. E., GOODSTADT, L. & PONTING, C. P. 2004. Elevated rates of protein secretion, evolution, and disease among tissue-specific genes. *Genome Res*, 14, 54-61.

WOLFF, H., SAUKKONEN, K., ANTTILA, S., KARJALAINEN, A., VAINIO, H. & RISTIMAKI, A. 1998. Expression of cyclooxygenase-2 in human lung carcinoma. *Cancer Research*, 58, 4997-5001.

WONG, R. C. & TSE, H. Y. 2009. *Lateral flow immunoassay*, New York, NY, Springer.

WOOD, P. A., DU-QUITON, J., YOU, S. J. & HRUSHESKY, W. J. M. 2006. Circadian clock coordinates cancer cell cycle progression, thymidylate synthase, and 5-fluorouracil therapeutic index. *Molecular Cancer Therapeutics*, 5, 2023-2033.

WU, C. H., SUI, G. P., ARCHER, S. N., SASSONE-CORSI, P., AITKEN, K., BAGLI, D. & CHEN, Y. 2014. Local receptors as novel regulators for peripheral clock expression. *Faseb Journal*, 28, 4610-4616.

WU, L., JOHNSON, M. & SATO, M. 2003a. Transcriptionally targeted gene therapy to detect and treat cancer. *Trends Mol Med*, 9, 421-9.

WU, Q., ESUVARANATHAN, K. & MAHENDRAN, R. 2004. Monitoring the response of orthotopic bladder tumors to granulocyte macrophage colony-stimulating factor therapy using the prostate-specific antigen gene as a reporter. *Clin Cancer Res*, 10, 6977-84.

WU, Q. H., MAHENDRAN, R. & ESUVARANATHAN, K. 2003b. Nonviral cytokine gene therapy on an orthotopic bladder cancer model. *Clinical Cancer Research*, 9, 4522-4528.

XIE, X. M., XIA, W. Y., LI, Z. K., KUO, H. P., LIU, Y. F., LI, Z., DING, Q. Q., ZHANG, S., SPOHN, B., YANG, Y., WEI, Y. K., LANG, J. Y., EVANS, D. B., CHIAO, P. J., ABBRUZZESE, J. L. & HUNG, M. C. 2007. Targeted expression of BikDD eradicates pancreatic tumors in noninvasive imaging models. *Cancer Cell*, 12, 52-65.

- XU, F. J., ZHANG, Z. X., PING, Y., LI, J., KANG, E. T. & NEOH, K. G. 2009. Star-shaped cationic polymers by atom transfer radical polymerization from beta-cyclodextrin cores for nonviral gene delivery. *Biomacromolecules*, 10, 285-93.
- YAMAMOTO, M., ALEMANY, R., ADACHI, Y., GRIZZLE, W. E. & CURIEL, D. T. 2001a. Characterization of the cyclooxygenase-2 promoter in an adenoviral vector and its application for the mitigation of toxicity in suicide gene therapy of gastrointestinal cancers. *Mol Ther*, 3, 385-94.
- YAMAMOTO, M., ALEMANY, R., ADACHI, Y., GRIZZLE, W. E. & CURIEL, D. T. 2001b. Characterization of the cyclooxygenase-2 promoter in an adenoviral vector and its application for the mitigation of toxicity in suicide gene therapy of gastrointestinal cancers. *Molecular Therapy*, 3, 385-394.
- YE, L., QIAN, Q., ZHANG, Y., YOU, Z., CHE, J., SONG, J. & ZHONG, B. 2015. Analysis of the sericin1 promoter and assisted detection of exogenous gene expression efficiency in the silkworm *Bombyx mori* L. *Sci Rep*, 5, 8301.
- YETISEN, A. K., AKRAM, M. S. & LOWE, C. R. 2013. Paper-based microfluidic point-of-care diagnostic devices. *Lab Chip*, 13, 2210-51.
- YILMAZ, K. B., DOGAN, L., NALBANT, H., AKINCI, M., KARAMAN, N., OZASLAN, C. & KULACOGU, H. 2011. Comparing scalpel, electrocautery and ultrasonic dissector effects: the impact on wound complications and pro-inflammatory cytokine levels in wound fluid from mastectomy patients. *J Breast Cancer*, 14, 58-63.
- YOSHIDA, Y., TOMIZAWA, M., BAHAR, R., MIYAUCHI, M., YAMAGUCHI, T., SAISHO, H., KADOMATSU, K., MURAMATSU, T., MATSUBARA, S., SAKIYAMA, S. & TAGAWA, M. 2002. A promoter region of midkine gene can activate transcription of an exogenous suicide gene in human pancreatic cancer. *Anticancer Research*, 22, 117-120.
- YOSHIMURA, R., SANO, H., MASUDA, C., KAWAMURA, M., TSUBOUCHI, Y., CHARGUI, J., YOSHIMURA, N., HLA, T. & WADA, S. 2000. Expression of cyclooxygenase-2 in prostate carcinoma. *Cancer*, 89, 589-596.
- YOU, S. J., WOOD, P. A., XIONG, Y., KOBAYASHI, M., DU-QUITON, J. & HRUSHESKY, W. J. M. 2005. Daily coordination of cancer growth and circadian clock gene expression. *Breast Cancer Research and Treatment*, 91, 47-60.
- YOUNG, D. C., KINGSLEY, S. D., RYAN, K. A. & DUTKO, F. J. 1993. Selective Inactivation of Eukaryotic Beta-Galactosidase in Assays for Inhibitors of Hiv-1 Tat Using Bacterial Beta-Galactosidase as a Reporter Enzyme. *Analytical Biochemistry*, 215, 24-30.
- YUAN, J. S., REED, A., CHEN, F. & STEWART, C. N., JR. 2006. Statistical analysis of real-time PCR data. *BMC Bioinformatics*, 7, 85.

ZAHAROFF, D. A., HOFFMAN, B. S., HOOPER, H. B., BENJAMIN, C. J., JR., KHURANA, K. K., HANCE, K. W., ROGERS, C. J., PINTO, P. A., SCHLOM, J. & GREINER, J. W. 2009. Intravesical immunotherapy of superficial bladder cancer with chitosan/interleukin-12. *Cancer Res*, 69, 6192-9.

ZHA, S., YEGNASUBRAMANIAN, V., NELSON, W. G., ISAACS, W. B. & DE MARZO, A. M. 2004. Cyclooxygenases in cancer: progress and perspective. *Cancer Letters*, 215, 1-20.

ZHANG, J. F., THOMAS, T. Z., KASPER, S. & MATUSIK, R. J. 2000. A small composite probasin promoter confers high levels of prostate-specific gene expression through regulation by androgens and glucocorticoids in vitro and in vivo. *Endocrinology*, 141, 4698-4710.

ZHANG, L. Q., ADAMS, J. Y., BILLICK, E., ILAGAN, R., IYER, M., LE, K., SMALLWOOD, A., GAMBHIR, S. S., CAREY, M. & WU, L. L. 2002. Molecular engineering of a two-step transcription amplification (TSTA) system for transgene delivery in prostate cancer. *Molecular Therapy*, 5, 223-232.

ZHANG, S., ZHAO, Y., ZHAO, B. & WANG, B. 2010. Hybrids of nonviral vectors for gene delivery. *Bioconjug Chem*, 21, 1003-9.

ZHANG, X., ATALA, A. & GODBEY, W. T. 2008. Expression-targeted gene therapy for the treatment of transitional cell carcinoma. *Cancer Gene Ther*, 15, 543-52.

ZHANG, X. & GODBEY, W. T. 2011a. Preclinical evaluation of a gene therapy treatment for transitional cell carcinoma. *Cancer Gene Therapy*, 18, 34-41.

ZHANG, X. & GODBEY, W. T. 2011b. Preclinical evaluation of a gene therapy treatment for transitional cell carcinoma. *Cancer Gene Ther*, 18, 34-41.

ZHANG, X., TURNER, C. & GODBEY, W. T. 2009. Comparison of caspase genes for the induction of apoptosis following gene delivery. *Mol Biotechnol*, 41, 236-46.

ZHU, Y. Q., GIDO, S. P., LATROU, H., HADJICHRISTIDIS, N. & MAYS, J. W. 2003. Microphase separation of cyclic block copolymers of styrene and butadiene and of their corresponding linear triblock copolymers. *Macromolecules*, 36, 148-152.

## **Biography**

Yunlan Fang was born on Jan 29<sup>th</sup>, 1986 in Hangzhou City of Zhejiang Province in China. Yunlan attended Sichuan University in September 2004 and completed her bachelor degree in polymer processing engineering in June 2008. In August 2009, Yunlan was admitted to Tulane University and began her oversea studies in the Department of Chemical and Biomolecular Engineering at Tulane. In Jan 2010, she joined Prof. W Godbey's group and started her research on cancer detection via expression-targeted gene delivery. She published 2 peer reviewed journal articles and one book chapter. She had a patent filed and presented her research in international conferences. She is eager to continue working on the area of biomedical engineering and make contribution to conquering cancer.